



Magnetic surfaces and Thin Films (Polarized Neutron Reflectometry)

25. October 2005

Hartmut Zabel

Ruhr University Bochum, Germany



School on Pulsed Neutron Sources
Trieste - Italy, 17 - 28 October 2005

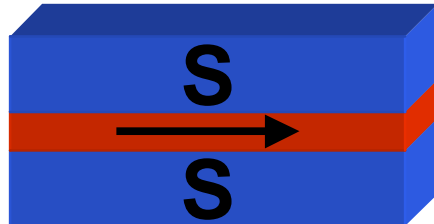
1



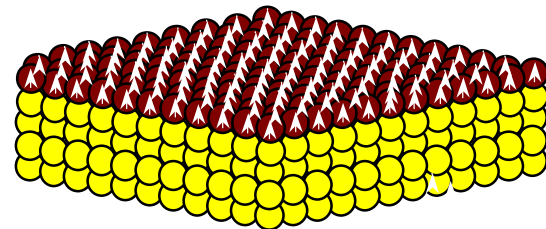
Surfaces, Interfaces and Thin Films

For fundamental properties in the area of
magneto- and spintronics

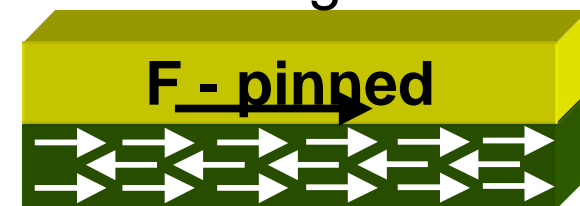
Proximity effects
and tunneling



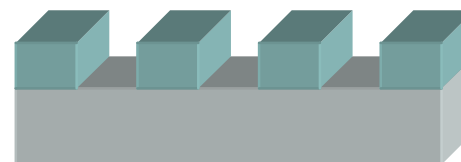
Magnetic films



Exchange bias



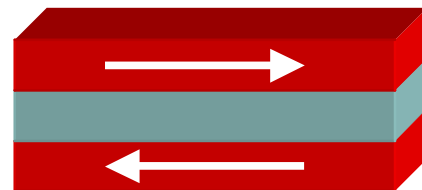
Lateral structures



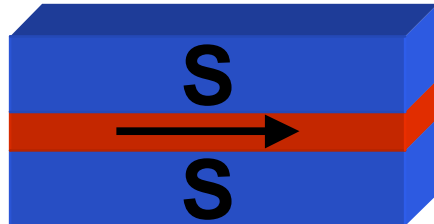
Surfaces, Interfaces and Thin Films

For fundamental properties in the area of
magneto- and spintronics

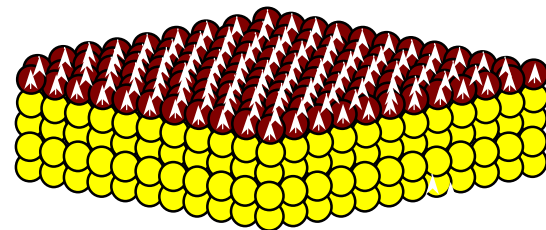
GMR heterostructures



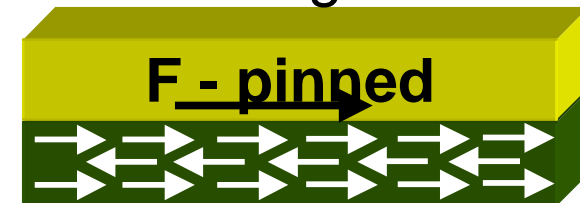
Proximity effects
and tunneling



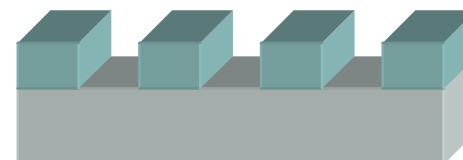
Magnetic films



Exchange bias



Lateral structures



Content

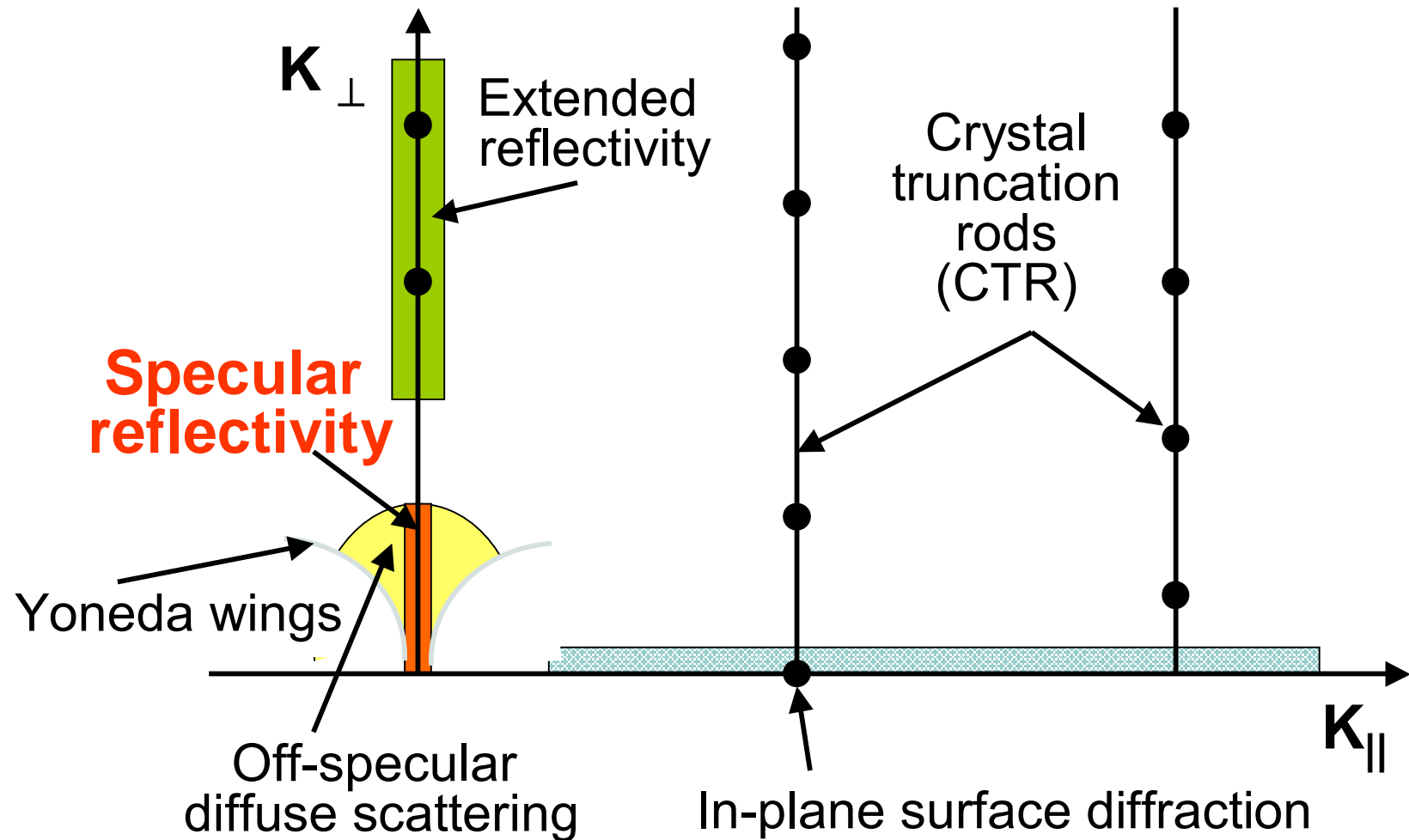
- 1. X-ray and neutron reflectivity**
- 2. Polarized neutron reflectivity (PNR)**
 - Methods
 - Instrumentation
 - Examples



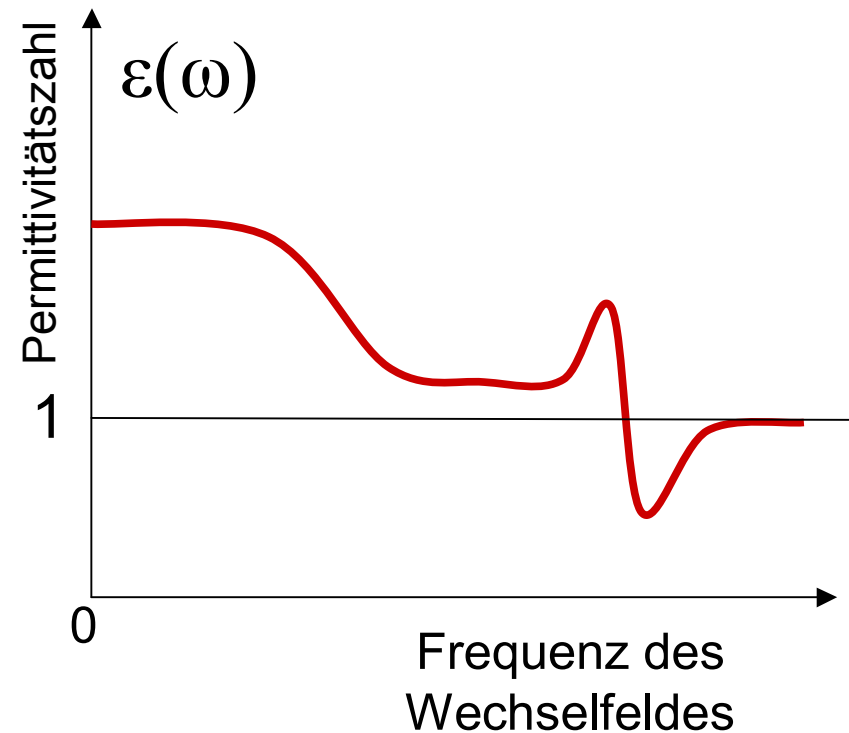
1. X-ray and neutron reflectivity



Specular reflectivity



Index of refraction



$$\sqrt{\epsilon(\omega)} = n(\omega) = \text{Brechungsindex} \Rightarrow \text{Optik}$$

X-ray refractive index

Refractive Index:

$$n^2(\omega) = 1 + \frac{4\pi\rho_A e^2}{m_e} \sum_i \frac{f_i}{\omega_i^2 - \omega^2 + i\gamma}$$

For x-ray's, the refractive index is always smaller than 1:

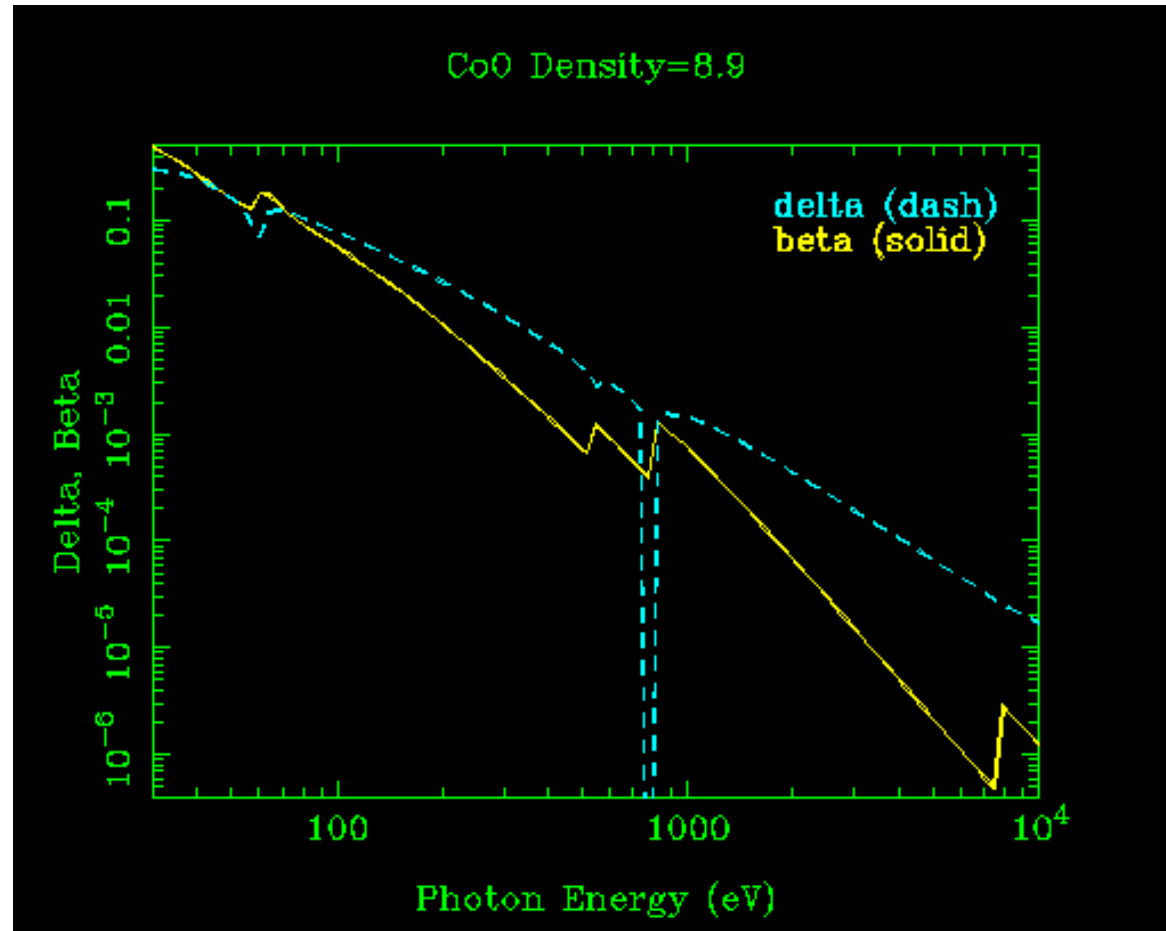
$$\begin{aligned} n(\lambda) &= 1 - \frac{r_0}{2\pi} \rho_e \lambda^2 \\ &\approx 1 - 10^{-5} < 1 \end{aligned}$$

Adding dispersion and absorption correction:

$$\begin{aligned} n(Q_z) &= 1 - \frac{2\pi r_0}{k_0^2} \rho_A [f(Q_z) + \Delta f] - \frac{i\mu}{2k_0} \\ &= 1 \quad -\delta \quad -i\beta \\ &\approx 1 \quad - \quad 10^{-5} \quad < \quad 1 \end{aligned}$$



Plot of δ and β for CoO



http://www-cxro.lbl.gov/optical_constants/getdb2.html 8



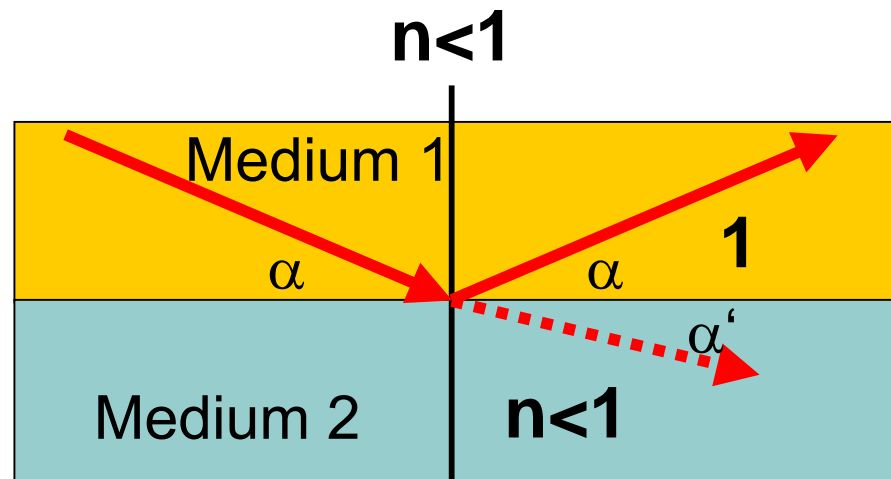
Snellius law for different media



9



Snellius law for different media

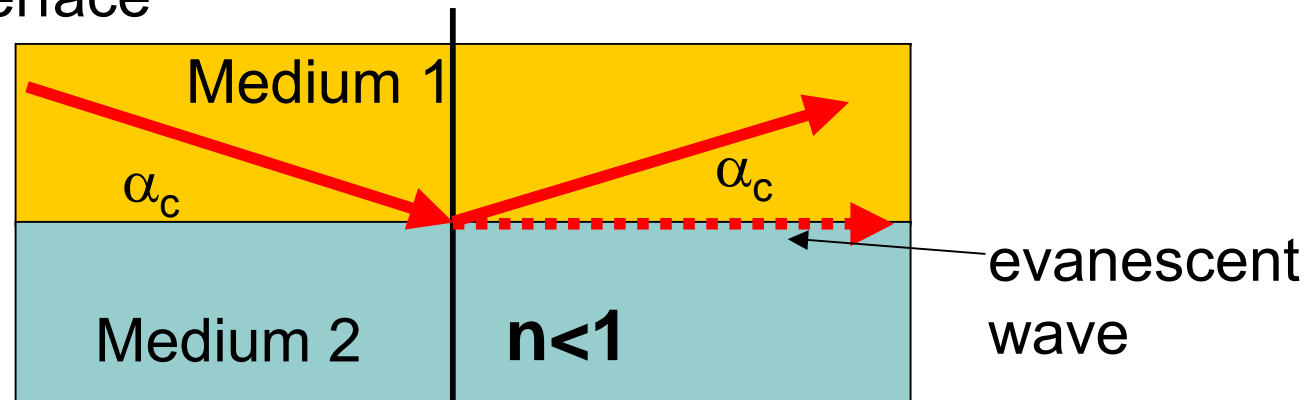


$$\frac{\cos \alpha}{\cos \alpha'} = n;$$

Critical angle for total reflection

Since $n < 1$, total reflection occurs at:

For all angles $\alpha < \alpha_c$ the wave can not penetrate into the medium, but at α_c there is an evanescent wave travelling along the interface

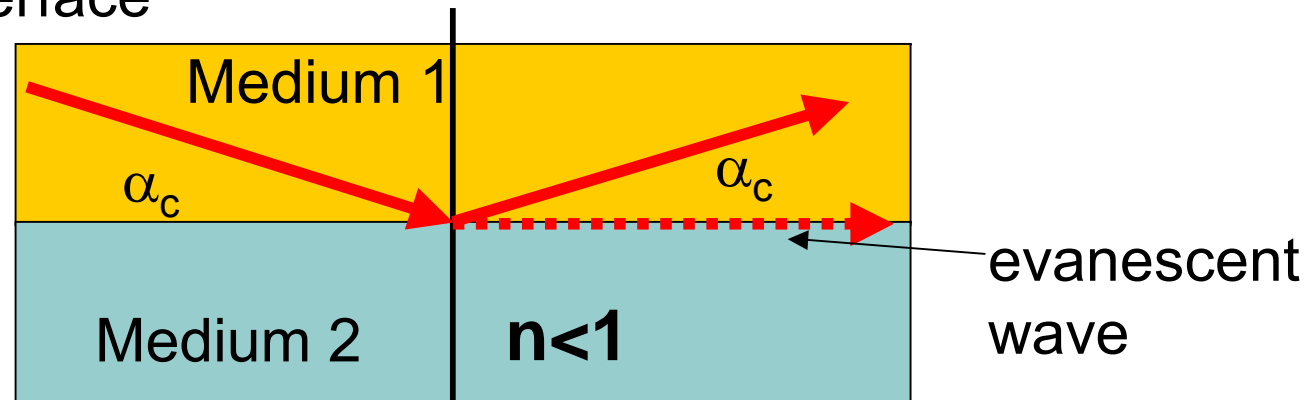


Critical angle for total reflection

Since $n < 1$, total reflection occurs at:

$$\frac{\cos \alpha_c}{\cos 0} = \cos \alpha_c = n$$

For all angles $\alpha < \alpha_c$ the wave can not penetrate into the medium, but at α_c there is an evanescent wave travelling along the interface



Critical Scattering Vector

Scattering vector is defined as:

$$Q = \frac{4\pi}{\lambda} \sin \alpha = 2k \sin \alpha$$

Accordingly the critical scattering vector is:

$$\begin{aligned} Q_c &= \frac{4\pi}{\lambda} \sin \alpha_c = 2k \sqrt{1 - \cos^2 \alpha_c} = \sqrt{4k^2(1 - n^2)} \\ &\simeq \sqrt{4k^2 2\delta} = \sqrt{16\pi r_0 \rho_e} \end{aligned}$$

The critical scattering vector is no more a function of the wavelength. It is entirely determined by the property of the material and in particular by the electron density ρ_e .



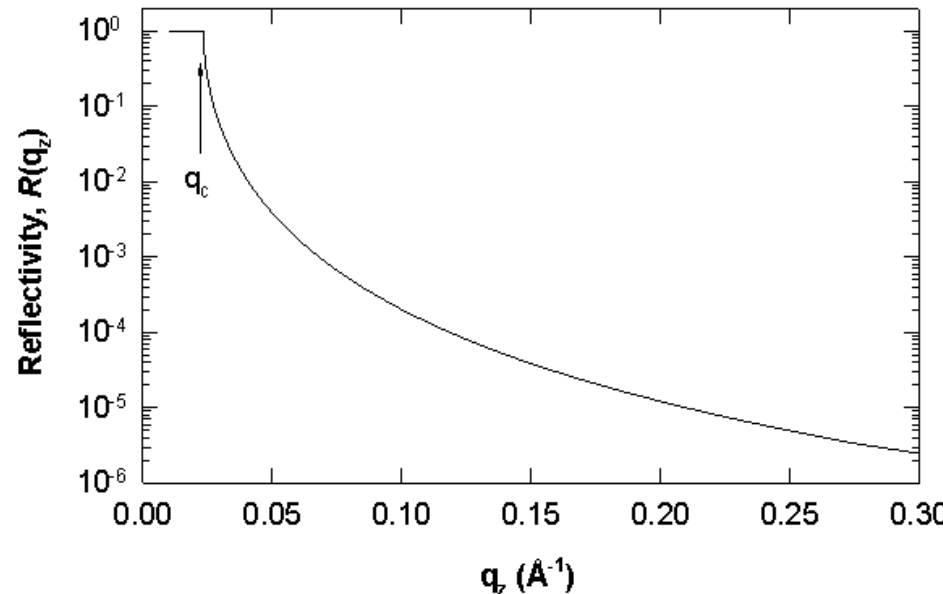
Fresnel reflectivity

For $Q_z < Q_c$: $R = 1$,

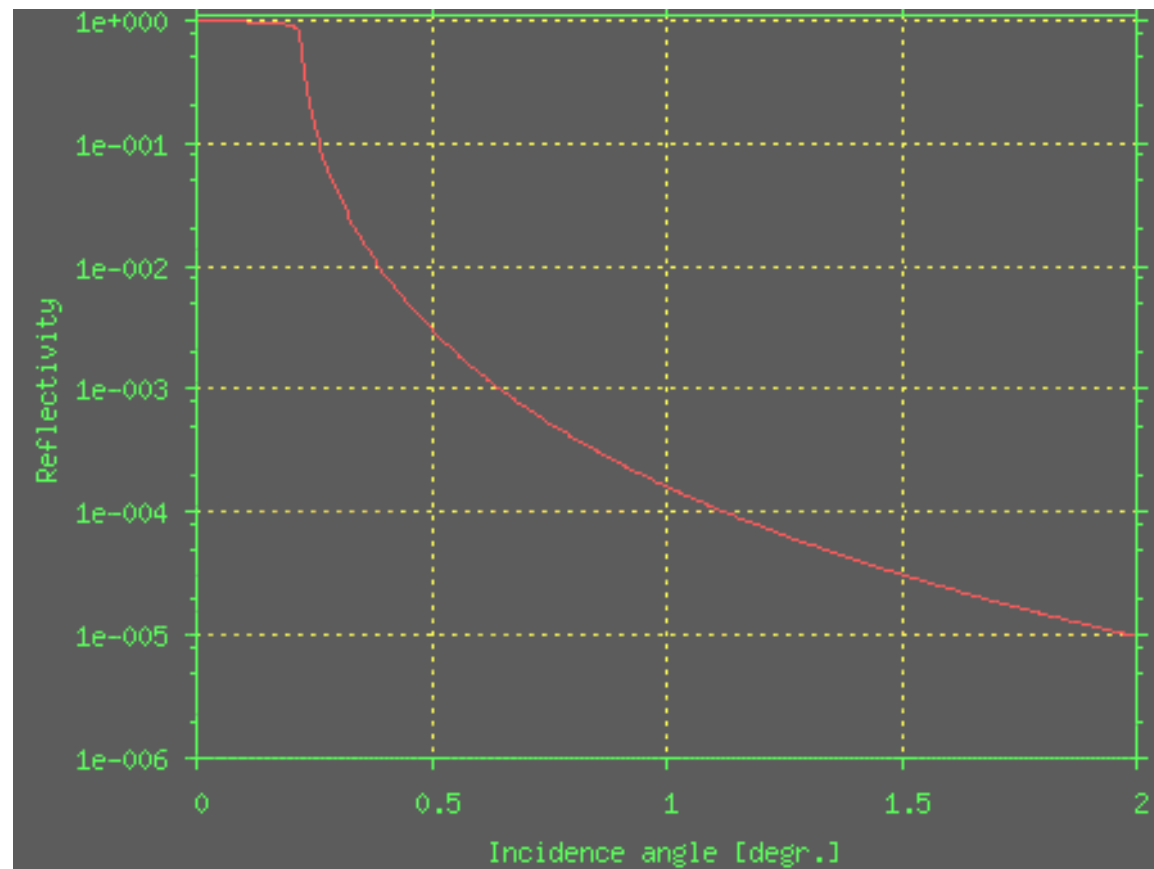
For $Q_z > Q_c$: $R = R_f$

The reflectivity drops with Q^4 , for scattering vectors $Q \gg Q_c$.

This applies for perfectly flat interfaces.



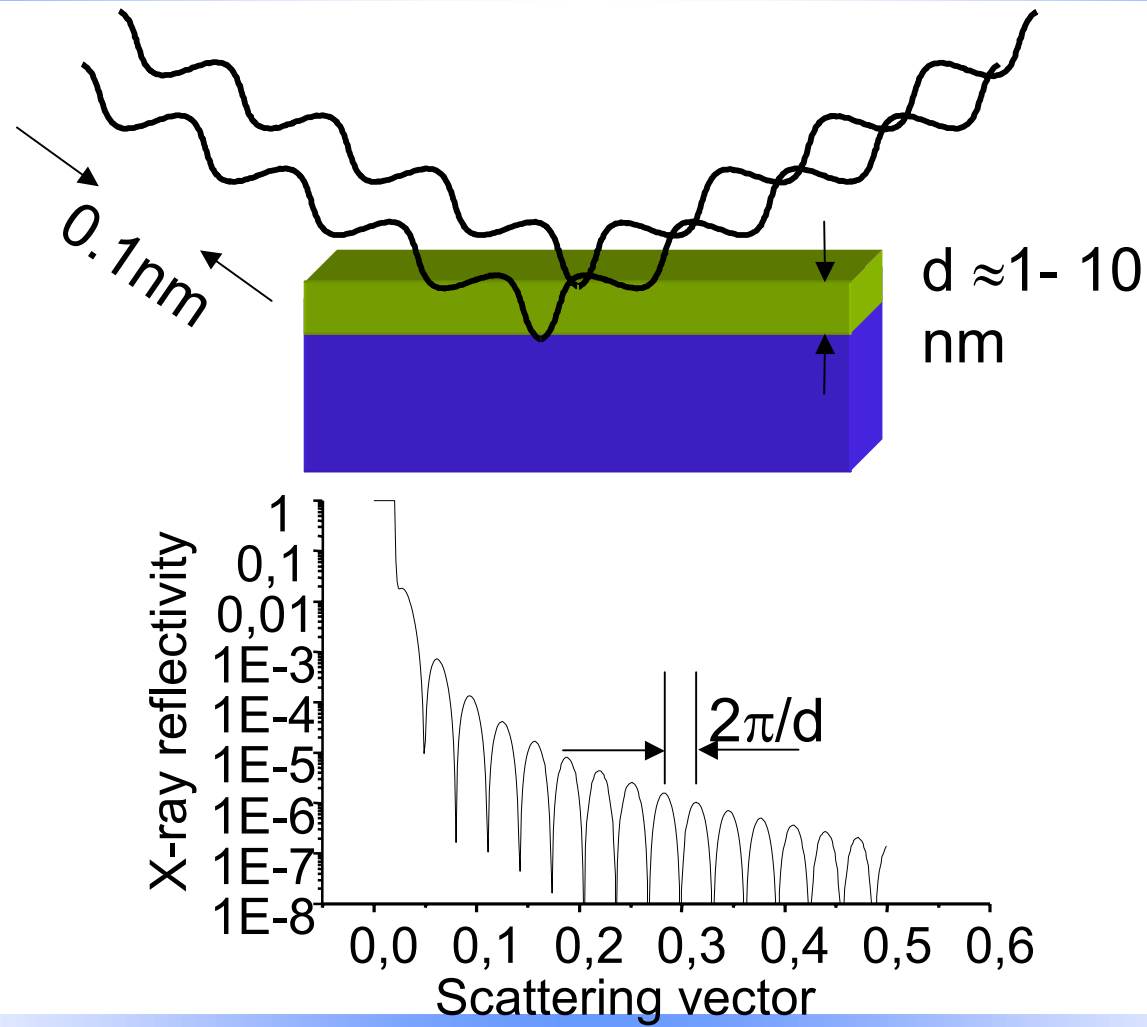
Fresnel reflectivity for Si



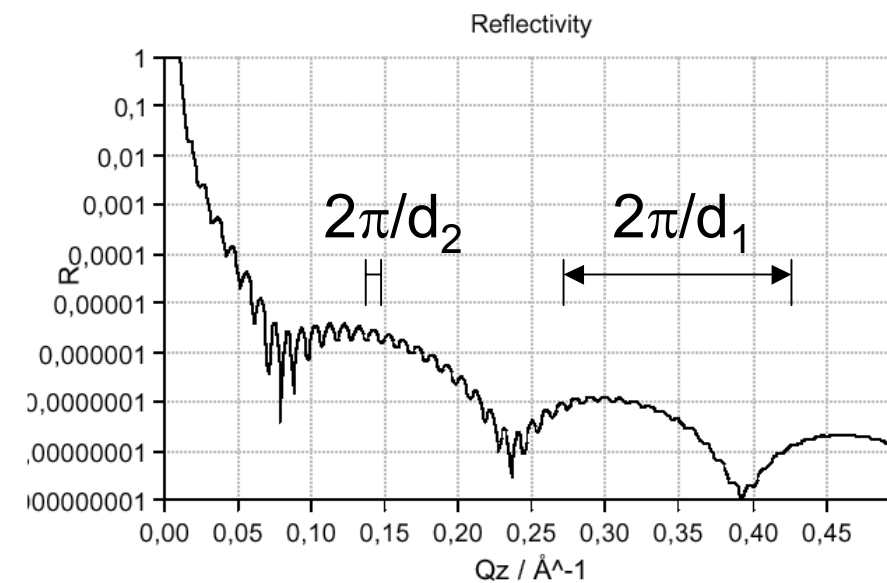
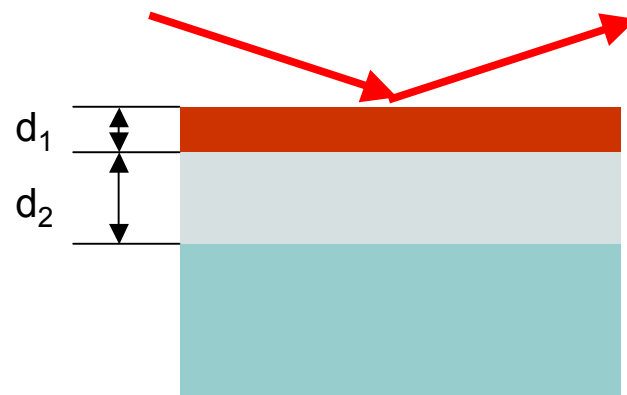
<http://sergey.gmca.aps.anl.gov/>



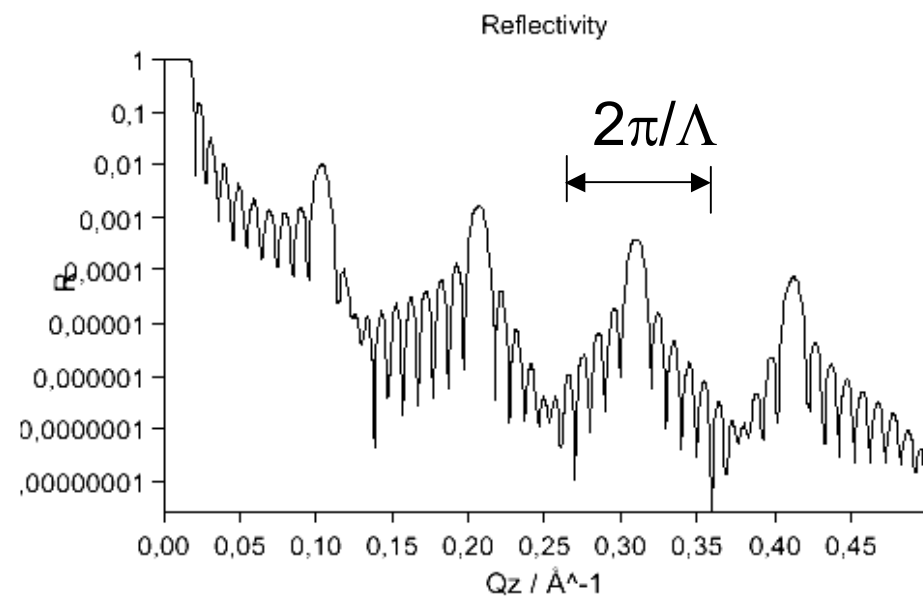
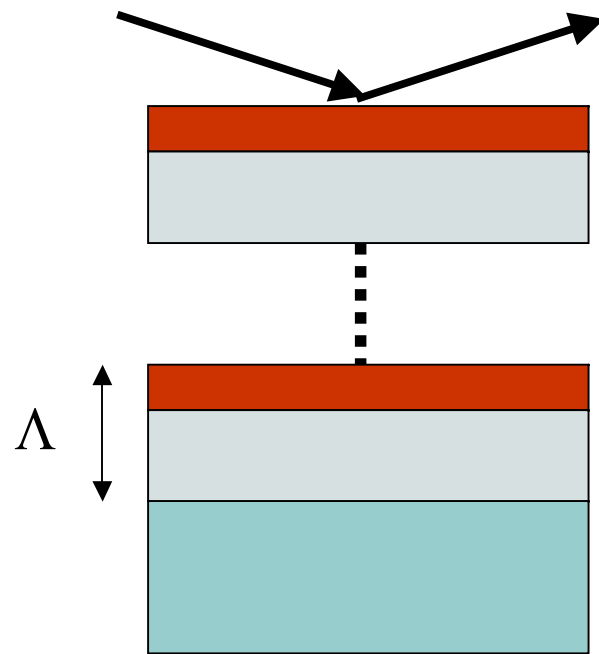
Reflectivity from a thin layer: Kiessig fringes



Reflectivity from a double layer

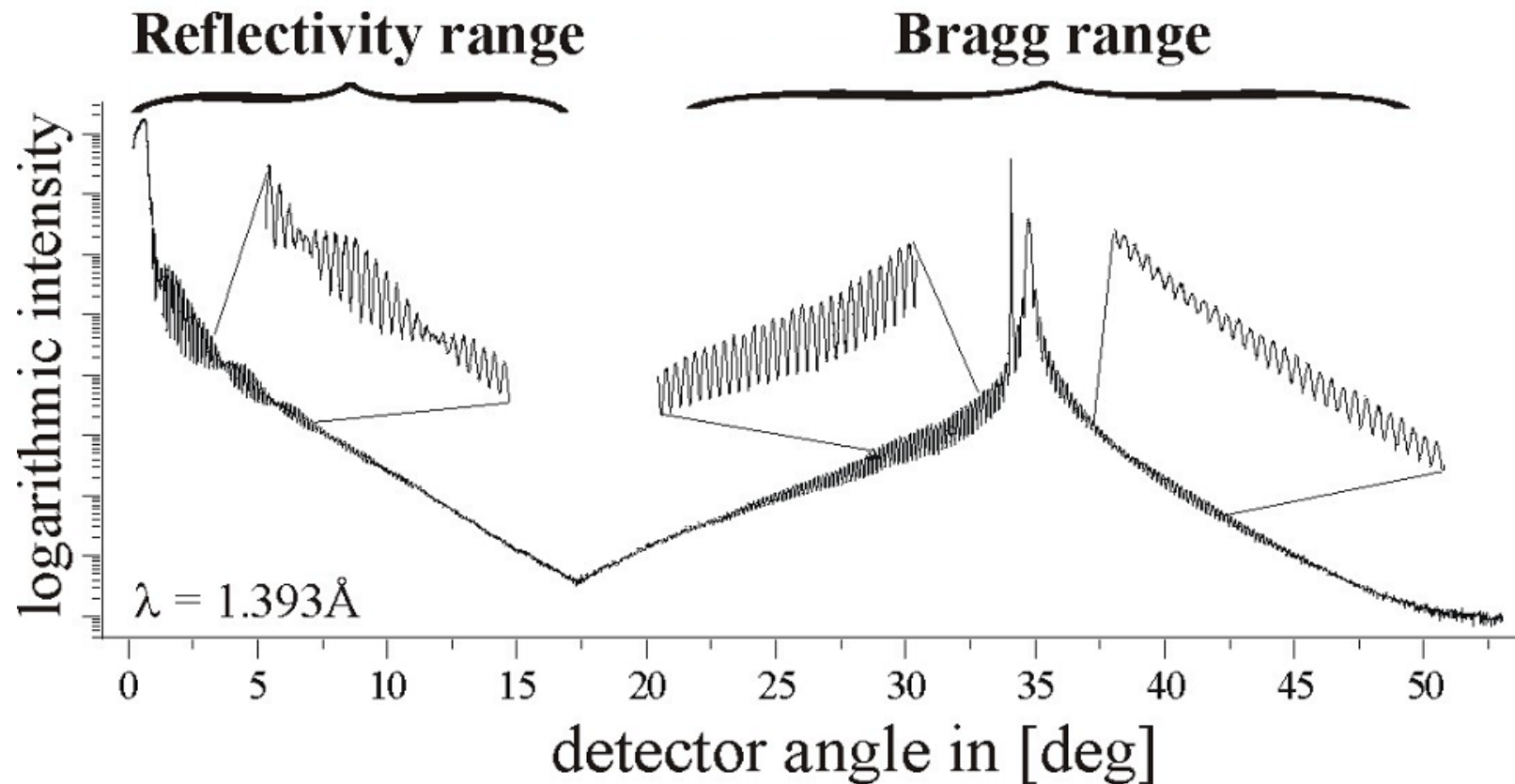


Reflectivity from a multilayer



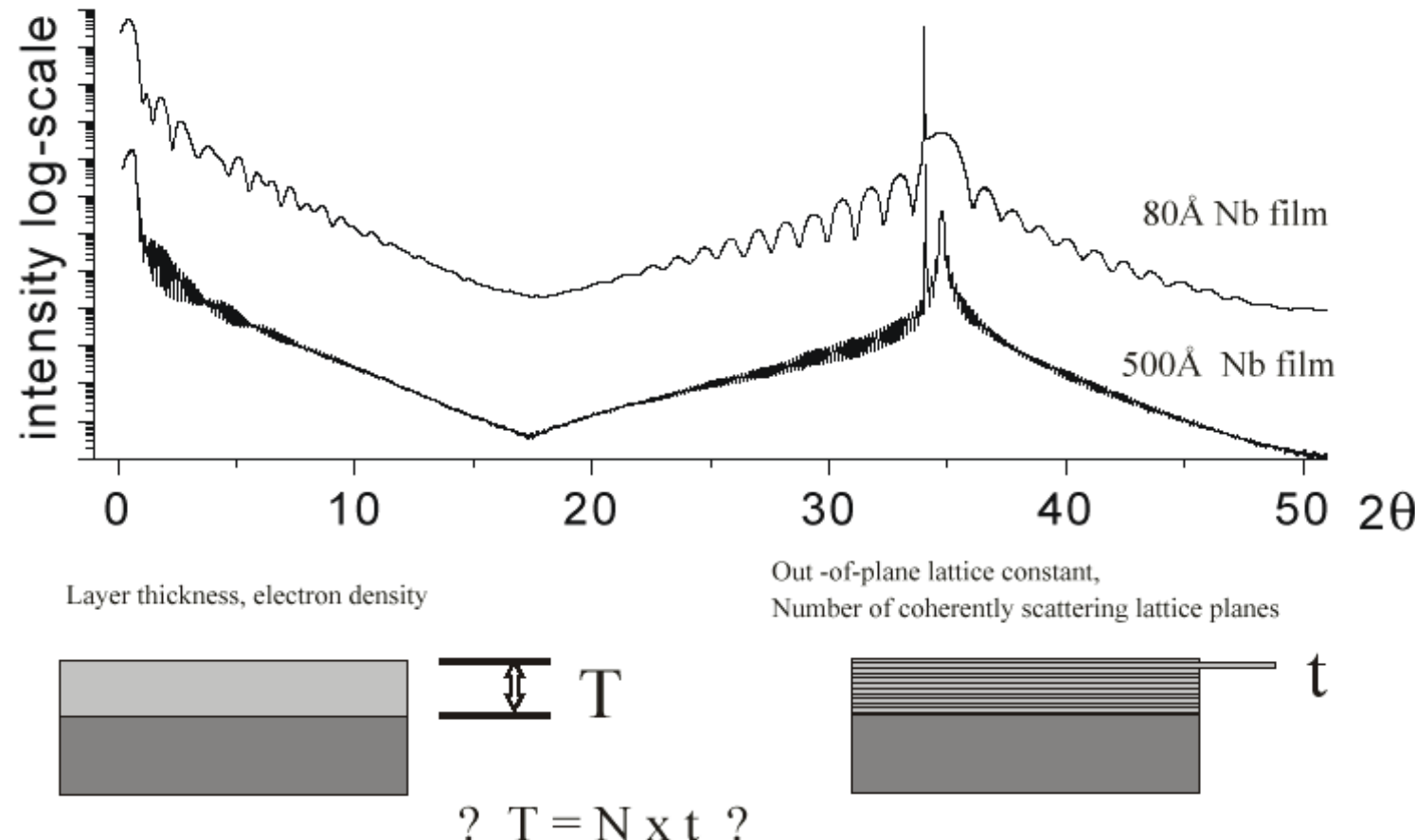
$$Q_l = \sqrt{Q_c^2 + l^2 \left(\frac{2\pi}{\Lambda} \right)^2}$$

Reflectivity and Bragg range

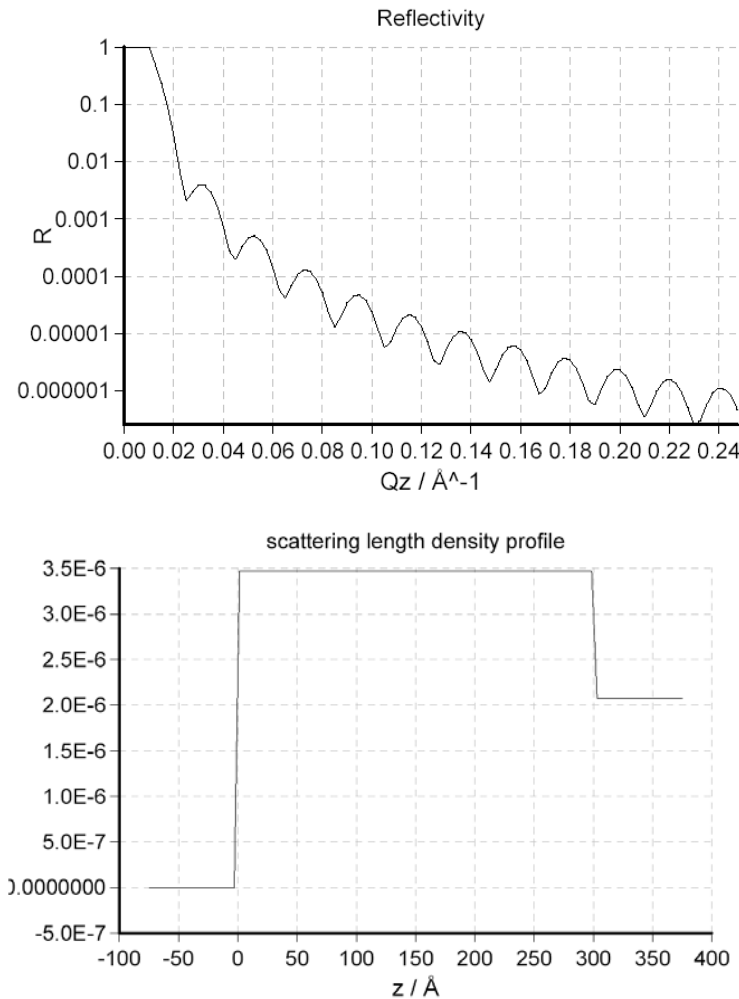


O. Hellwig, PhD Thesis, RUB 2000

In-situ control of layer thickness and oxide growth

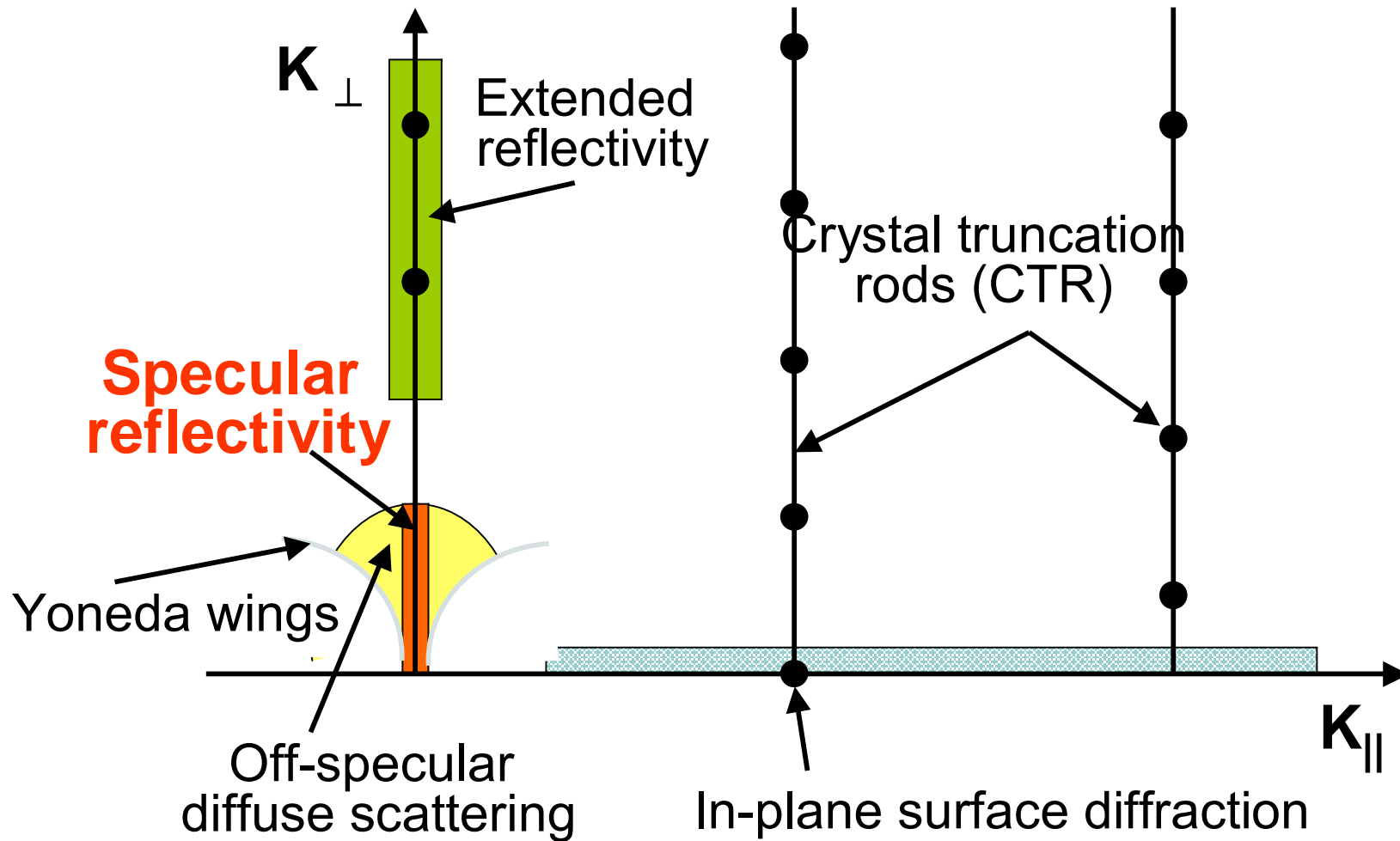


Electron density profile from reflectivity data



Back transformation from reflectivity data to electron densities and thickness profiles is the ultimate goal. However, the back transformation is not always uniquely possible.

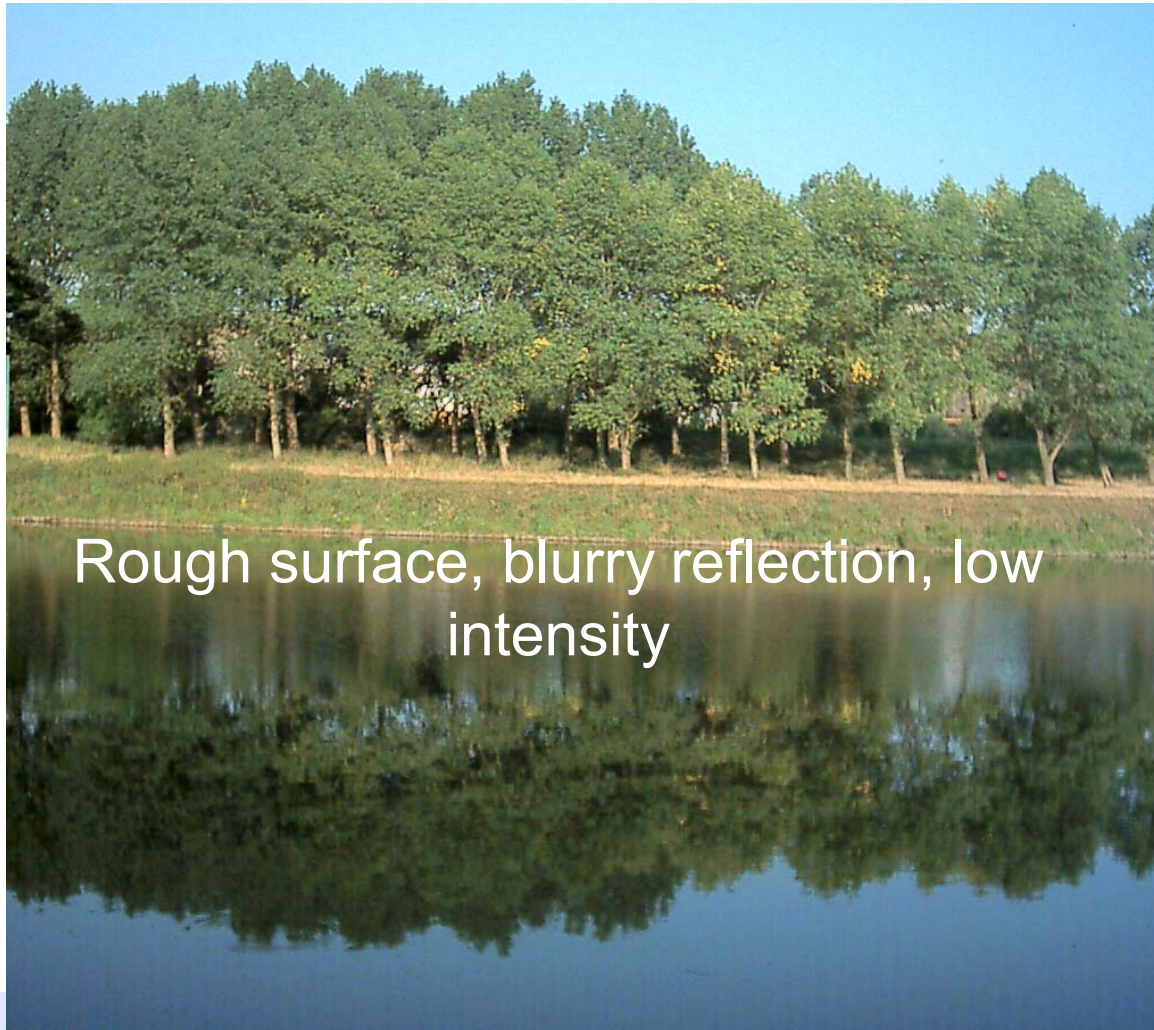
Reflectivity with surface roughness



Smooth and rough surfaces

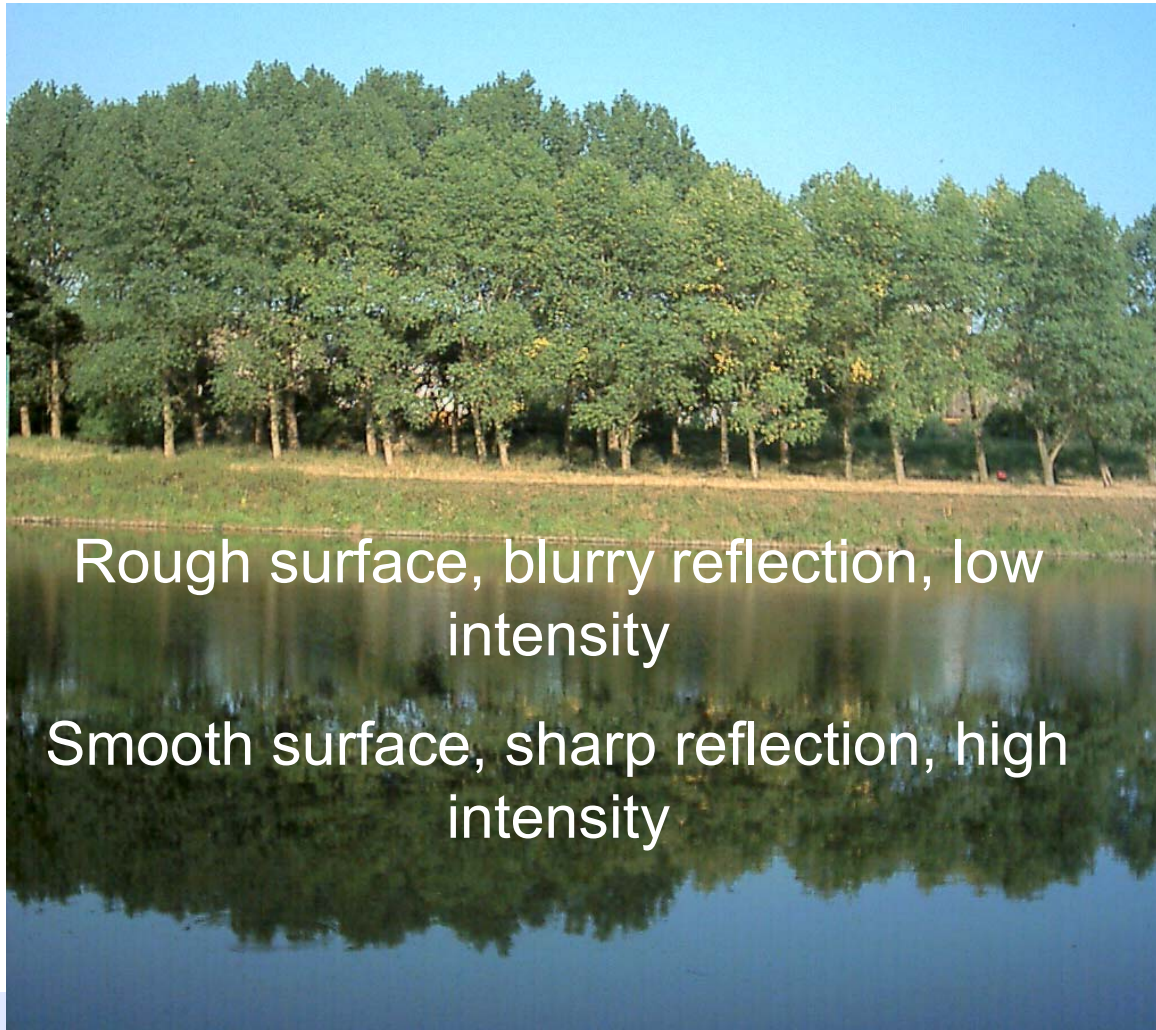


Smooth and rough surfaces



Rough surface, blurry reflection, low intensity

Smooth and rough surfaces



Rough surface, blurry reflection, low intensity

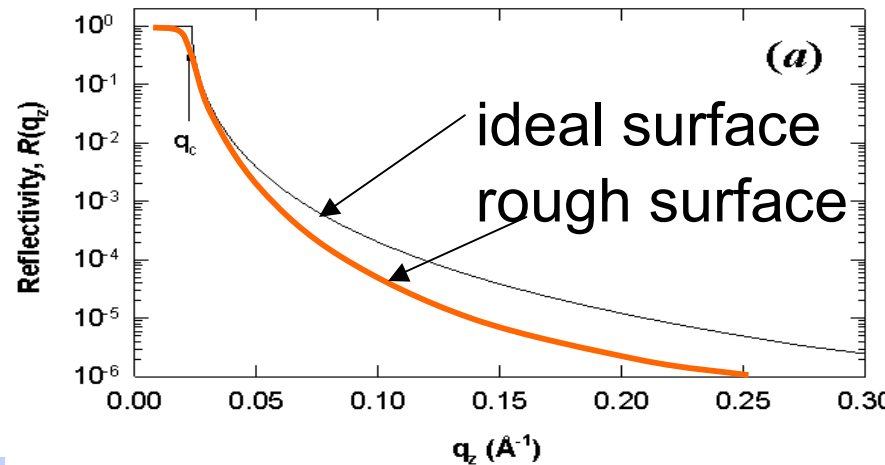
Smooth surface, sharp reflection, high intensity

Reflectivity of rough surface

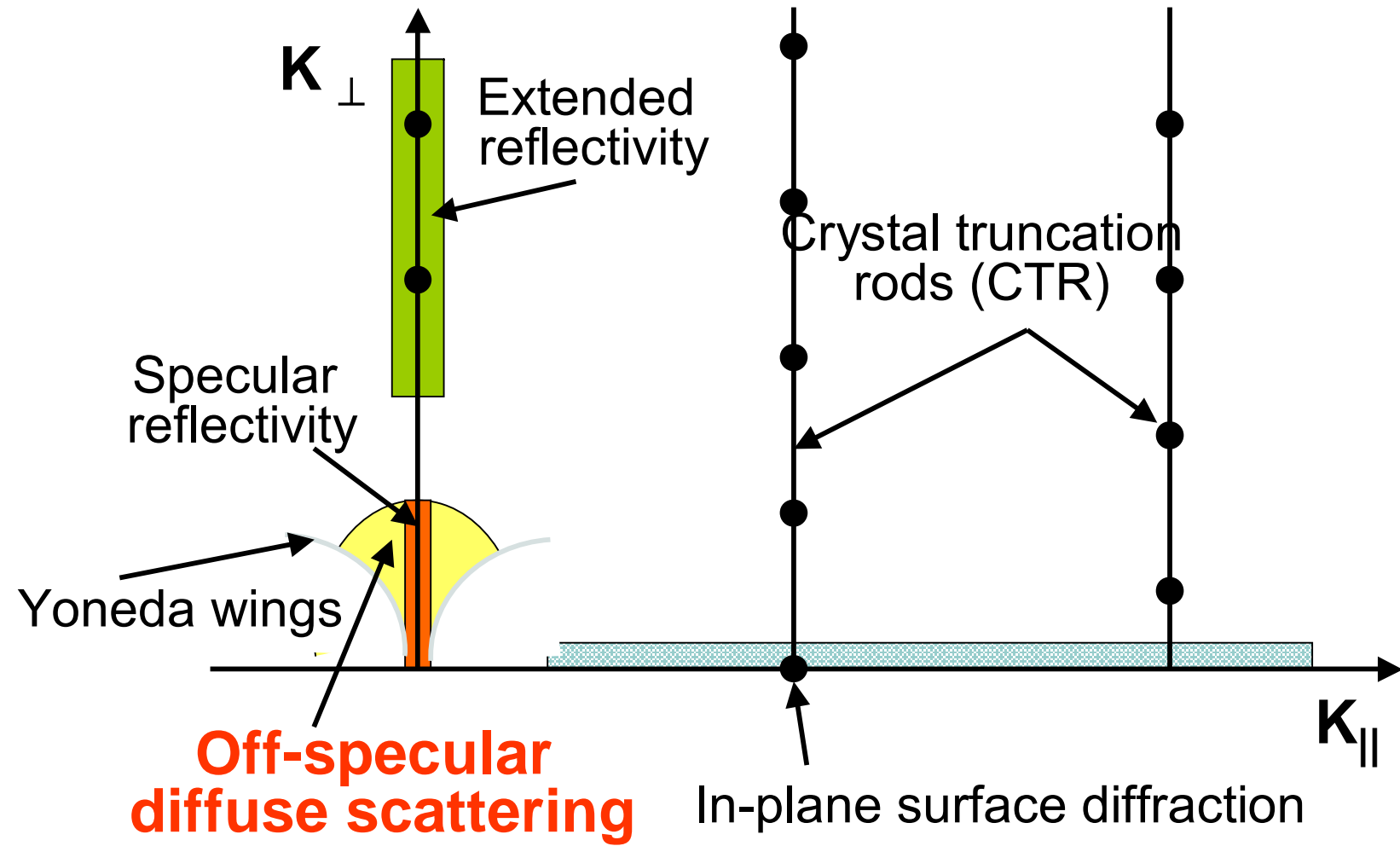
Master formular yields for a Gaussian roughness a damped Fresnel reflectivity:

$$R(Q_z) = R_F(Q_z) \exp(-Q_z^2 \sigma^2)$$

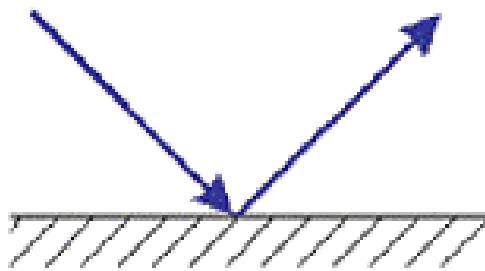
$R_F(Q_z)$ is the Fresnel reflectivity of the ideal surface.
Roughness adds a damping factor, similar to the Debye-Waller factor:



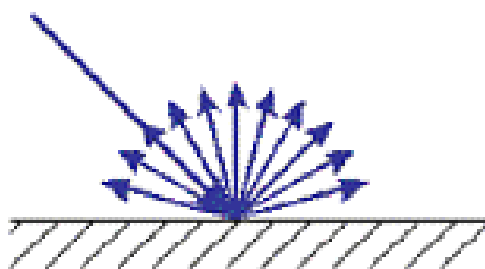
Off-specular diffuse scattering



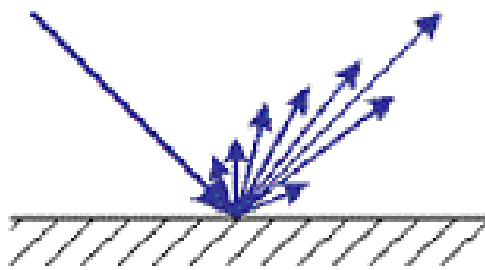
Off-specular scattering from rough interfaces



Perfectly specular surface,
100% reflection, mirror image



Perfectly rough surface,
100% diffuse scattering, projector wall



Partially reflecting and scattering from
rough surface

Diffuse Scattering

Scattering function in the Born approximation:

$$S(\vec{Q}) = \int \langle \rho(0) \rho(R) \rangle e^{i\vec{Q} \cdot \vec{R}} d^3 R$$

Pair correlation function:

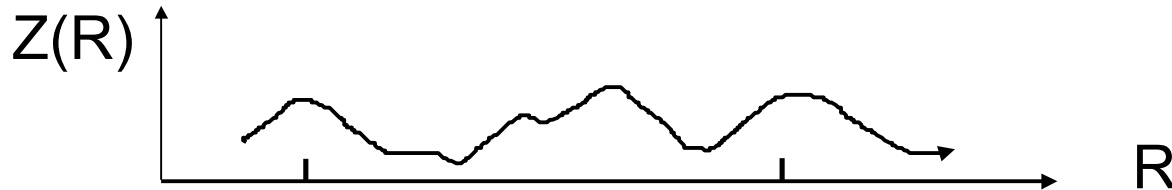
$$\begin{aligned} G(\vec{R}) &= \langle (\rho(0) - \langle \rho(0) \rangle)(\rho(\vec{R}) - \langle \rho(\vec{R}) \rangle) \rangle \\ &= \langle \rho(0) \rho(\vec{R}) \rangle - \langle \rho(0) \rangle \langle \rho(\vec{R}) \rangle \\ &= \langle \rho(0) \rho(\vec{R}) \rangle - \langle \rho(0) \rangle^2 \end{aligned}$$

Inserting:

$$\begin{aligned} S_{tot}(\vec{Q}) &= \underbrace{\langle \rho(0) \rangle^2 \int e^{i\vec{Q} \cdot \vec{R}} d^3 R}_{\textbf{Specular Reflection}} + \underbrace{\int C(\vec{R}) e^{i\vec{Q} \cdot \vec{R}} d^3 R}_{\textbf{Diffuse Scattering}} \\ &= S_{spec}(\vec{Q}) + S_{diff}(\vec{Q}) \end{aligned}$$



Height-height correlation function



Height-height correlation function for a single self-affine, fractal surface:

$$C(R) = \langle z(0)z(R) \rangle = \sigma^2 \exp[-(R / \xi)^{2h}]$$

σ = rms roughness

ξ = cut-off length:

for $R > \xi$, interface appears smooth,

for $R < \xi$, interface appears rough, fractal behavior

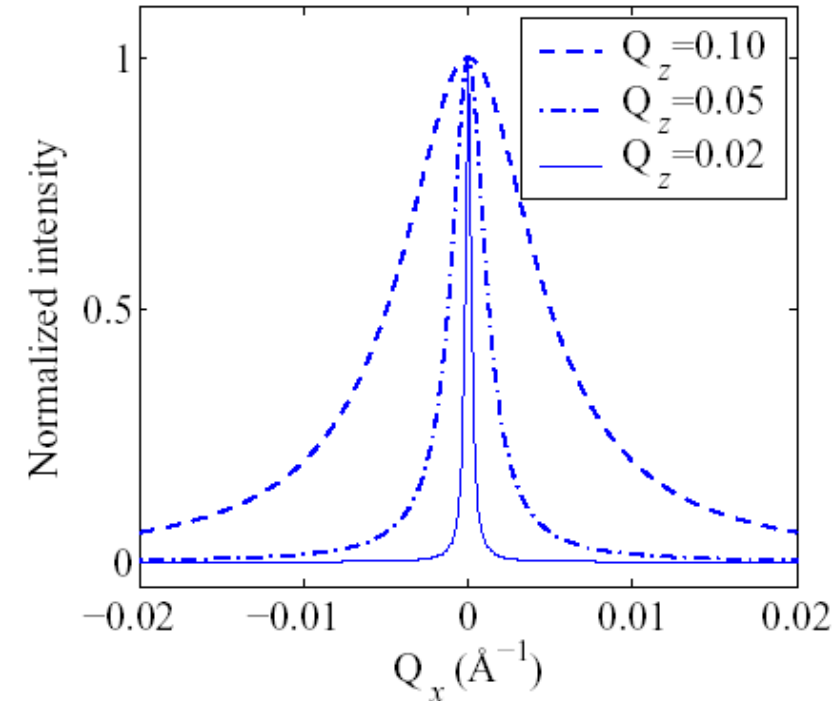
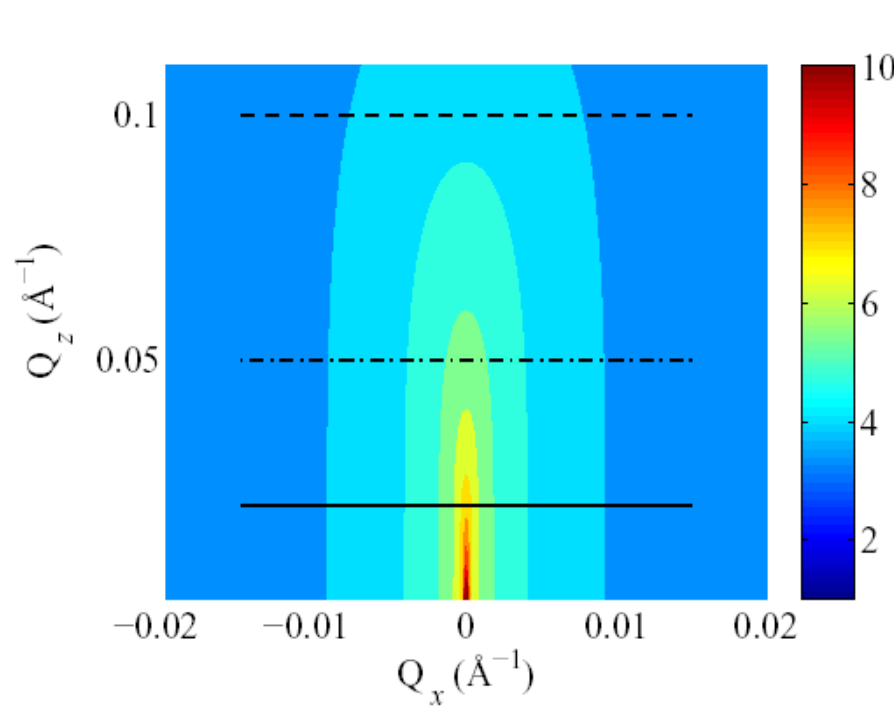
$$S_{diff}(\vec{Q}) = \frac{\exp(-Q_z^2 \sigma^2)}{Q_z^2} \times \int [\exp(Q_z^2 C(R)) - 1] \exp(iQ_{\parallel}R) d^2R$$



S.K. Sinha, E.B. Sirota, S. Garoff, and H.B. Stanley, Phys. Rev. B 38 2297 (1988)³⁶

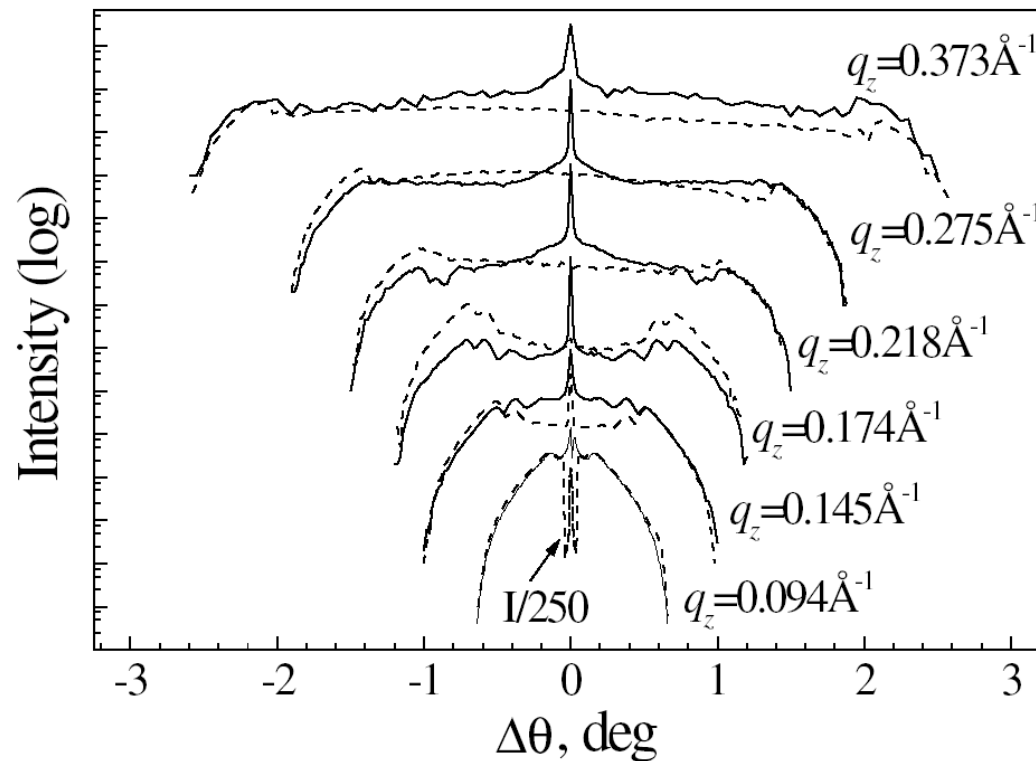


Specular and off-specular scattering



Transverse scans

Transverse scan from an FePt film on GaAs

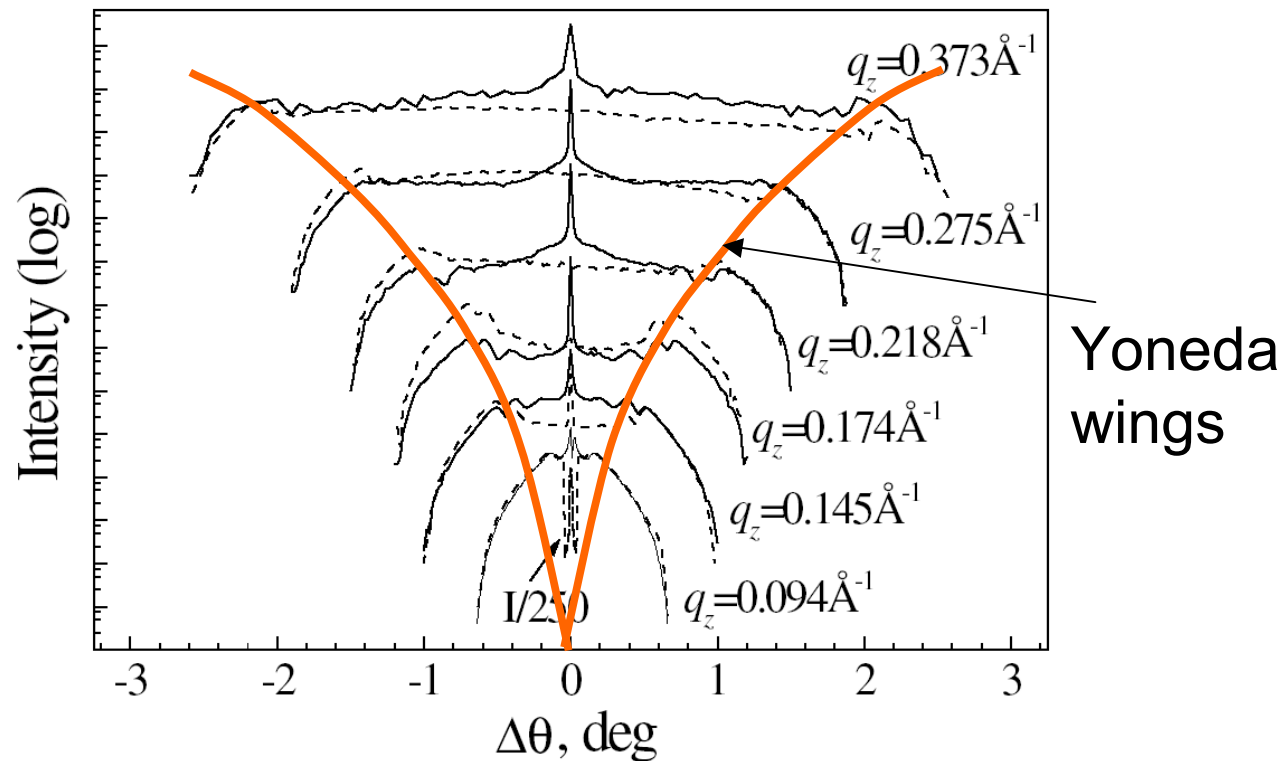


A. Nefedov et al. J. Phys.: Condens. Matter **14**, 12273 (2002)



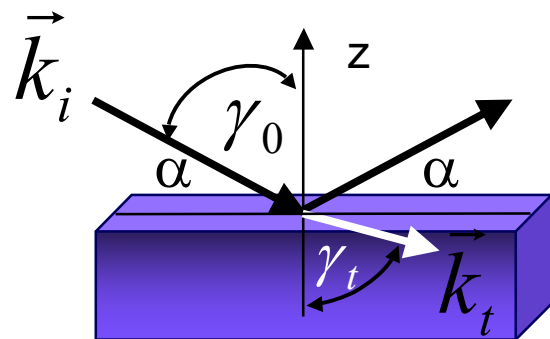
Transverse scans

Transverse scan from an FePt film on GaAs



Refractive index for neutrons

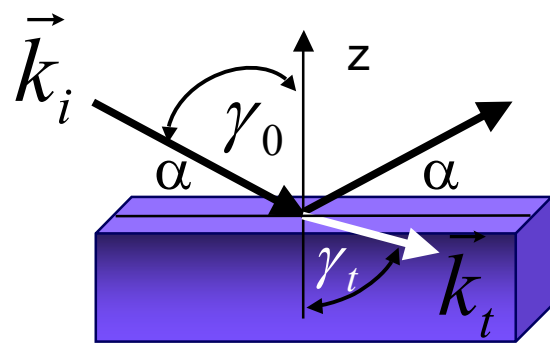
Snell's law for specular reflection:



$$n = \frac{\sin \gamma_0}{\sin \gamma_t} = \frac{|\vec{k}_t|}{|\vec{k}_i|}$$

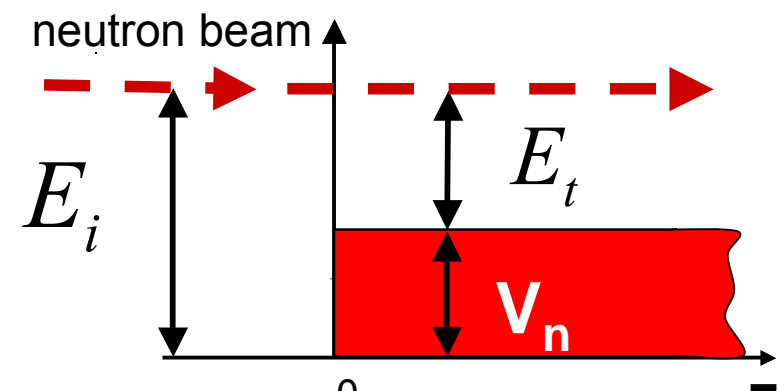
Refractive index for neutrons

Snell's law for specular reflection:



$$n = \frac{\sin \gamma_0}{\sin \gamma_t} = \frac{|\vec{k}_t|}{|\vec{k}_i|}$$

QM potential step for the z-component of the kinetic energy:



Nuclear potential:

$$V_n = \frac{2\pi\hbar^2}{m} N_A b_{coh}$$

Combining both

$$n^2 = \frac{\sin^2 \gamma_0}{\sin^2 \gamma_t} = \frac{|\vec{k}_t|^2}{|\vec{k}_i|^2} = \frac{E_t}{E_i} = \frac{E_i - V_n}{E_i} = 1 - \frac{4\pi}{k_i^2} N_A b_{coh}$$

N_A = nuclei number density

b_{coh} = coherent scattering length of nuclei A

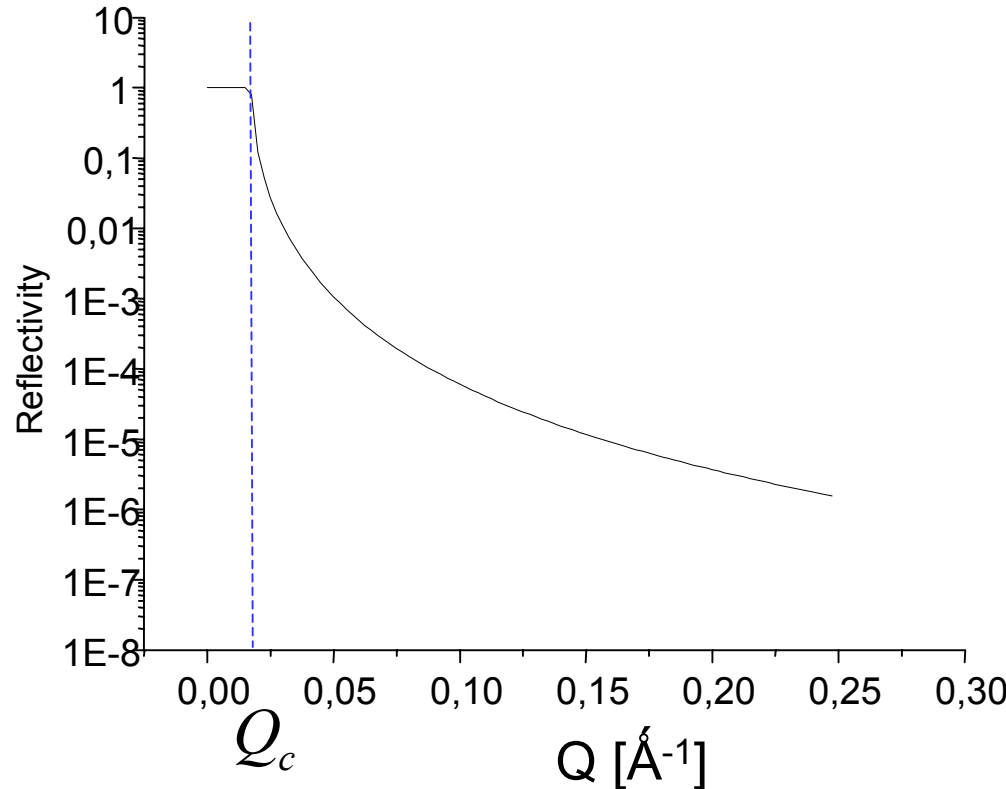
Notice that $n \leq 1$, only for $b_{coh} \geq 0$

Total reflection only for $b_{coh} \geq 0$



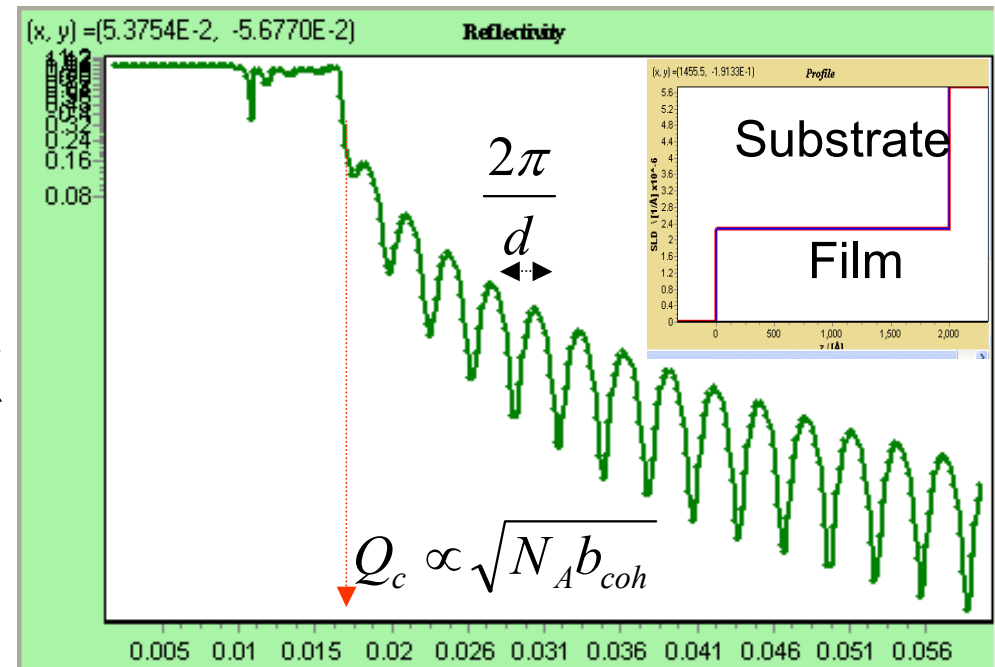
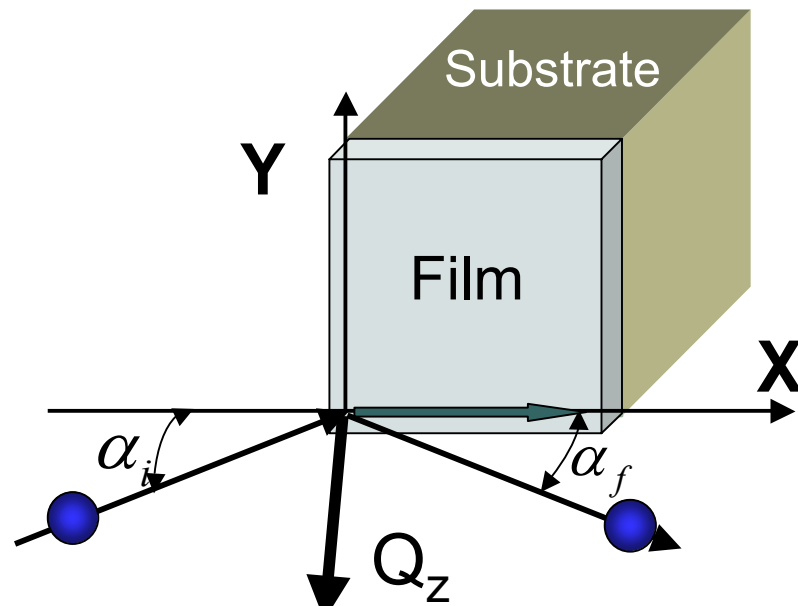
Example:

Neutron reflectivity from a non-magnetic, infinite thick and flat sample

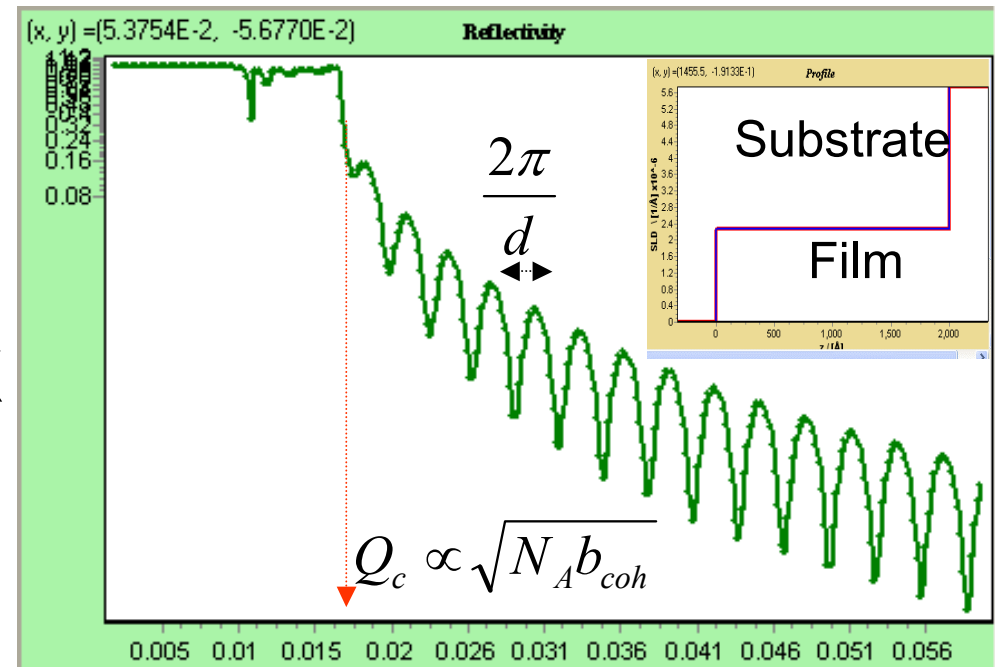
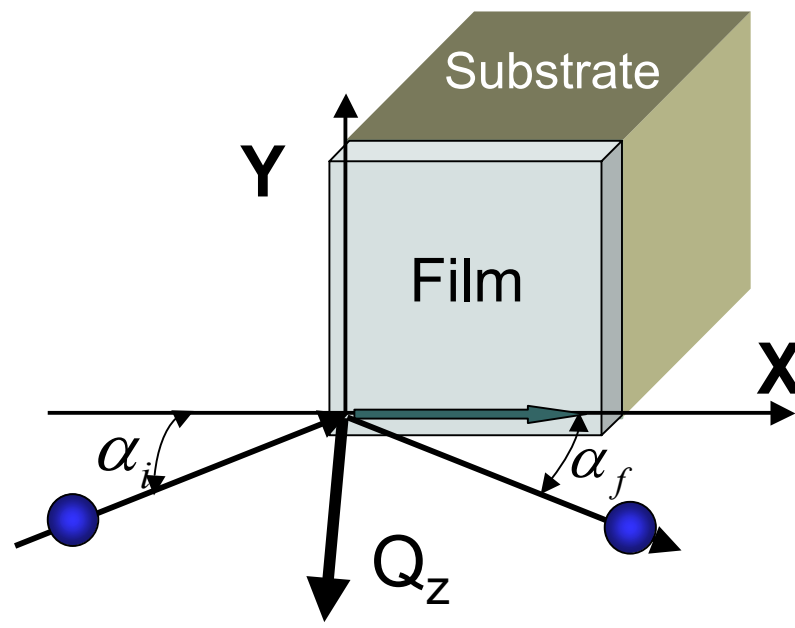


For $Q_z < Q_c$: $R = 1$, only for $b > 0$, i.e. for coherent scattering length.

Neutron Reflectivity

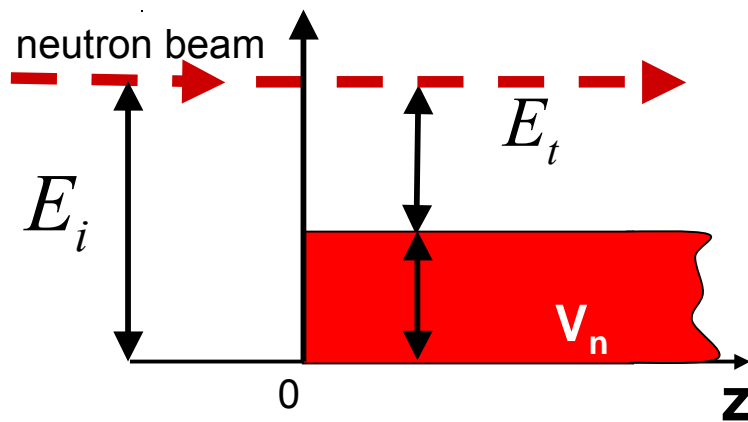


Neutron Reflectivity



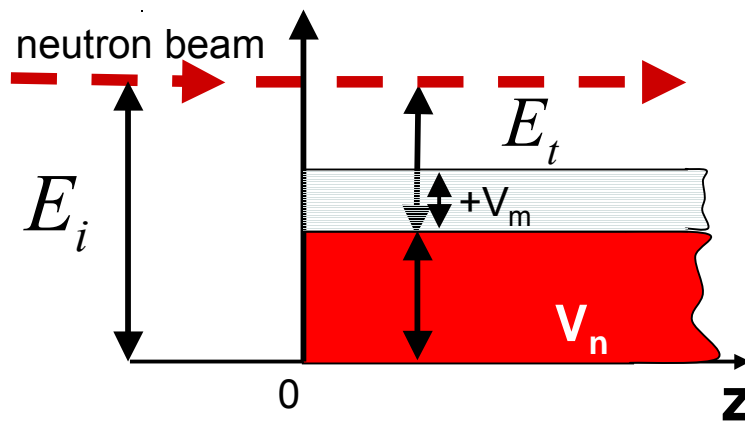
- ❖ Film thickness
- ❖ Interface roughness
- ❖ Density profiles

Reflectivity from single domain FM sample with flat surface



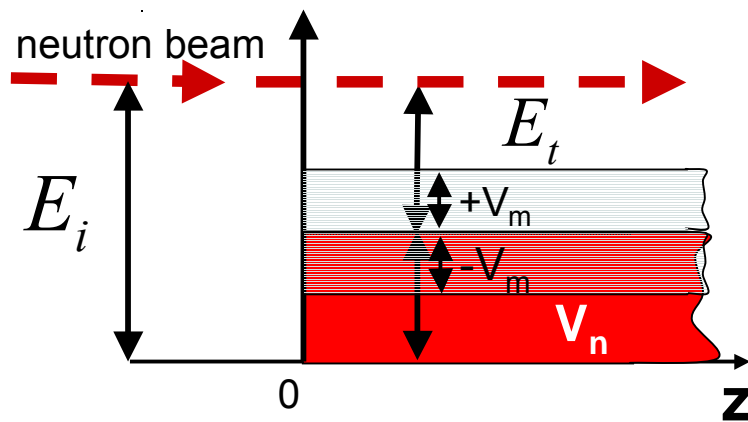
$$V = V_n \pm V_m = \frac{2\pi\hbar^2}{m} N_A (b_n \pm p_m)$$

Reflectivity from single domain FM sample with flat surface



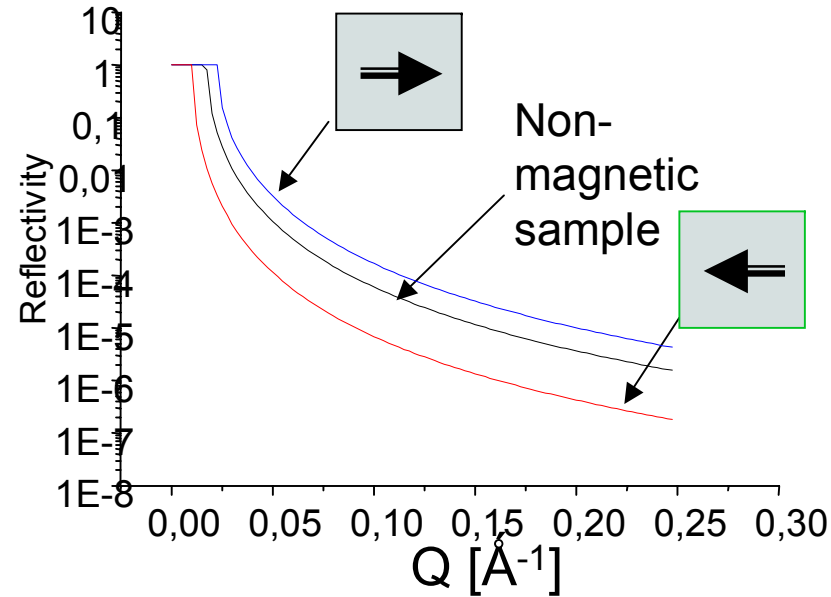
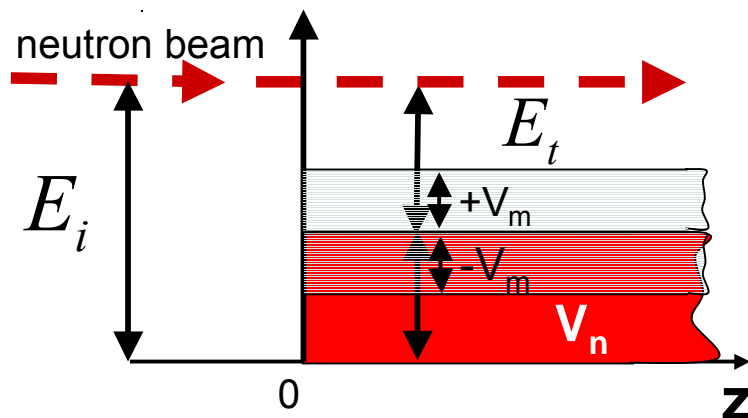
$$V = V_n \pm V_m = \frac{2\pi\hbar^2}{m} N_A (b_n \pm p_m)$$

Reflectivity from single domain FM sample with flat surface



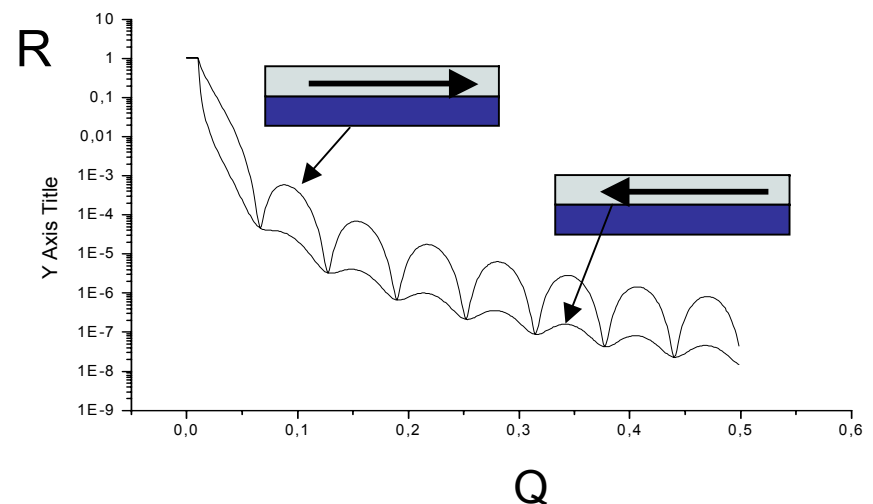
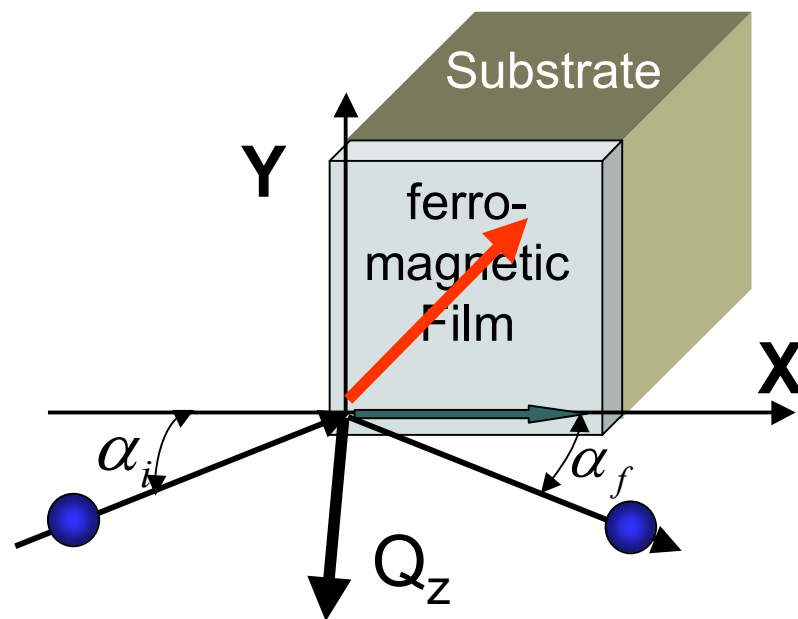
$$V = V_n \pm V_m = \frac{2\pi\hbar^2}{m} N_A (b_n \pm p_m)$$

Reflectivity from single domain FM sample with flat surface



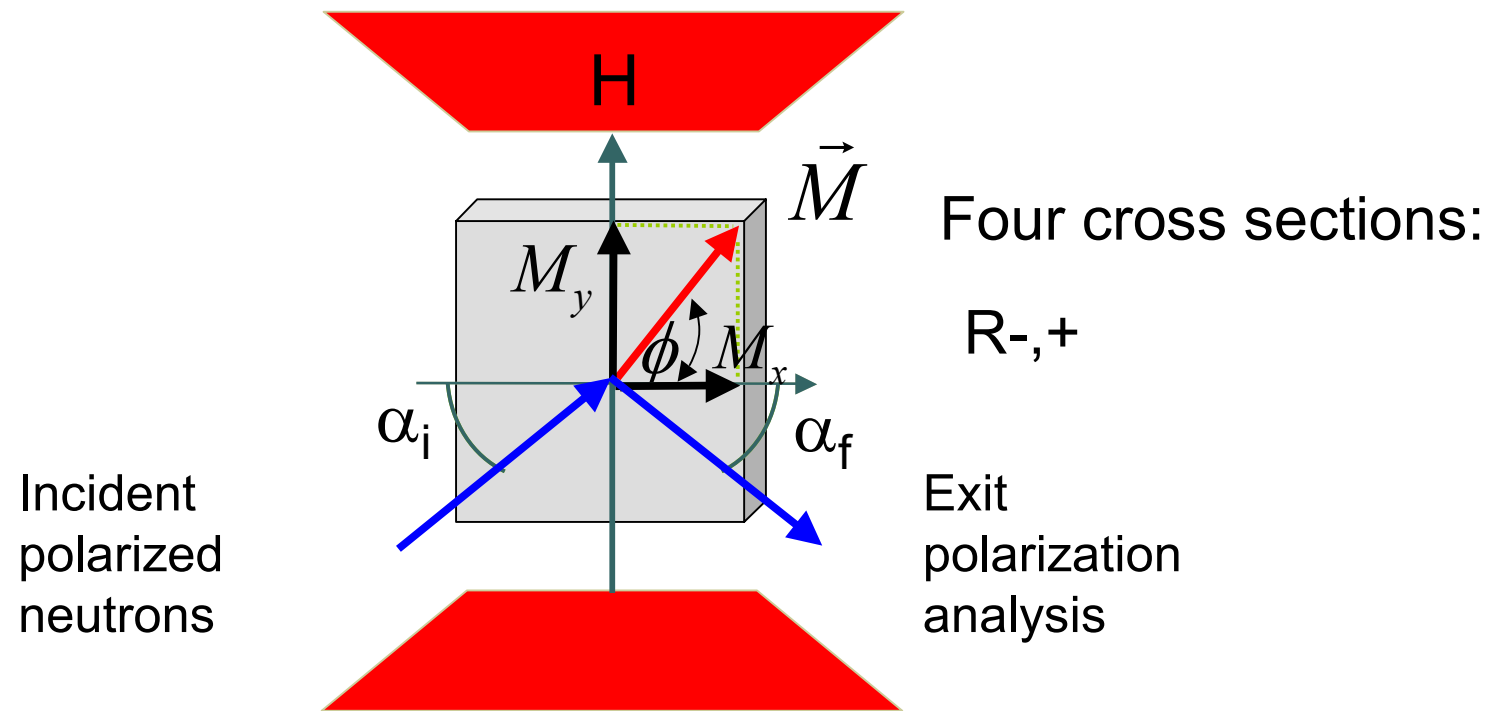
$$V = V_n \pm V_m = \frac{2\pi\hbar^2}{m} N_A (b_n \pm p_m)$$

Reflectivity from thin FM film

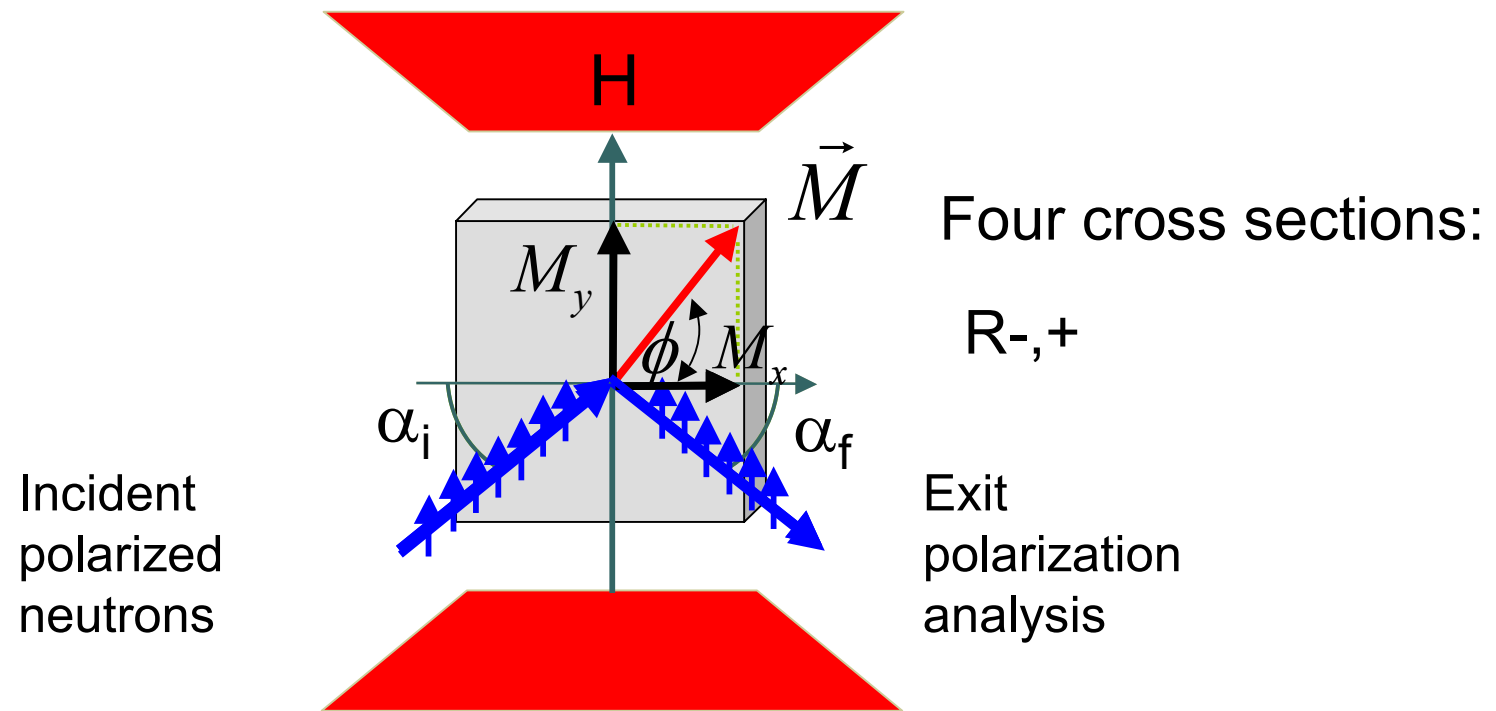


2. Polarized neutron reflectivity

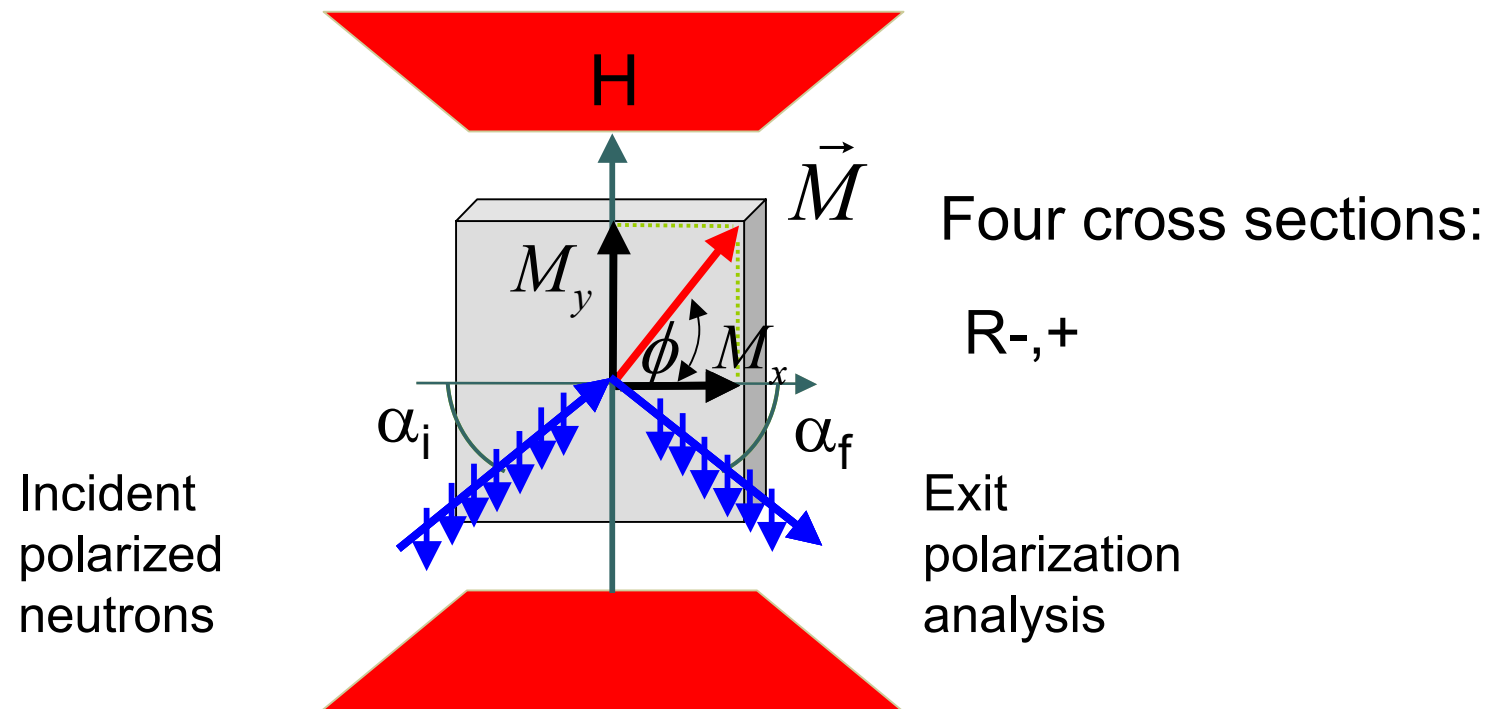
Polarized Neutron Reflectivity: The four cross-sections



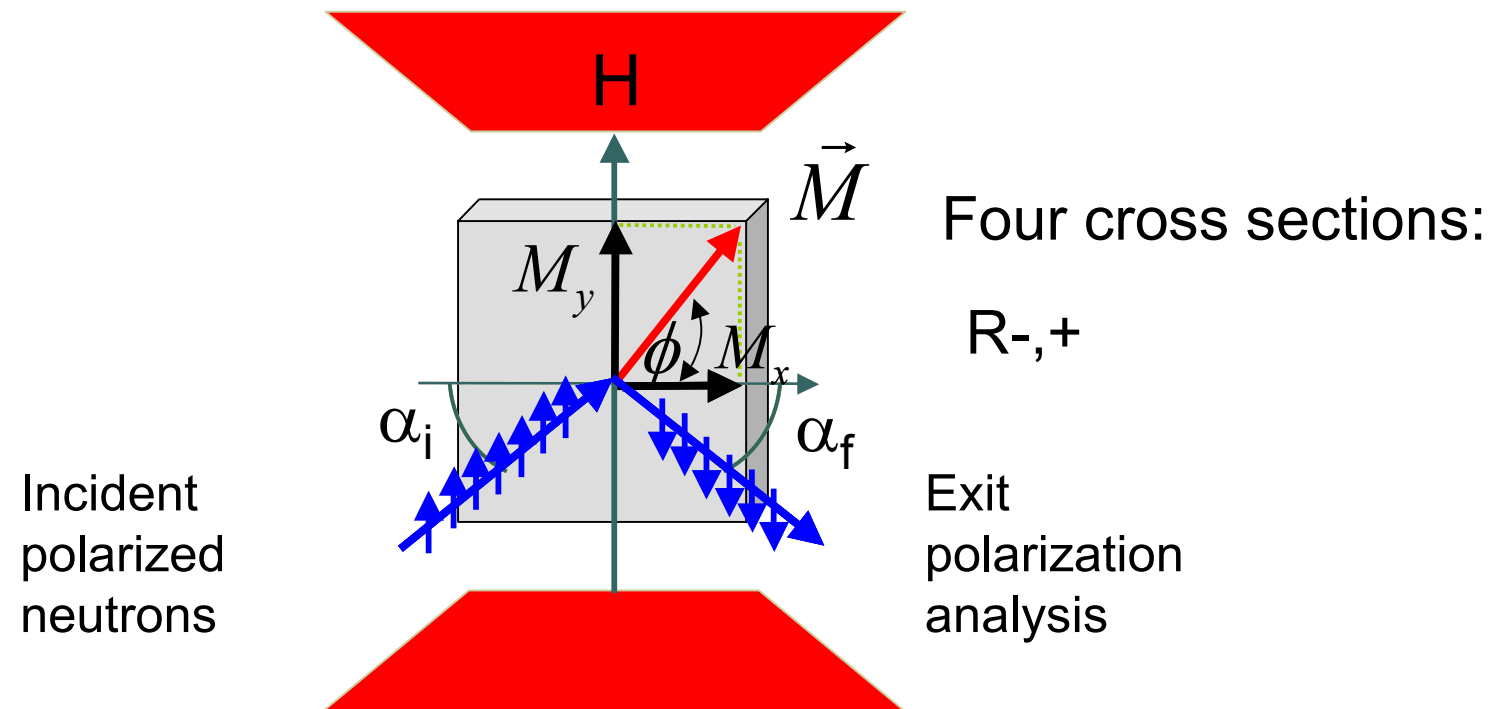
Polarized Neutron Reflectivity: The four cross-sections



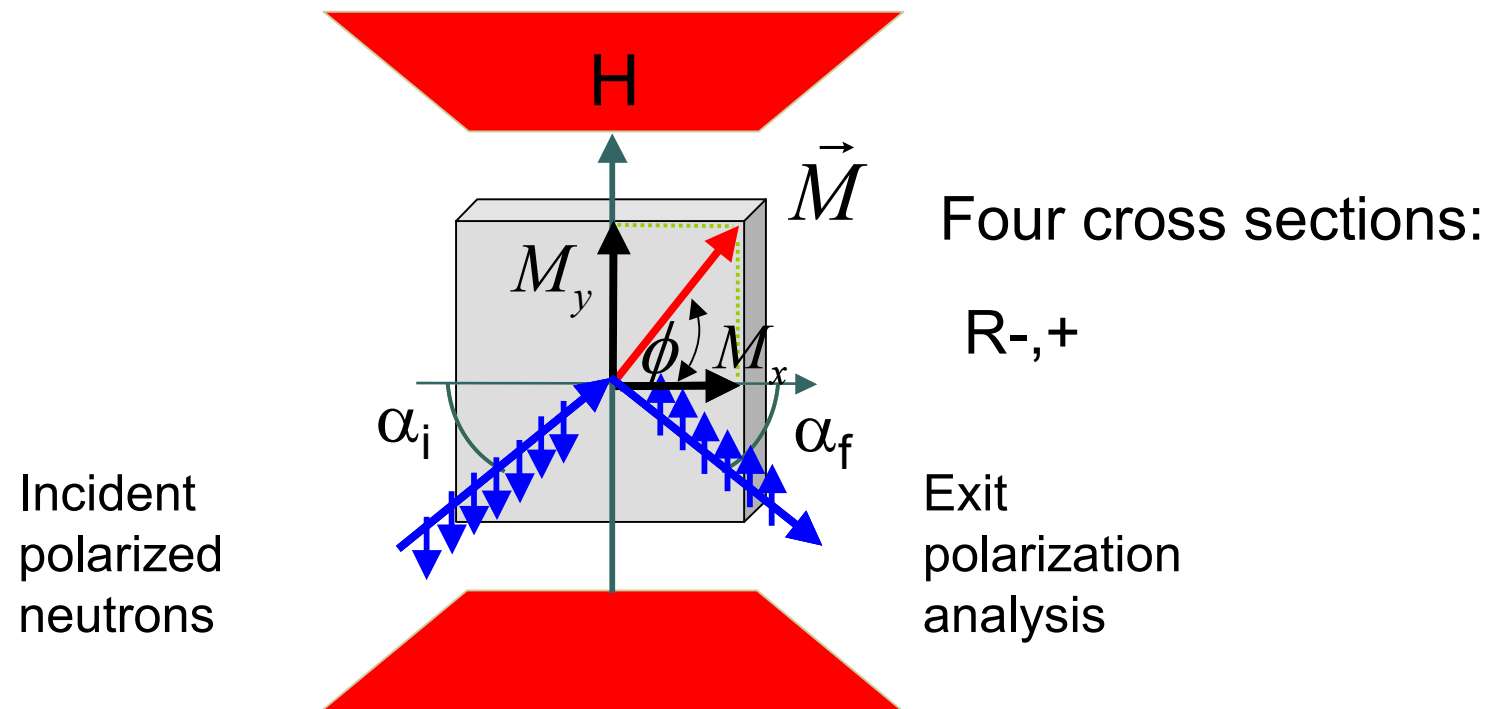
Polarized Neutron Reflectivity: The four cross-sections



Polarized Neutron Reflectivity: The four cross-sections



Polarized Neutron Reflectivity: The four cross-sections

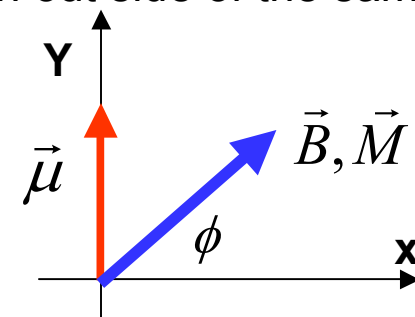


Magnetic potential of neutrons V_m (Spinor potential)



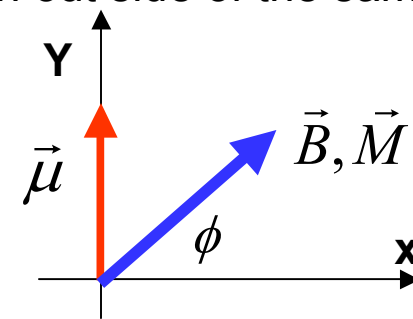
Magnetic potential of neutrons V_m (Spinor potential)

Initial state and polarization of neutron out side of the sample:

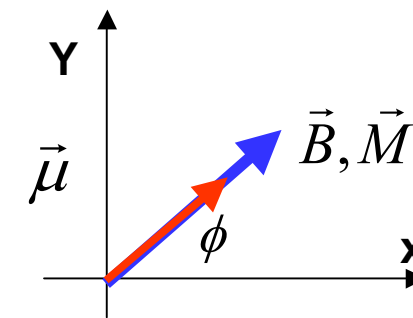


Magnetic potential of neutrons V_m (Spinor potential)

Initial state and polarization of neutron out side of the sample:



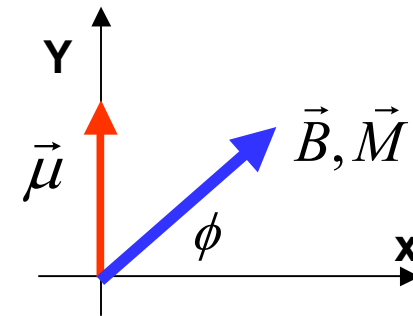
State and polarization of neutron inside of the sample:



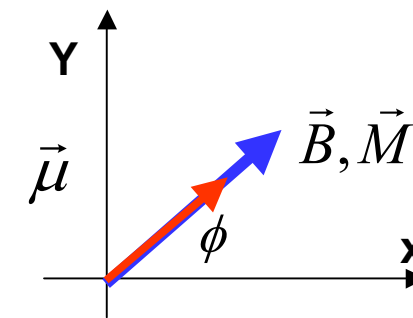
Magnetic potential of neutrons V_m (Spinor potential)

$$\begin{aligned} V_{m,Y}(z) &= -|\vec{\mu}_n| |\vec{B}(z)| \\ &= -4\pi |\vec{\mu}_n| |\vec{M}(z)| \\ &= -\frac{2\pi\hbar^2}{m_n} p_m(z) \end{aligned}$$

Initial state and polarization of neutron out side of the sample:



State and polarization of neutron inside of the sample:



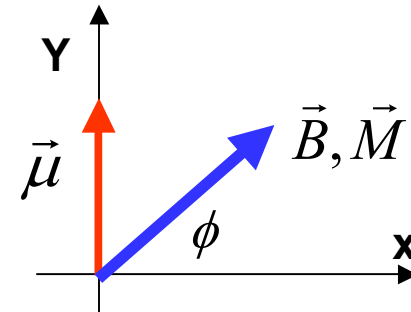
Magnetic potential of neutrons V_m (Spinor potential)

$$\begin{aligned} V_{m,Y}(z) &= -|\vec{\mu}_n| |\vec{B}(z)| \\ &= -4\pi |\vec{\mu}_n| |\vec{M}(z)| \\ &= -\frac{2\pi\hbar^2}{m_n} p_m(z) \end{aligned}$$

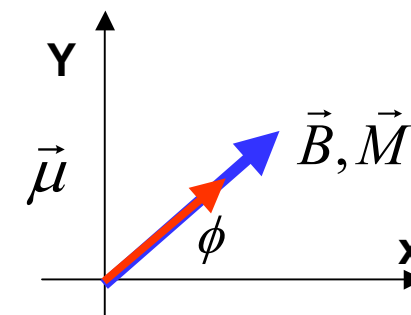
Total neutron – sample potential
(independent of the angle ϕ):

$$V = V_n \pm V_m = \frac{2\pi\hbar^2}{m_n} N_A (b_n \pm p_m)$$

Initial state and polarization of neutron out side of the sample:



State and polarization of neutron inside of the sample:



Schrödinger equation

Potential for polarized neutron scattering at magnetic samples:

$$V = \begin{pmatrix} V_{++} & V_{+-} \\ V_{-+} & V_{--} \end{pmatrix} = \frac{2\pi\hbar}{m_n} N_A \begin{pmatrix} b_{coh} + p_Y & p_X \\ p_X & b_{coh} - p_Y \end{pmatrix}$$

Inserting in Schrödinger equation:

$$\left(-\frac{\hbar^2}{2m} \frac{\partial^2}{\partial z^2} + V \right) \begin{pmatrix} \psi_+ \\ \psi_- \end{pmatrix} = E \begin{pmatrix} \psi_+ \\ \psi_- \end{pmatrix}$$

Yields the respective reflectivities R^{++} , R^{--} , R^{+-} , R^{-+} .

Reflectivity and Asymmetry

$$R^+ = R^{++} + R^{+-}$$

$$R^- = R^{--} + R^{-+}$$

$$R^+ - R^- = R^{++} - R^{--}$$

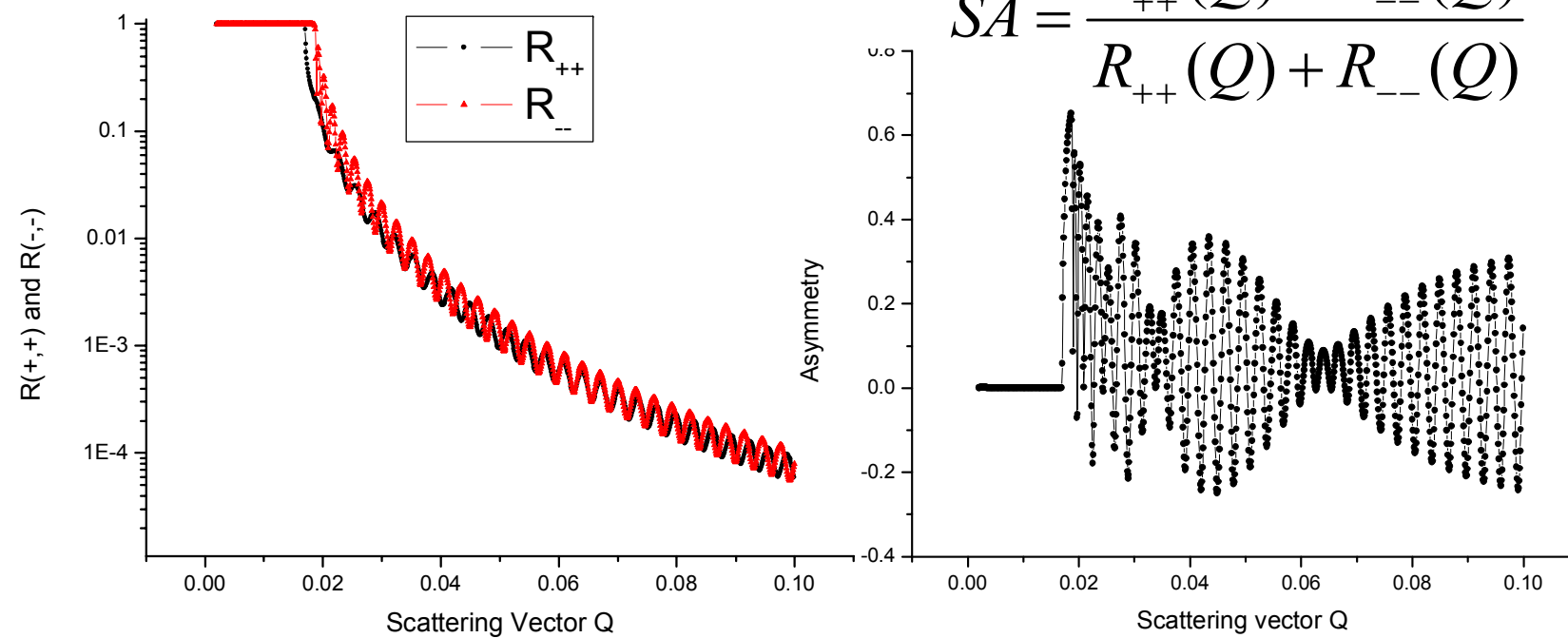
$$R^+ + R^- = R^{++} + R^{--} + 2R^{+-}$$

Spin Asymmetry:

$$SA = \frac{R^+ - R^-}{R^+ + R^-} = \frac{R^{++} - R^{--}}{R^{++} + R^{--} + 2R^{+-}}$$



Spin asymmetry (SA), single surface



Reflectivity and Asymmetry for single thin ferromagnetic film (Fe)

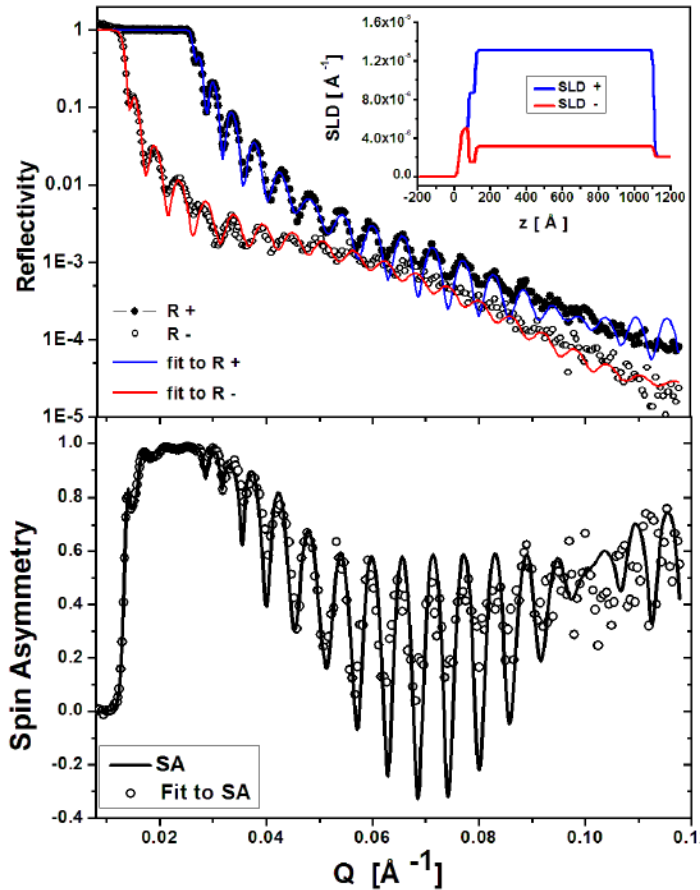
Reflectivities :

$$R^+ \text{ and } R^-$$

Spin Asymmetry :

$$SA = \frac{R^+ - R^-}{R^+ + R^-}$$

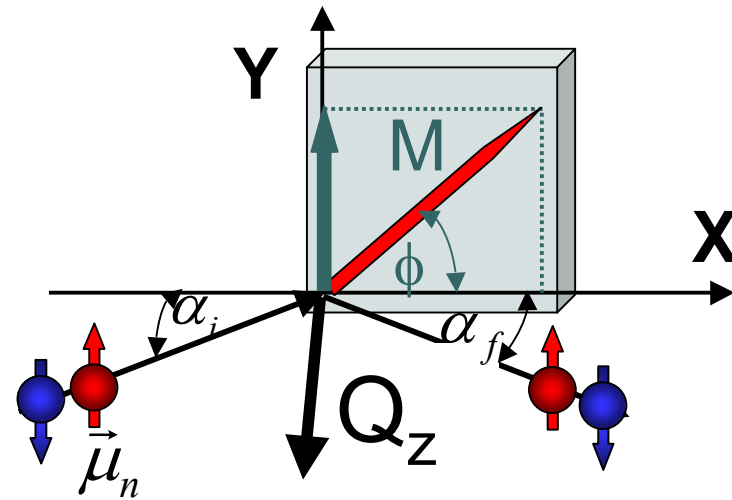
F. Radu et al. submitted



Non-spin flip (NSF) scattering

For an inclined magnetization follows:

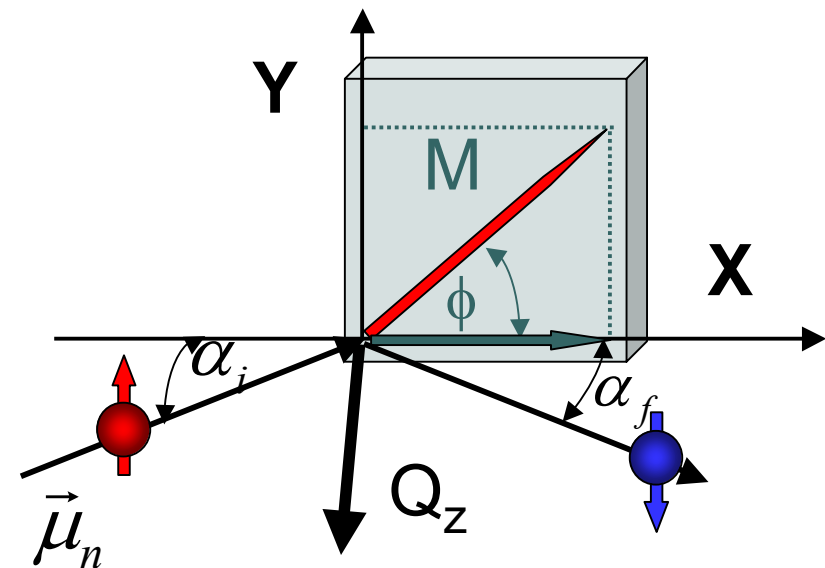
$$\begin{aligned} & SA(Q_z, \vec{M}(\phi)) \\ &= SA(Q_z, \vec{M}(0)) \sin \phi \\ &\sim \frac{M_Y}{|\vec{M}|} \end{aligned}$$



NSF – scattering measures the Y-component of the magnetization vector: M_Y (longitudinal component)

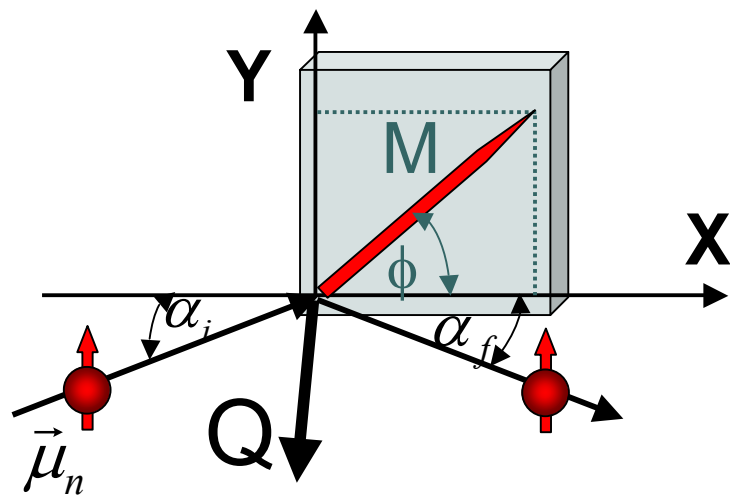
Spin-flip (SF) scattering

$$R^{+-} = R^{-+} \sim \cos^2 \phi \sim \left(\frac{M_x}{|\vec{M}|} \right)^2$$

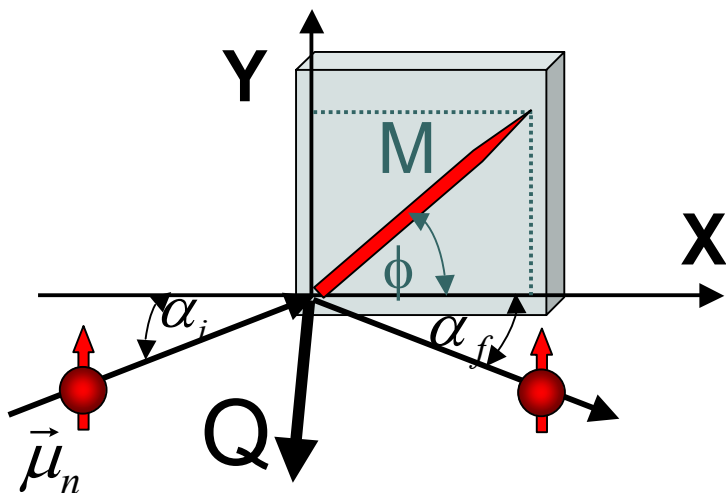


SF – scattering measures the X-component of the magnetization vector: M_x (transverse component)

Vector Magnetometry



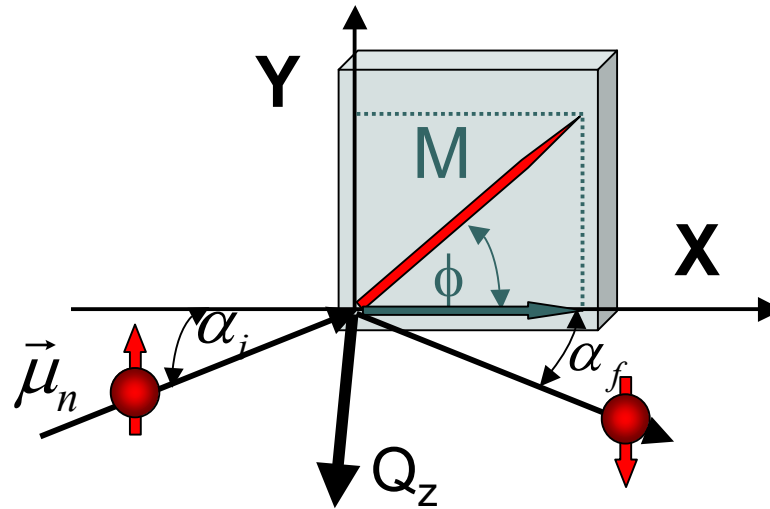
Vector Magnetometry



$$\phi = \arctan\left(\frac{M_y}{M_x}\right)$$

$$|\vec{M}| = \frac{M_y}{\sin \phi}$$

Selection rule for magnetic neutron scattering



$$\left(\frac{d\sigma}{d\Omega}(M(\vec{r}), Q_z) \right)_m = |M(\vec{r})|^2 \sin^2(Q_z, \vec{M}(\vec{r}))$$

Magnetization components parallel to the scattering vector are not visible to the neutrons!

Instrumention: two types

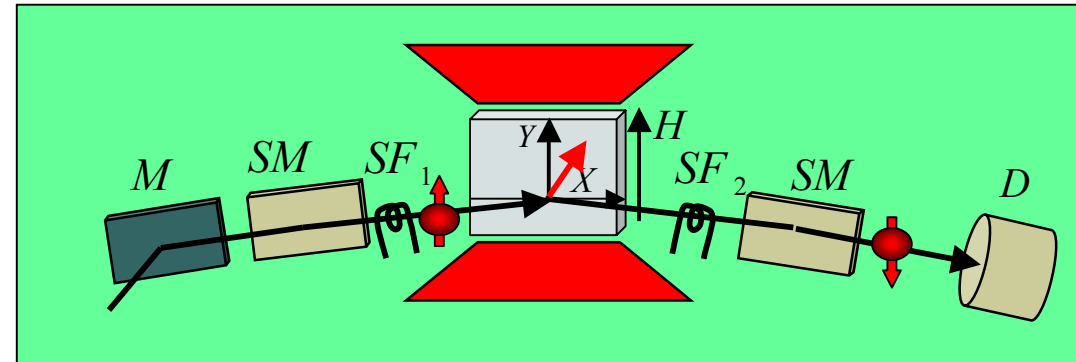


46



Instrumentation: two types

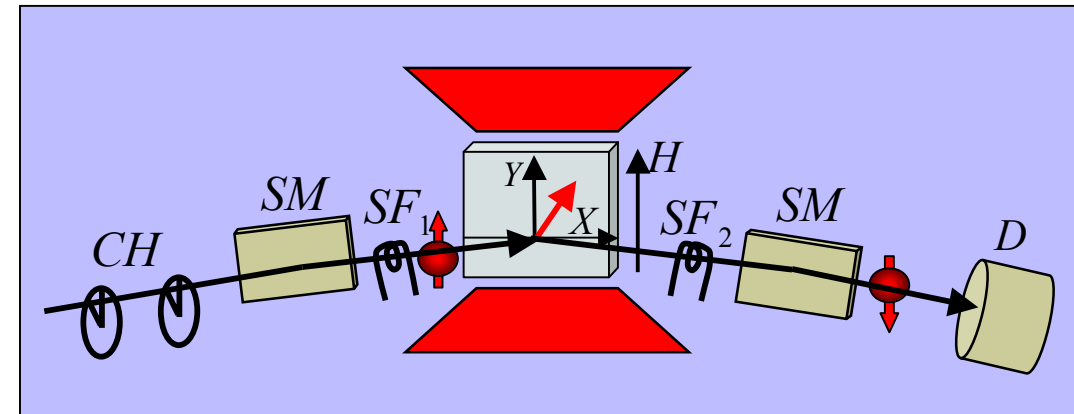
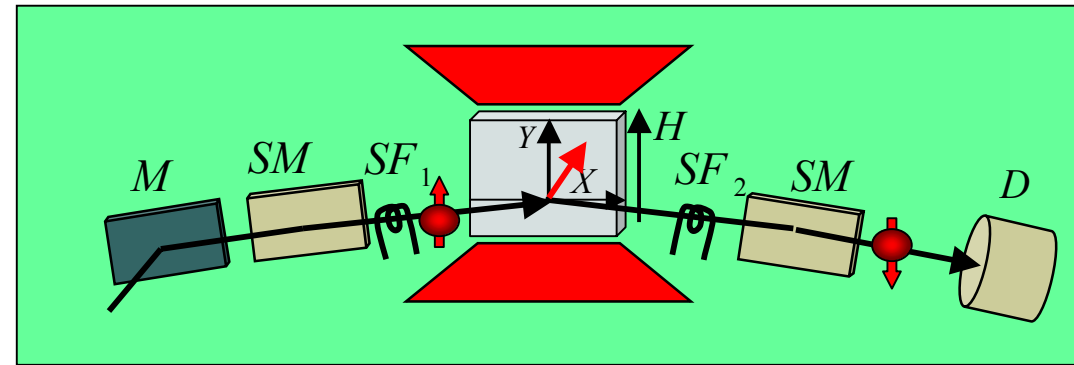
- Angle dispersive
- monochromatic beam
- scanning of α



Instrumentation: two types

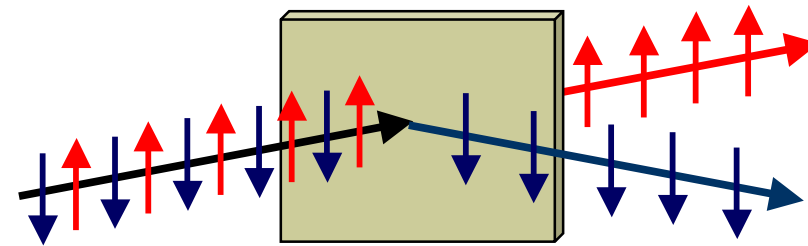
- Angle dispersive
- monochromatic beam
- scanning of α

- Wavelength dispersive
- White beam
- TOF method,
- fixed α



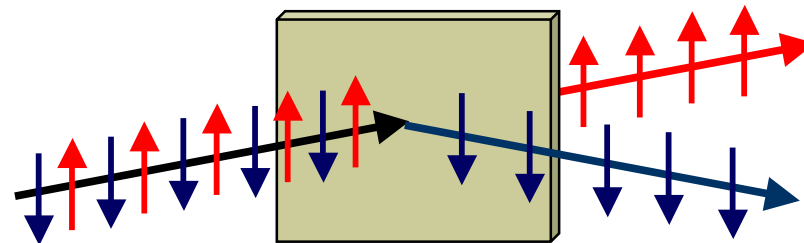
Polarizer, analyzer, and spin flipper

transmission
supermirror:

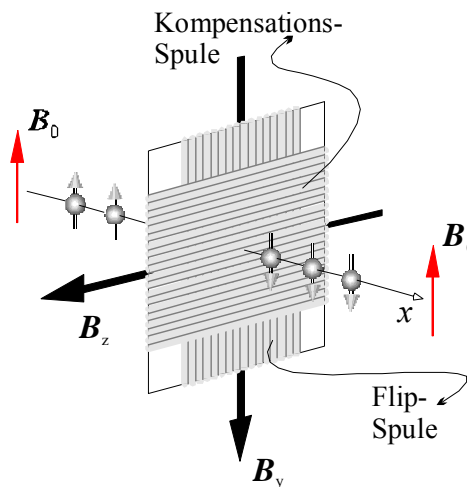


Polarizer, analyzer, and spin flipper

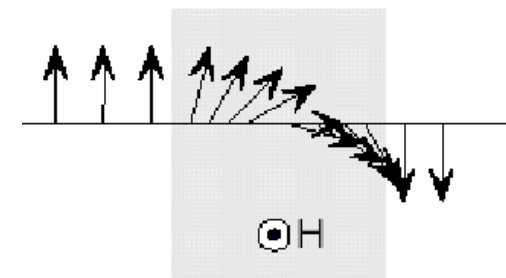
transmission
supermirror:



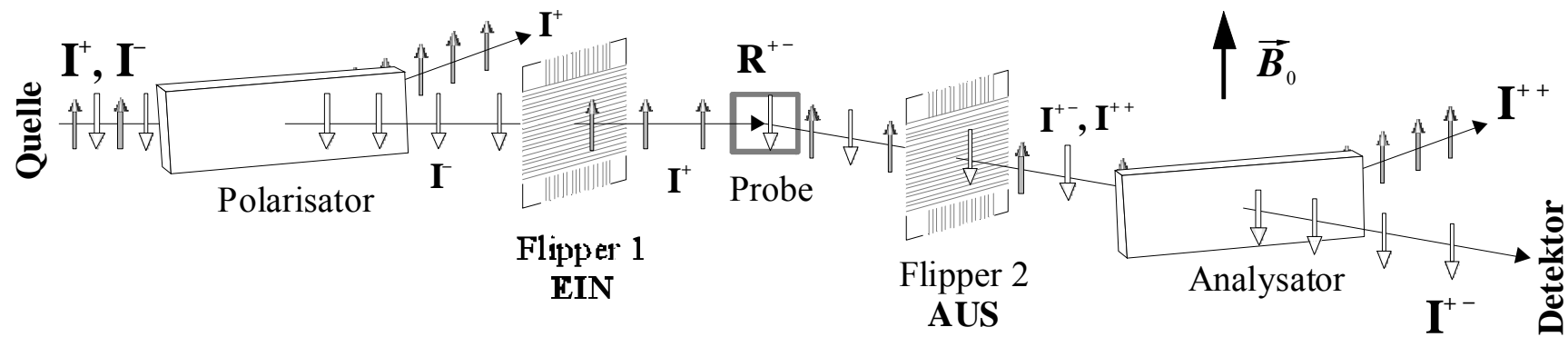
**Mezei spin- π
neutron–flipper**



Adiabatic spin rotation

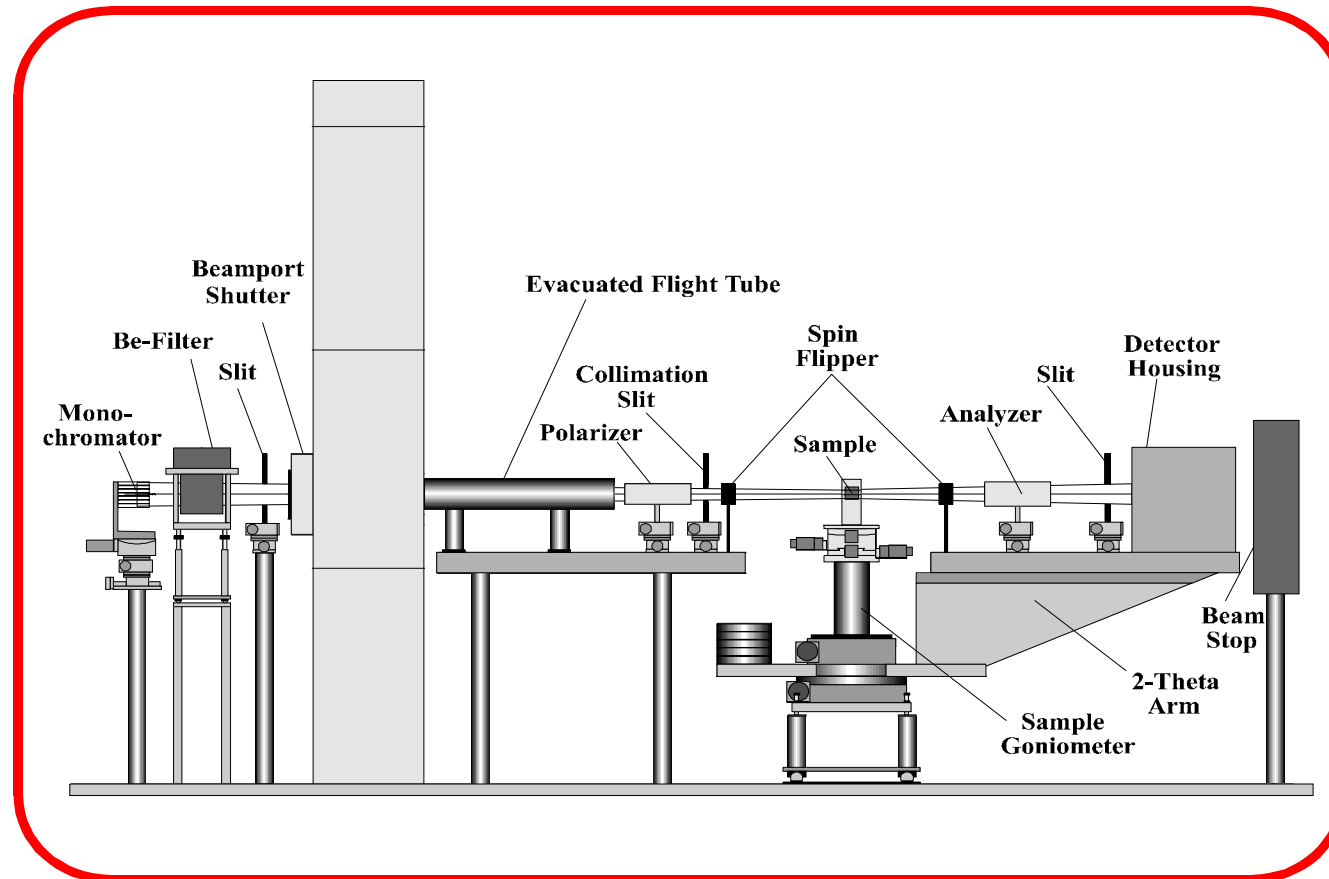


Schematics: neutron reflectometer with complete polarization analysis



This part is identical for angle dispersive and wavelength dispersive instruments

Schematics of an angle dispersive (fixed wavelength) reflectometer

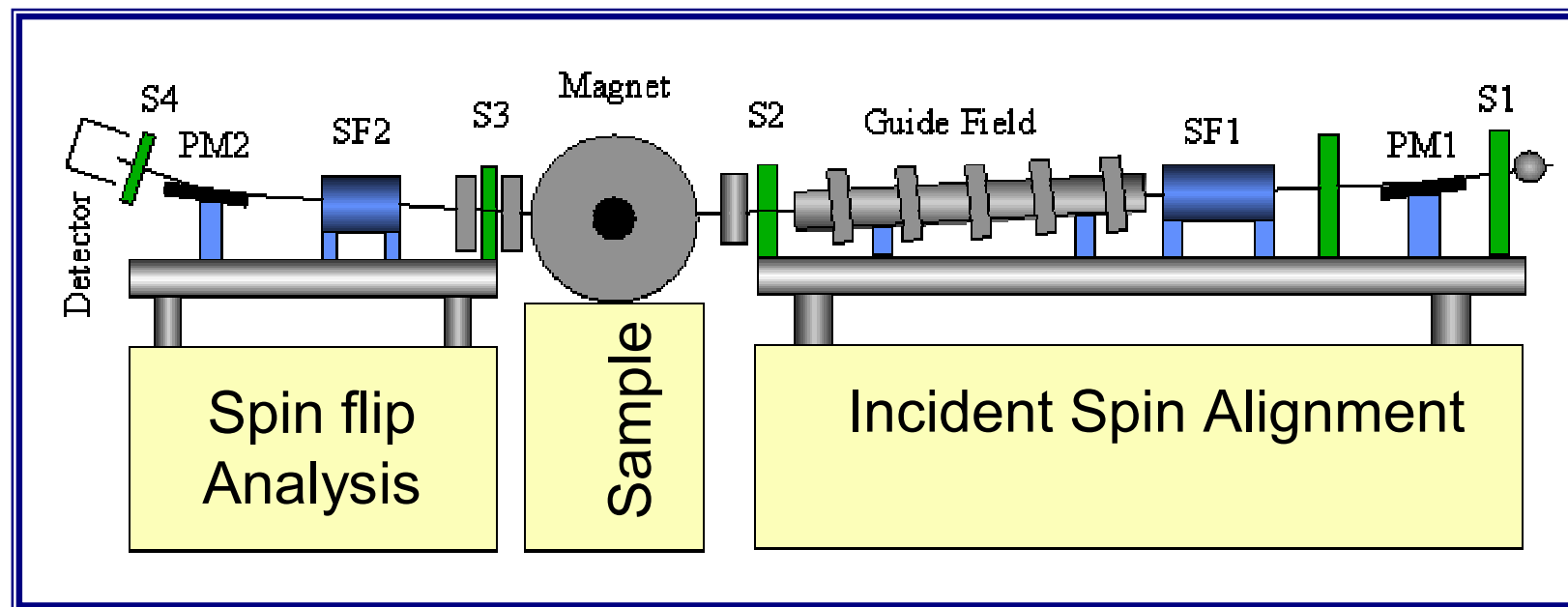


The ADAM Reflectometer at the ILL



<http://www.ill.fr/YellowBook/ADAM/>

TOF - PNR - CRISP-ISIS

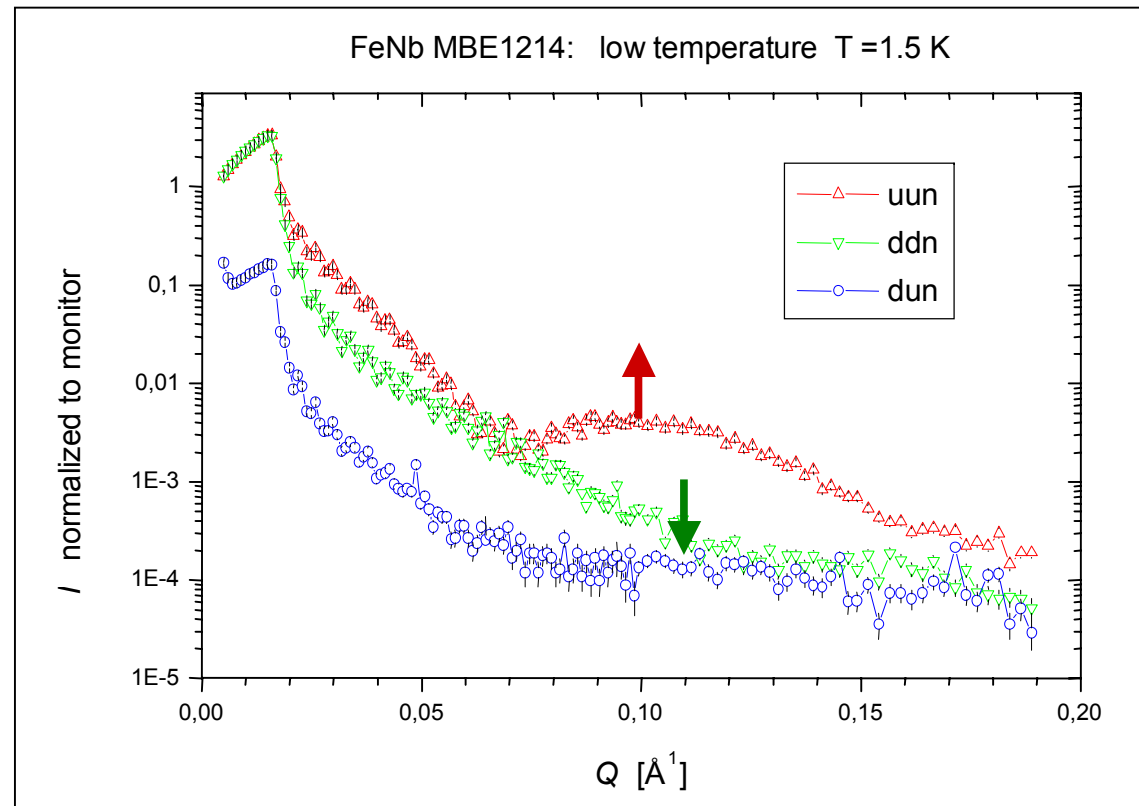
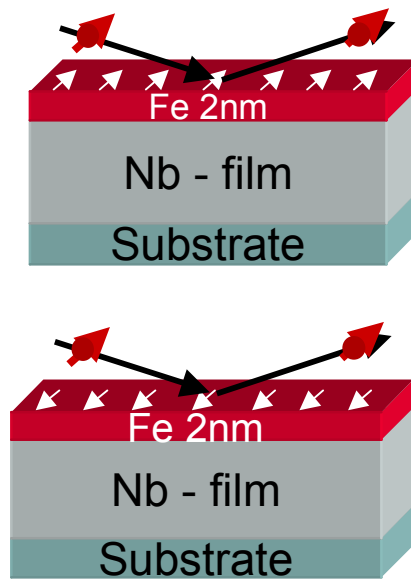


Examples

- a. Thin films
- b. Superlattices and roughness
- c. Exchange bias
- d. Magnetic patterns

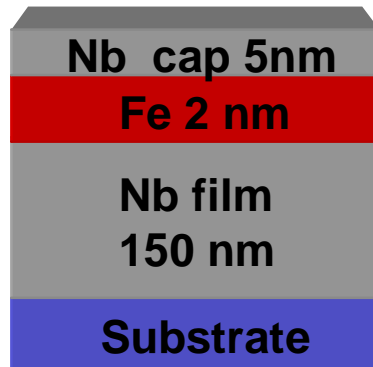


PNR of 2 nm Fe film on 150 nm Nb on sapphire substrate

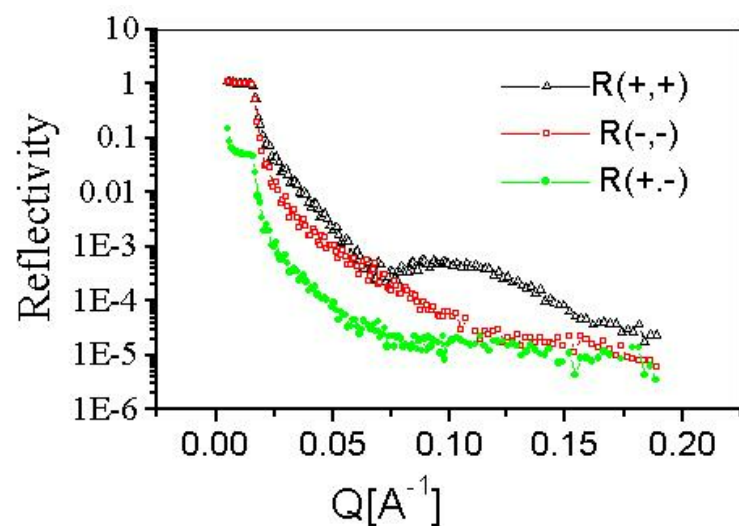
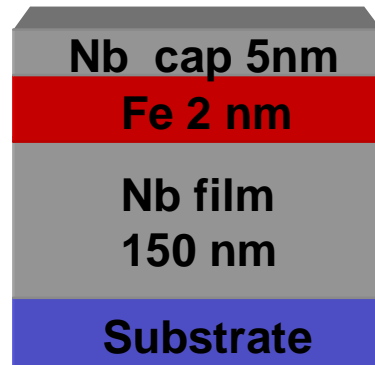


Amount of magnetic material: 10^{-3} emu

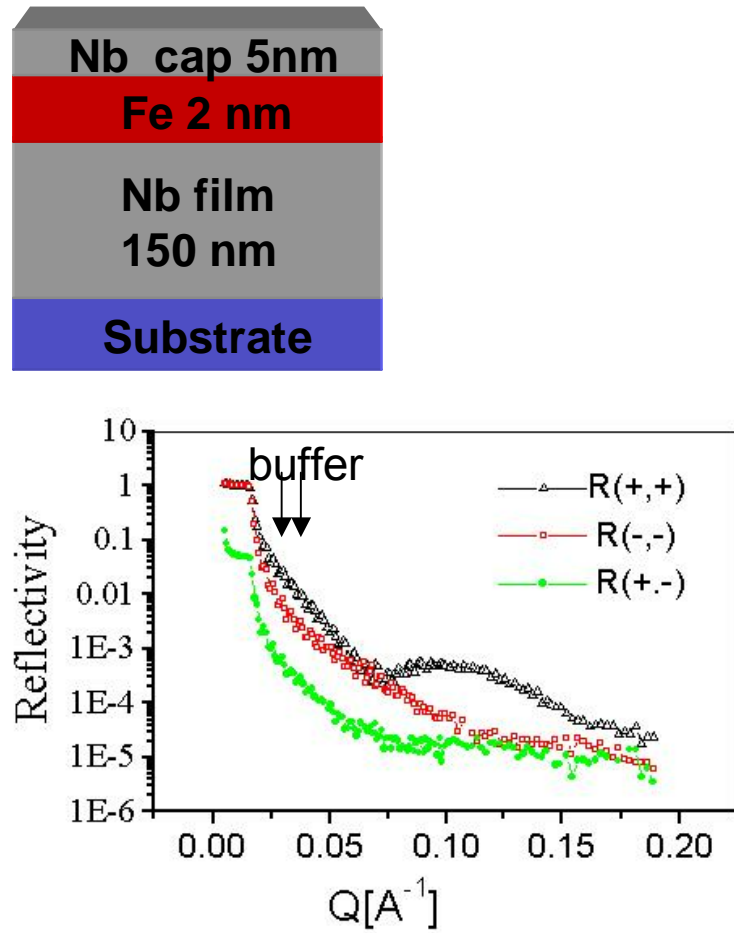
Interpretation of results



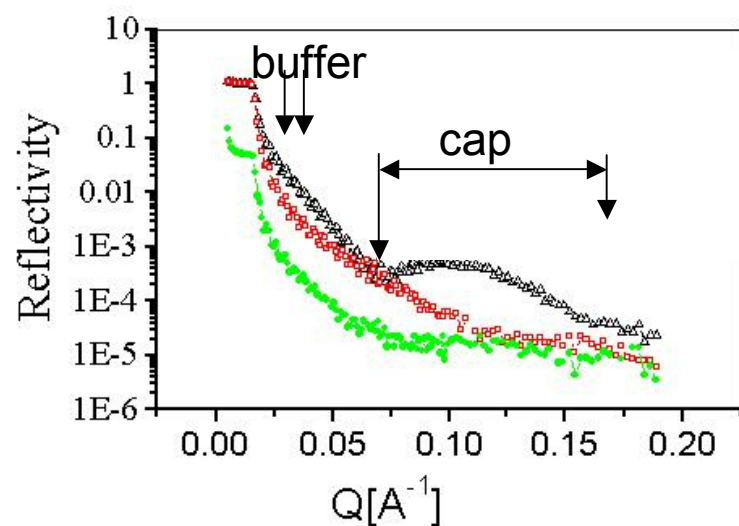
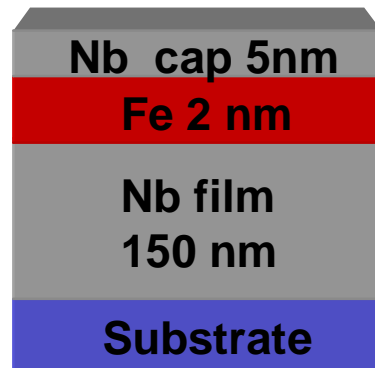
Interpretation of results



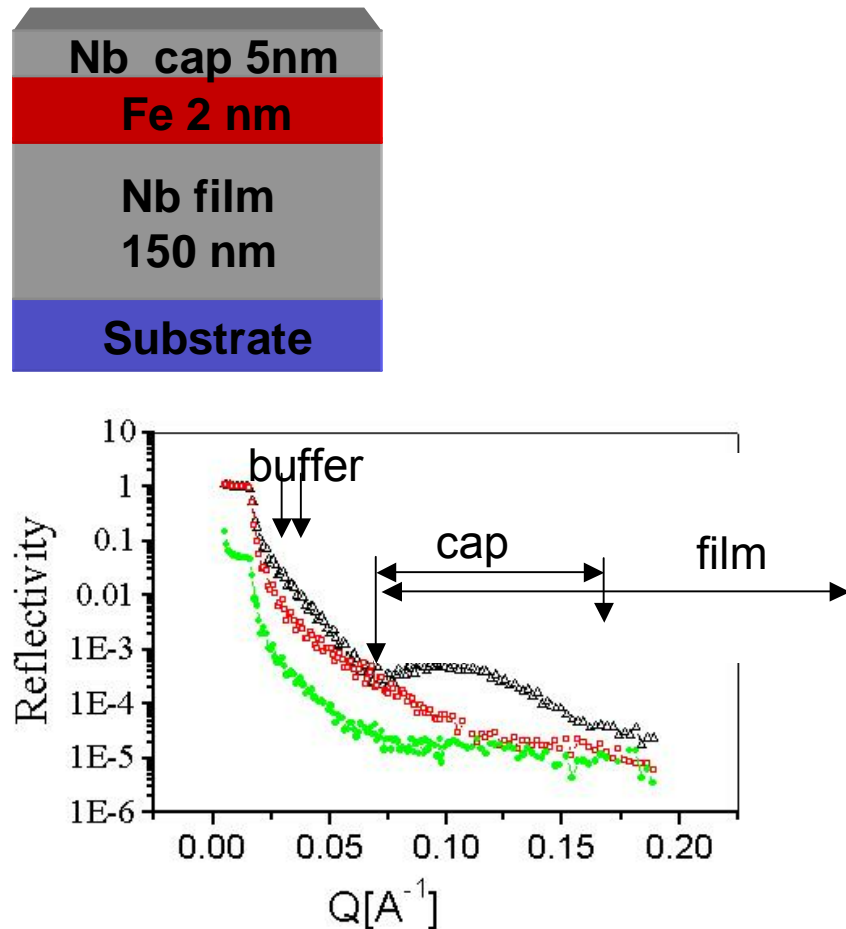
Interpretation of results



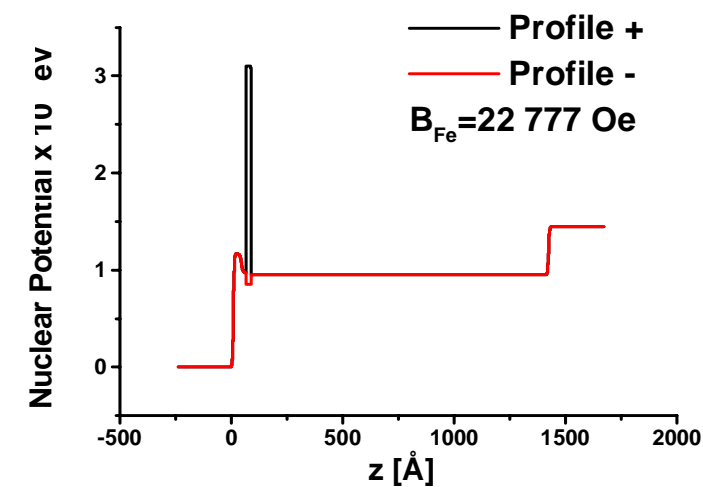
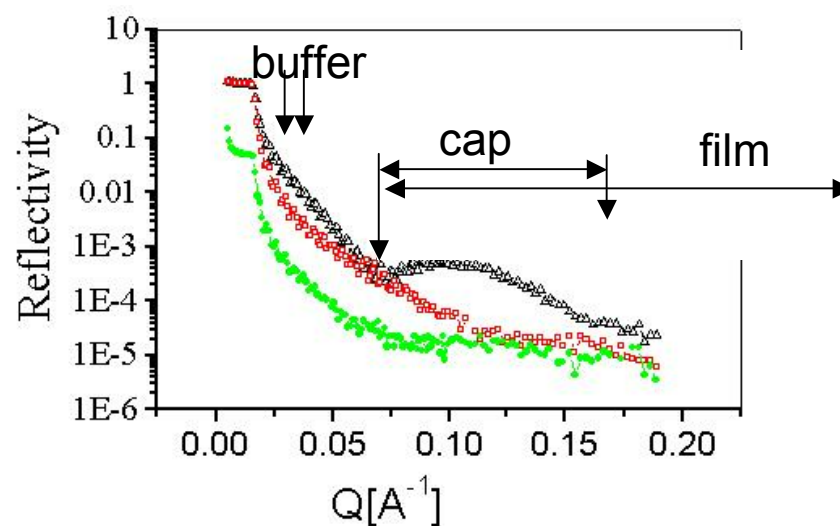
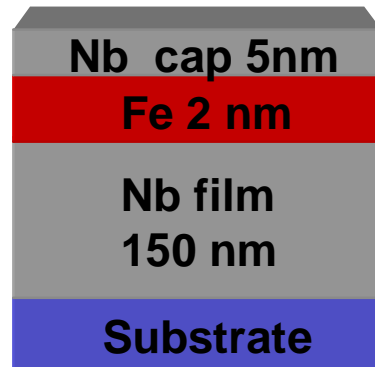
Interpretation of results



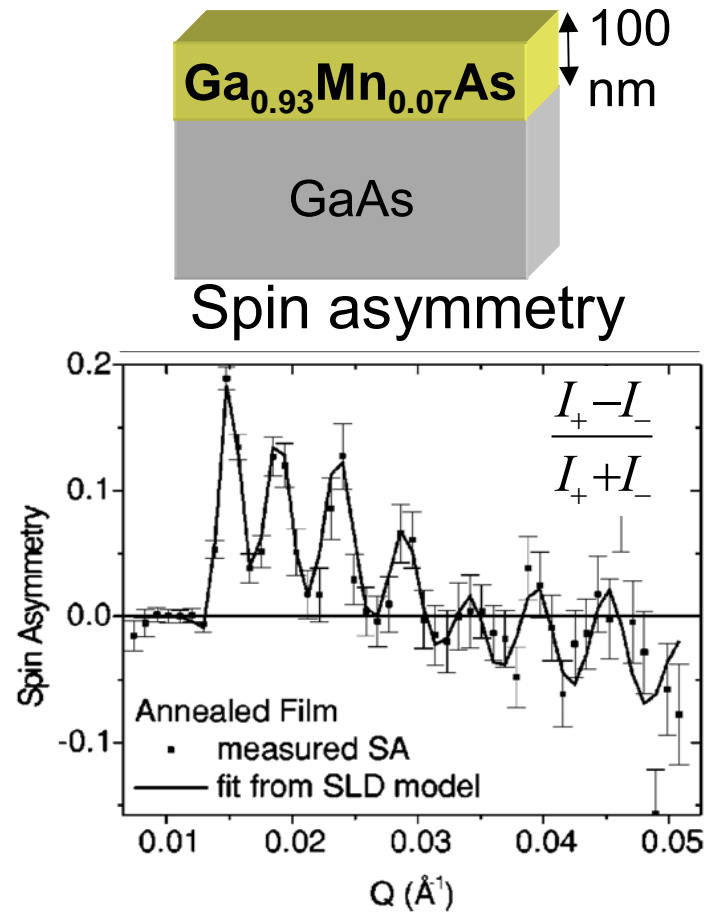
Interpretation of results



Interpretation of results

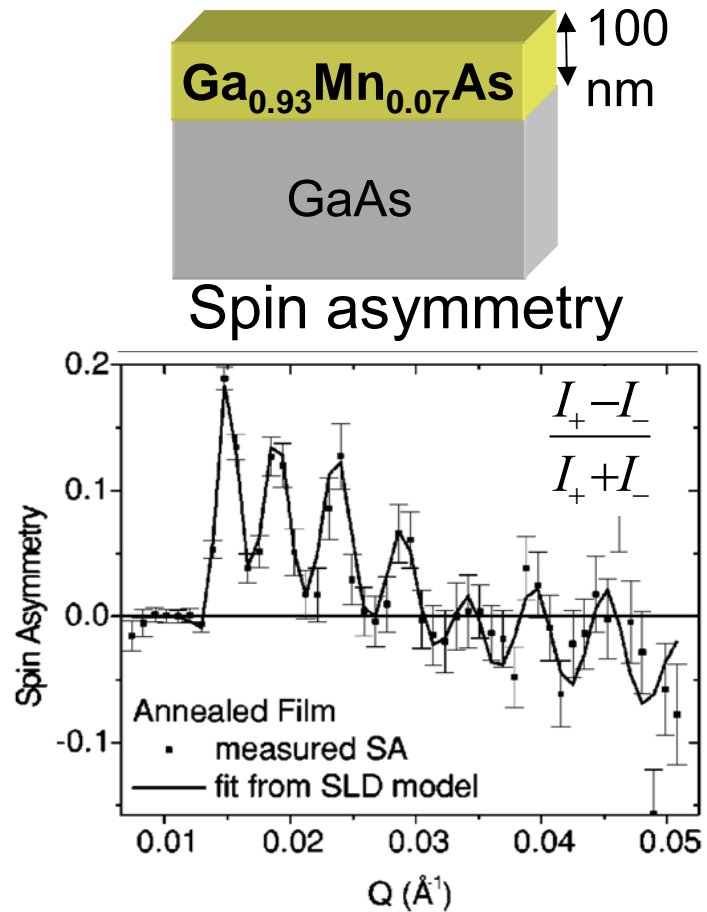


Nuclear and magnetic density profile in (GaMn)As

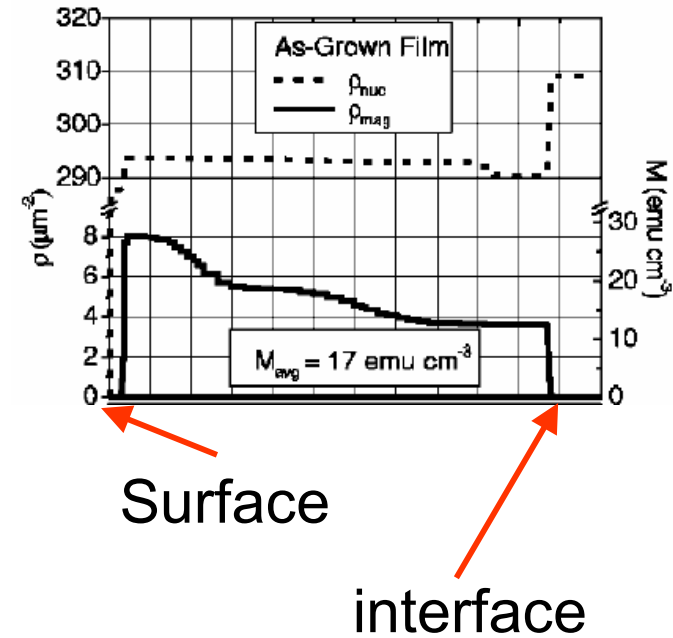


B.J. Kirby et al. Phys. Rev. B **69** (2004) 081307

Nuclear and magnetic density profile in (GaMn)As

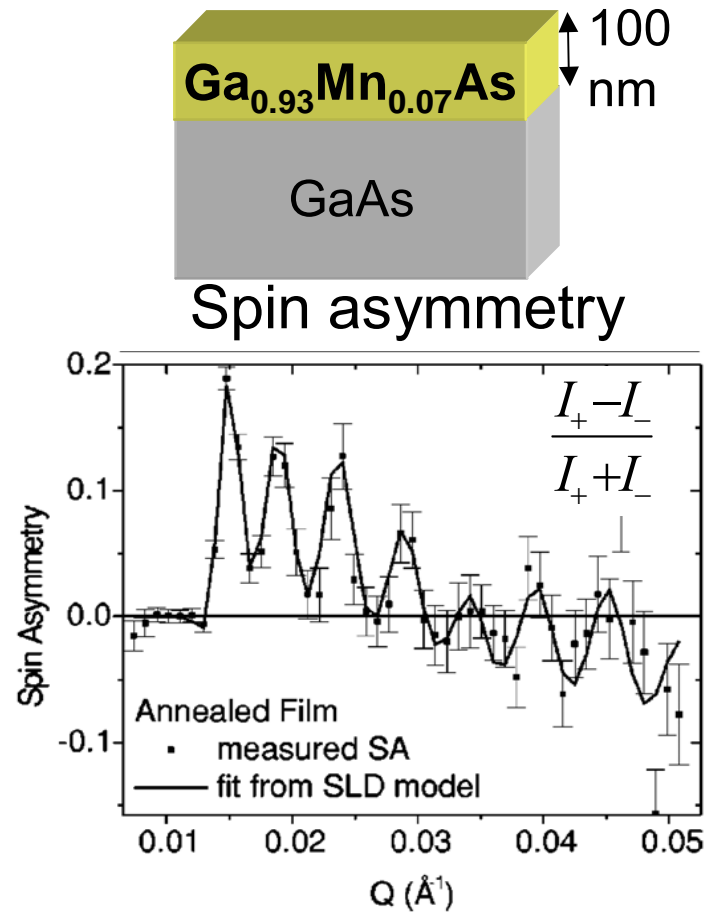


before
annealing



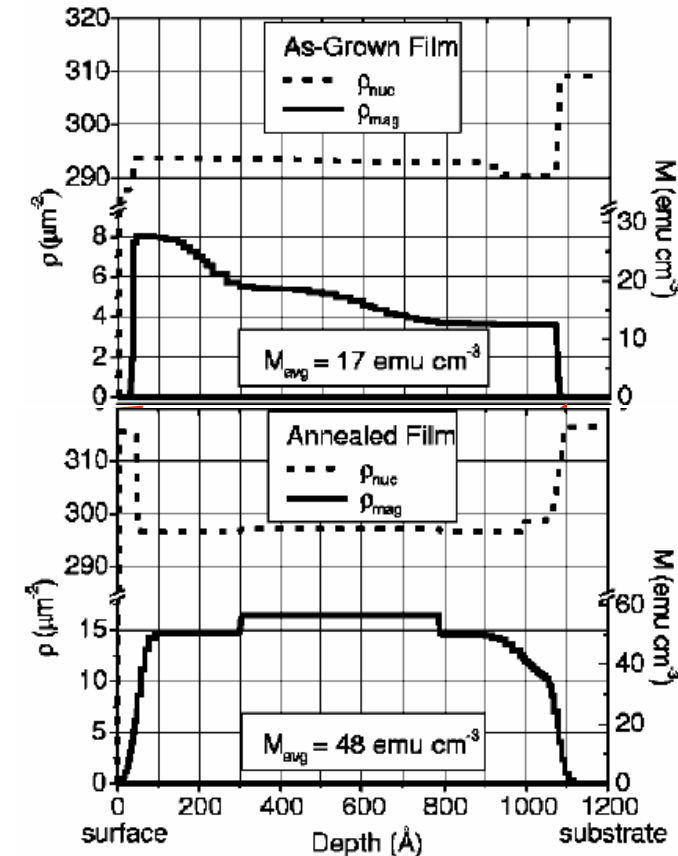
B.J. Kirby et al. Phys. Rev. B **69** (2004) 081307

Nuclear and magnetic density profile in (GaMn)As



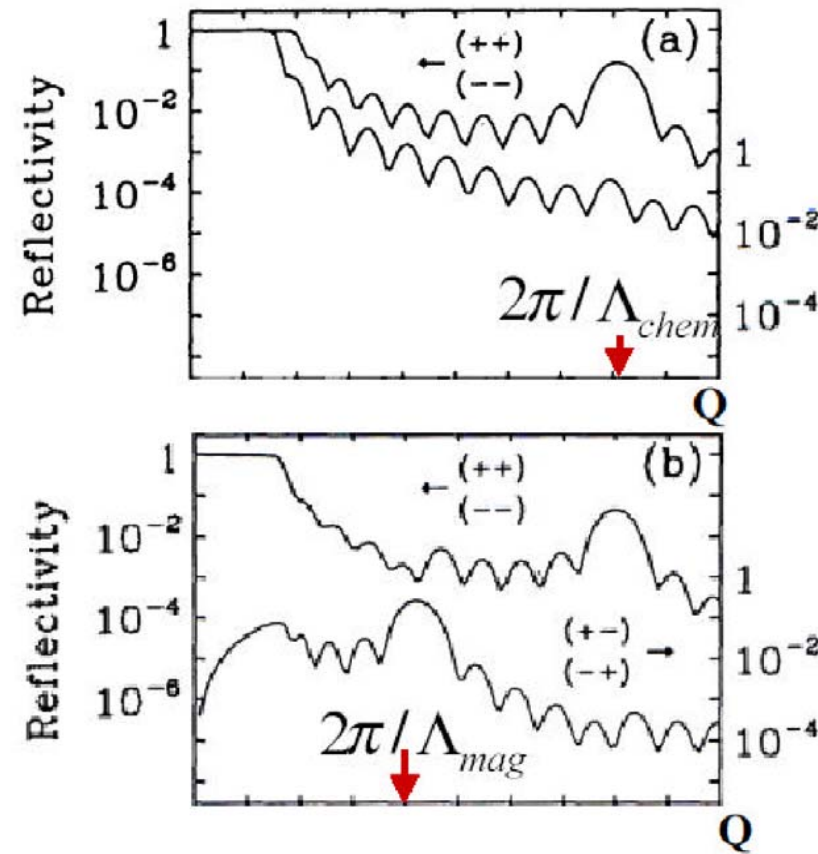
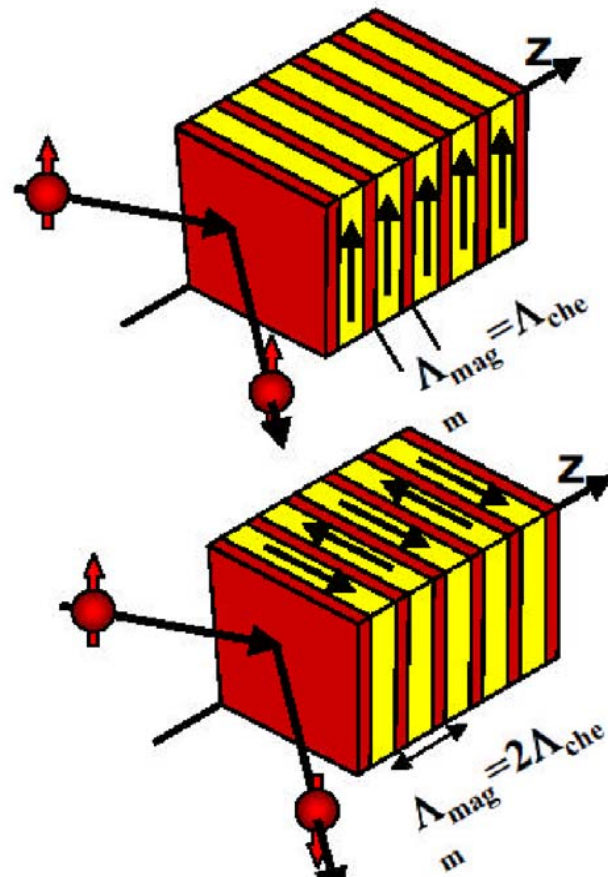
before
annealing

after
annealing
at 280°C
for 1 h

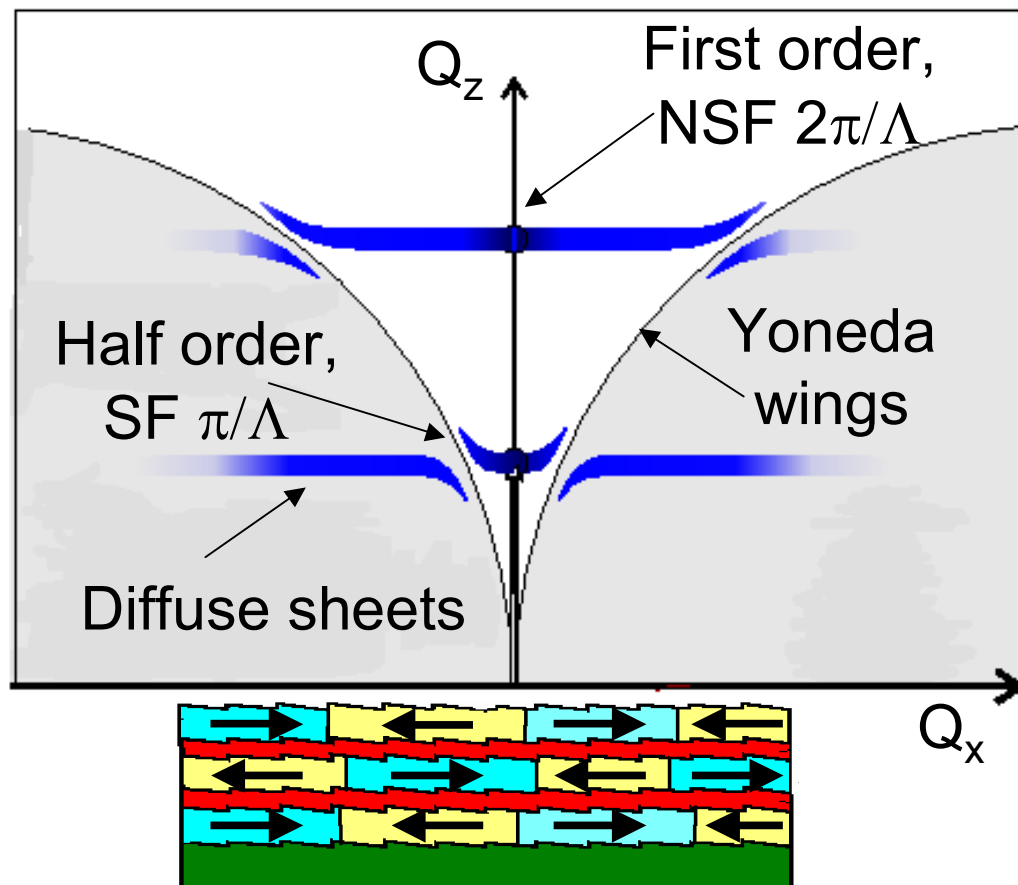


B.J. Kirby et al. Phys. Rev. B **69** (2004) 081307

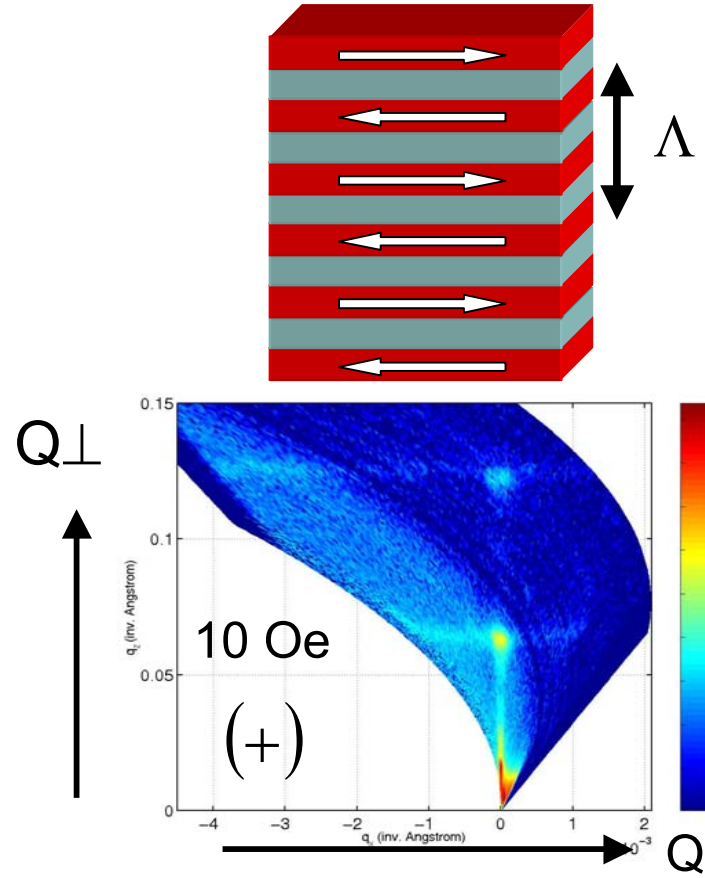
PNR from model-spinstructures in magnetic multilayers



Reciprocal space maps in the small angle regime

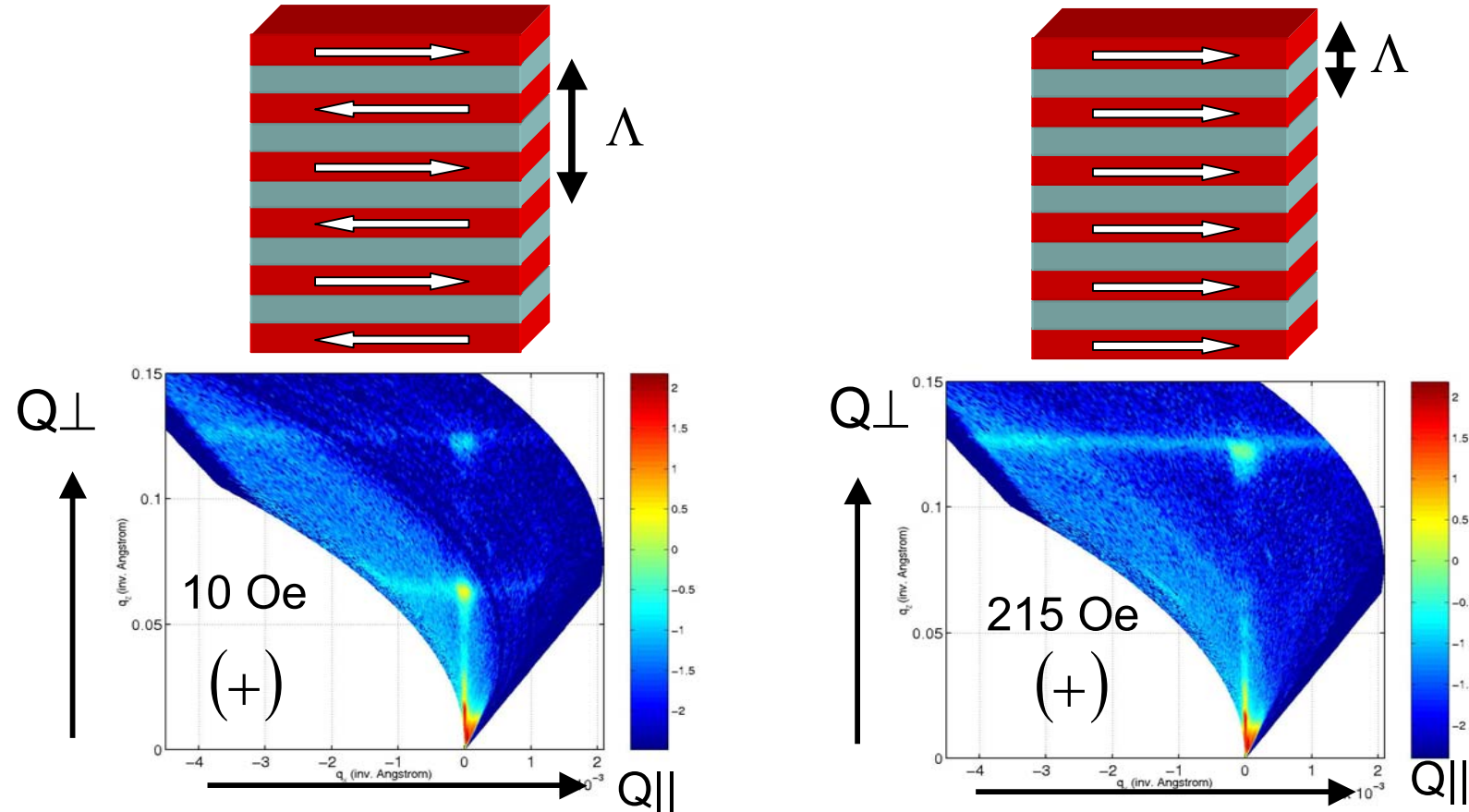


Exchange coupling in [Fe_{0.43}Cr_{0.57}(24Å)/Cr(28Å)]



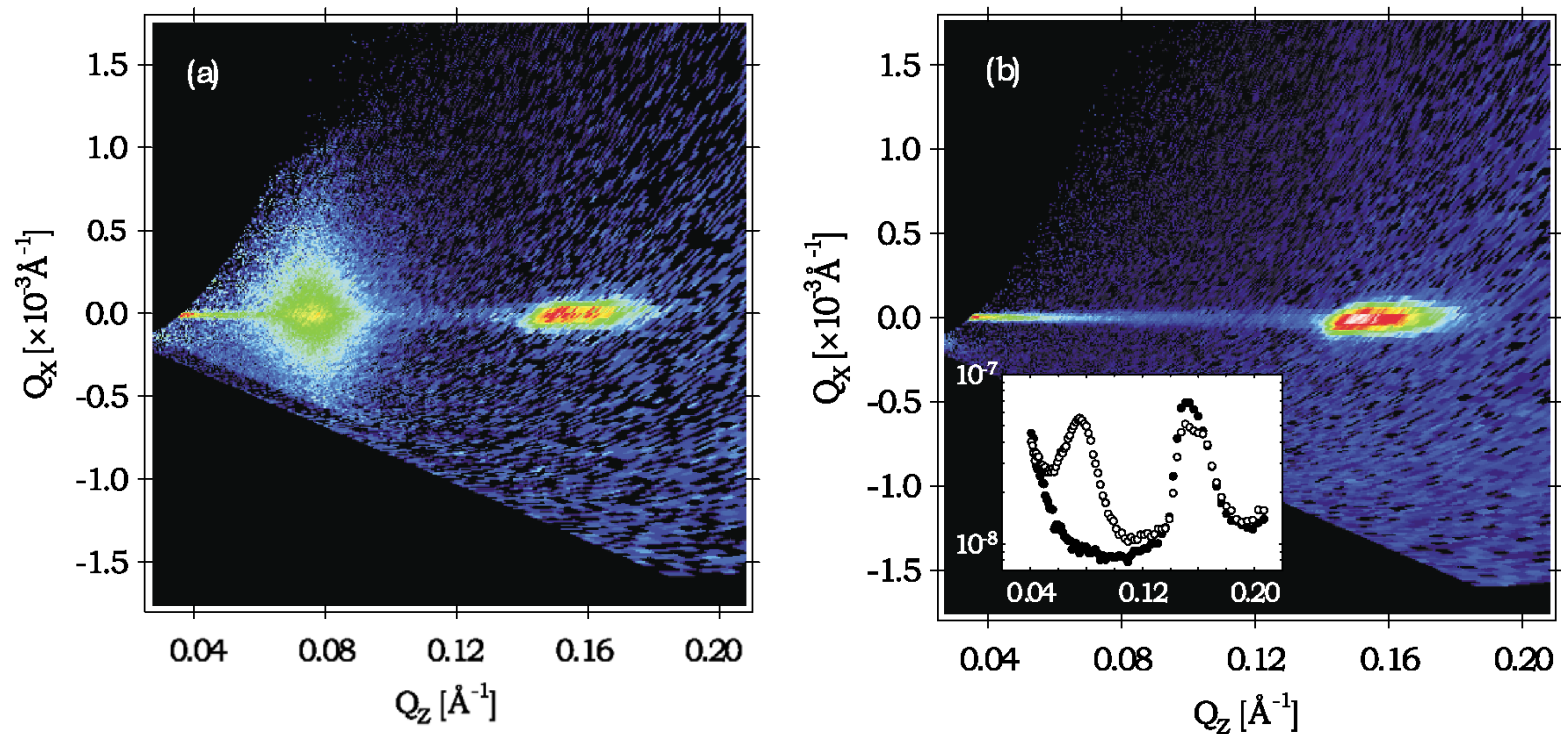
R. Siebrecht, et al. 2000

Exchange coupling in [Fe_{0.43}Cr_{0.57}(24Å)/Cr(28Å)]



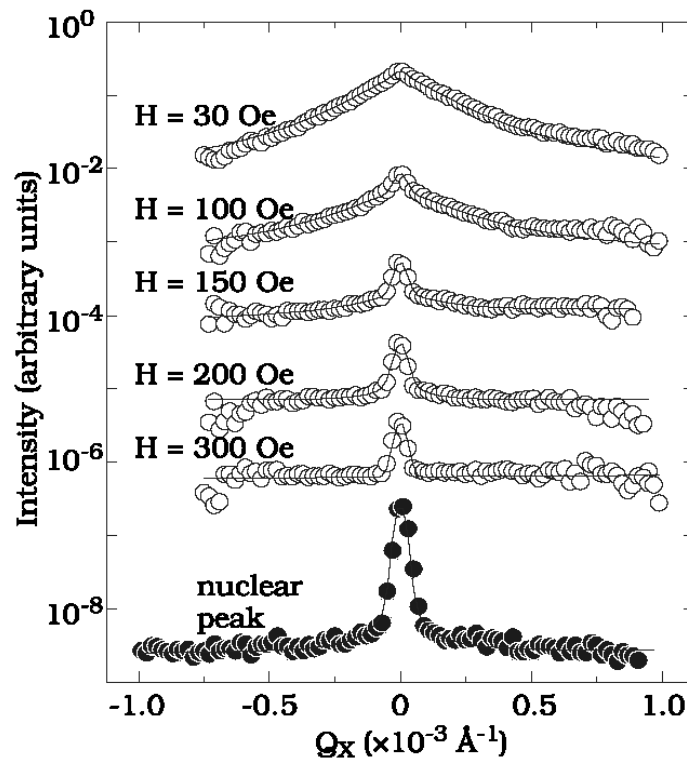
R. Siebrecht, et al. 2000

Magnetic roughness in Co/Cu superlattices



S. Langridge, J. Schamlian, C.H. Marrows, D.T. Dekadjevi, B.J. Hickey, PRL **85**, 4964 (2000).

Transverse scans across half-order AF peak



$$S_{Diff}(Q) = DW \int d^2\vec{r} e^{i\vec{Q}_\parallel \cdot \vec{r}} [s + m + sm]$$

s = structural roughness

m = domain distribution roughness

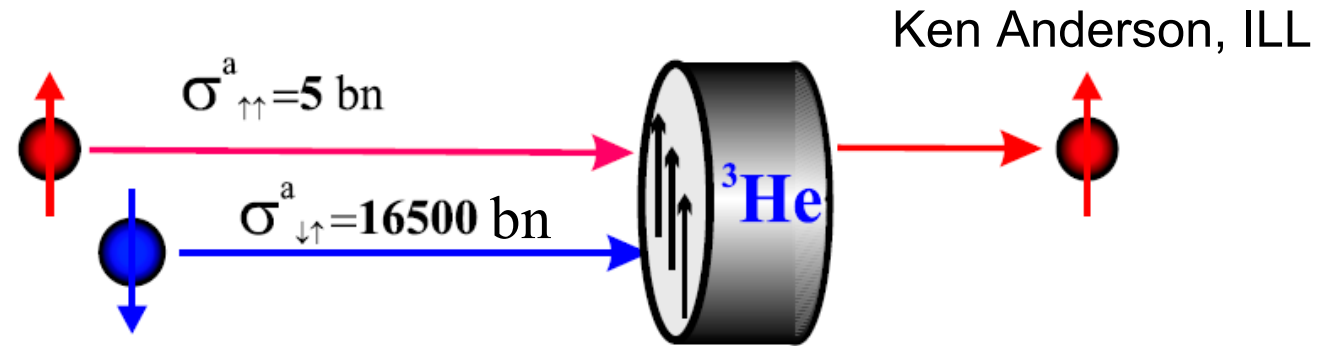
sm = cross term contains magnetic roughness

Diffuse scattering due to:

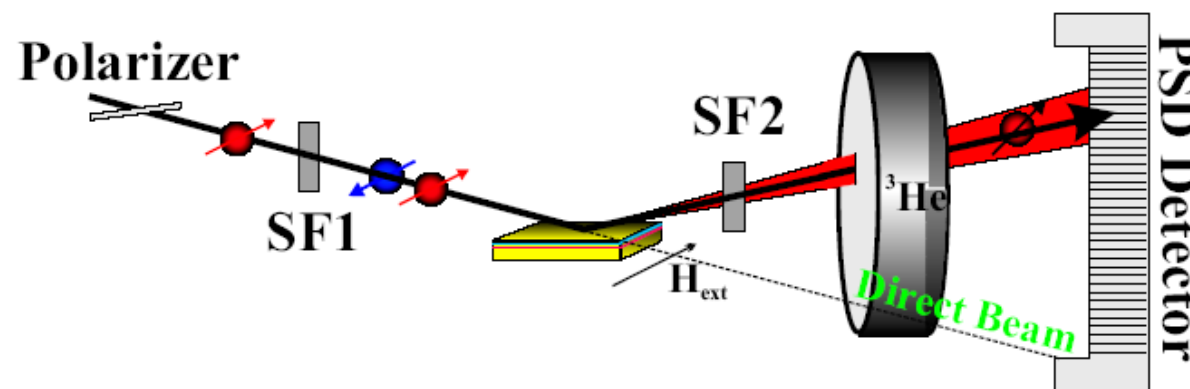
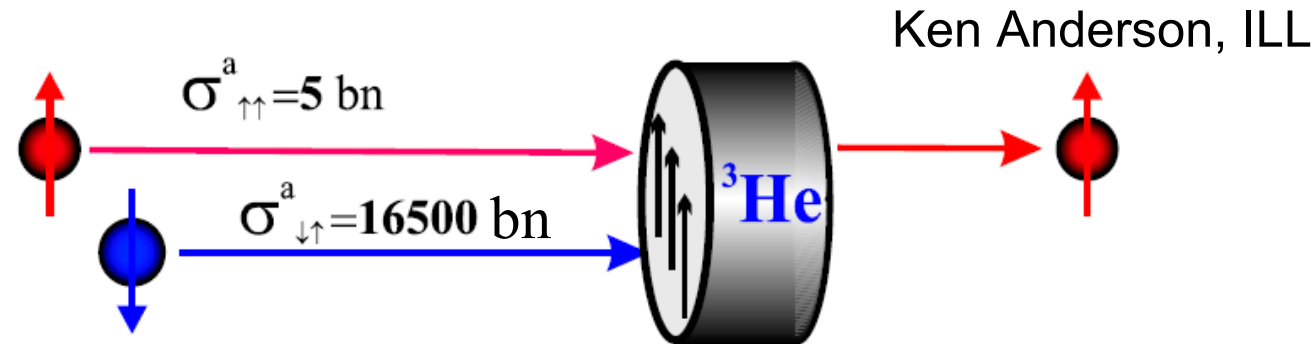
- domain size distribution
- orientational domain distribution

Diffuse scattering diminishes in high fields

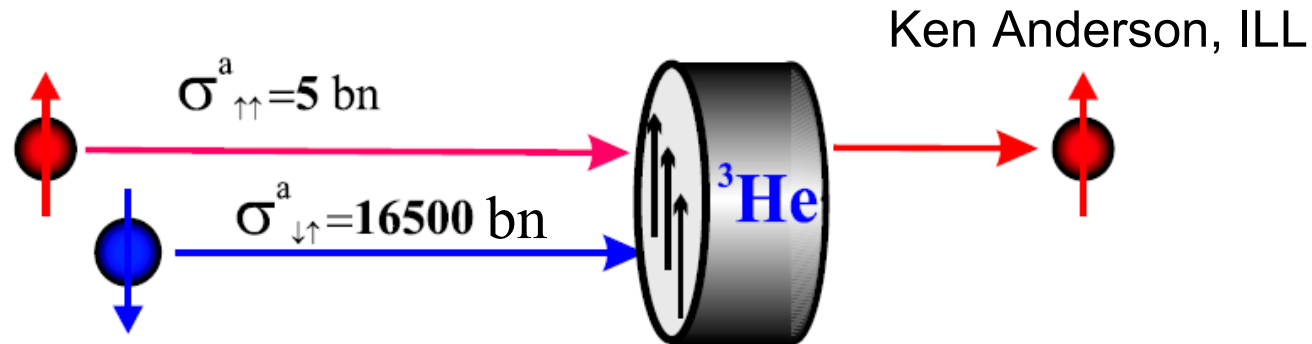
New ${}^3\text{He}$ Spin-Filter



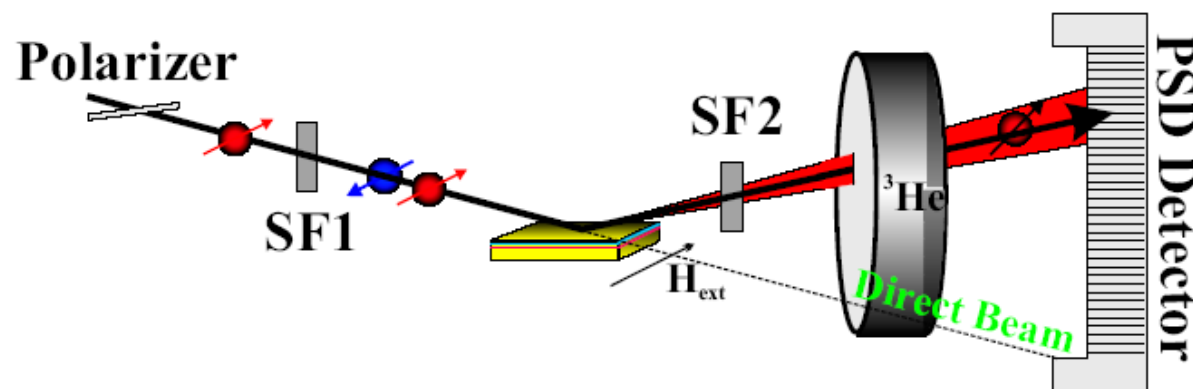
New ${}^3\text{He}$ Spin-Filter



New ${}^3\text{He}$ Spin-Filter

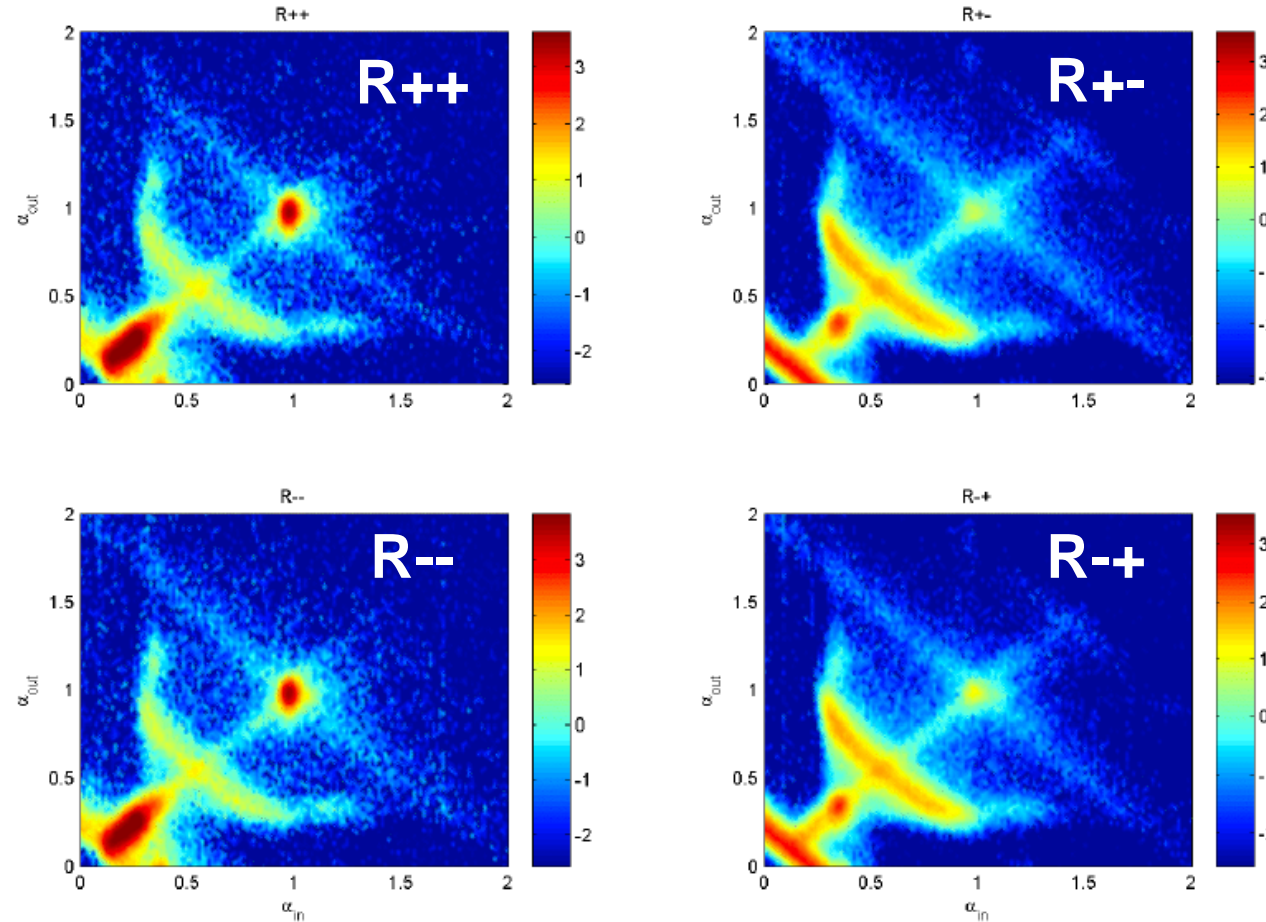


Ken Anderson, ILL



${}^3\text{He}$ spin-filter technique is very useful for the polarization analysis of off-specular scattering. Compared to solid-state analyzer, the spin-filter covers a wider angular range and is free of small angle scattering.

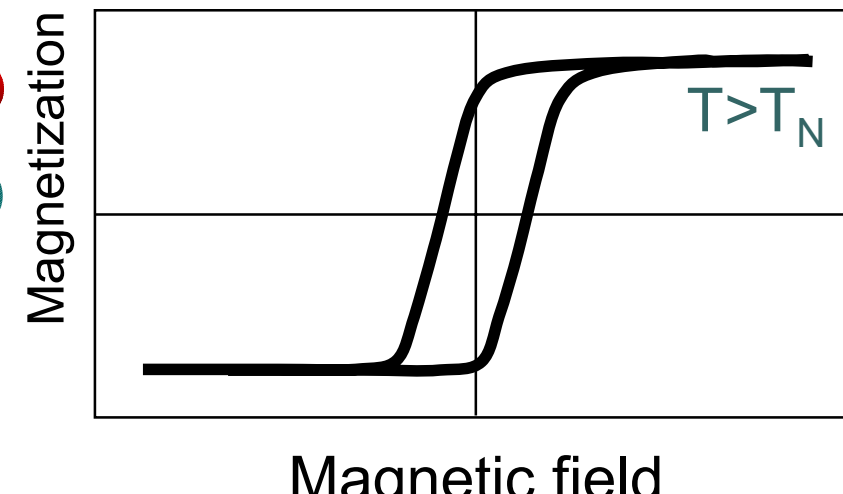
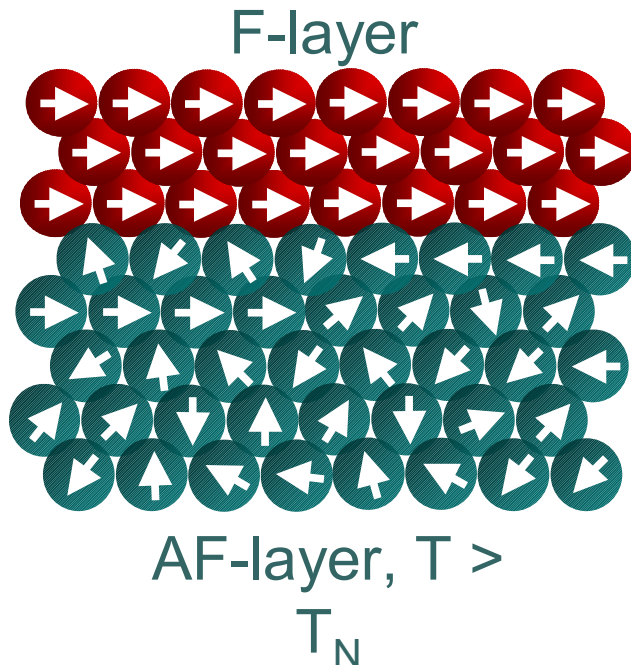
AF-coupled Co/CoO multilayer



F. Radu et al. (2005) unpublished

Exchange bias effect

Exchange interaction of a F and AF layer across a common interface



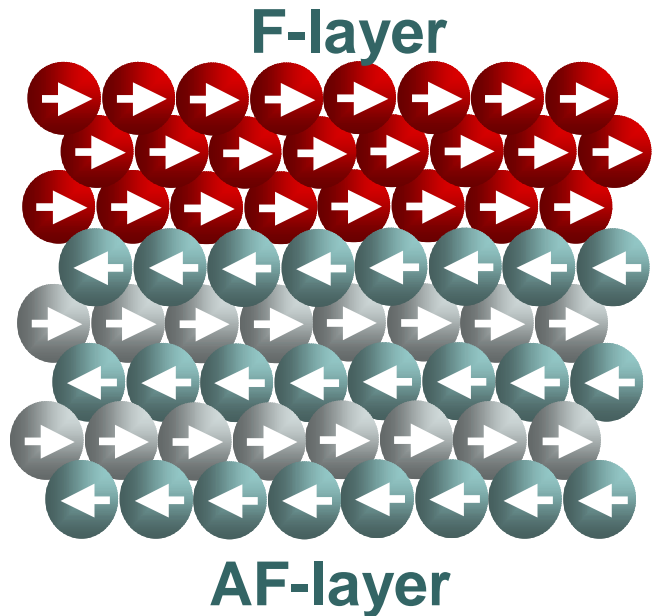
1. F-layer saturation in positive field

Exchange bias

2. Field cooling of AF below T_N

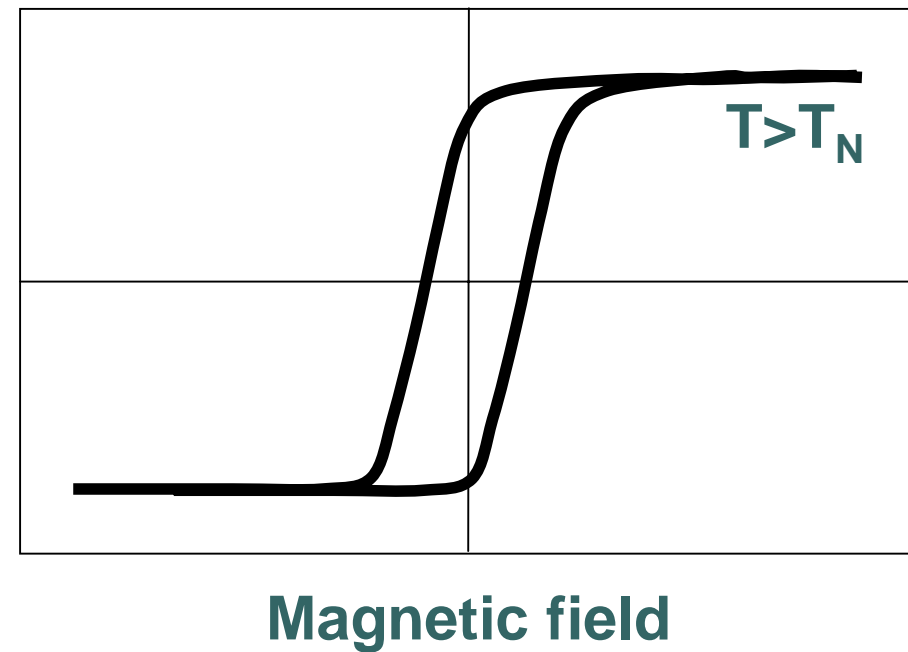
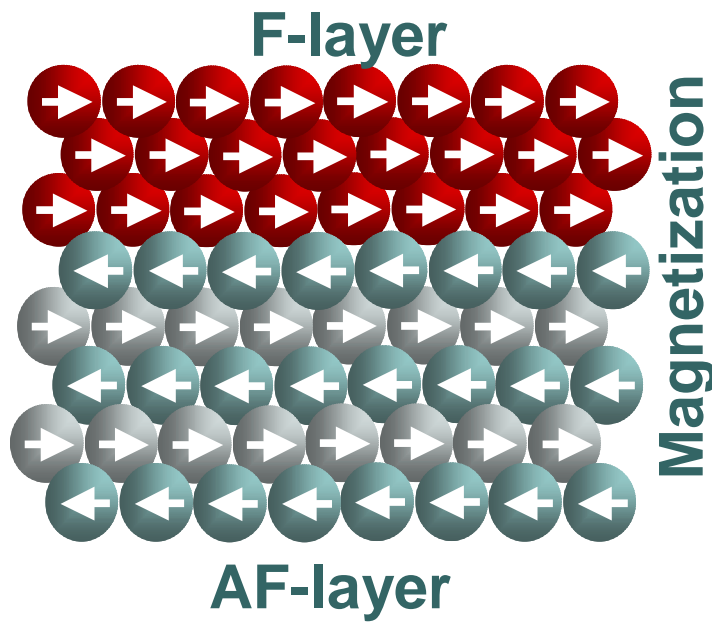


Exchange bias



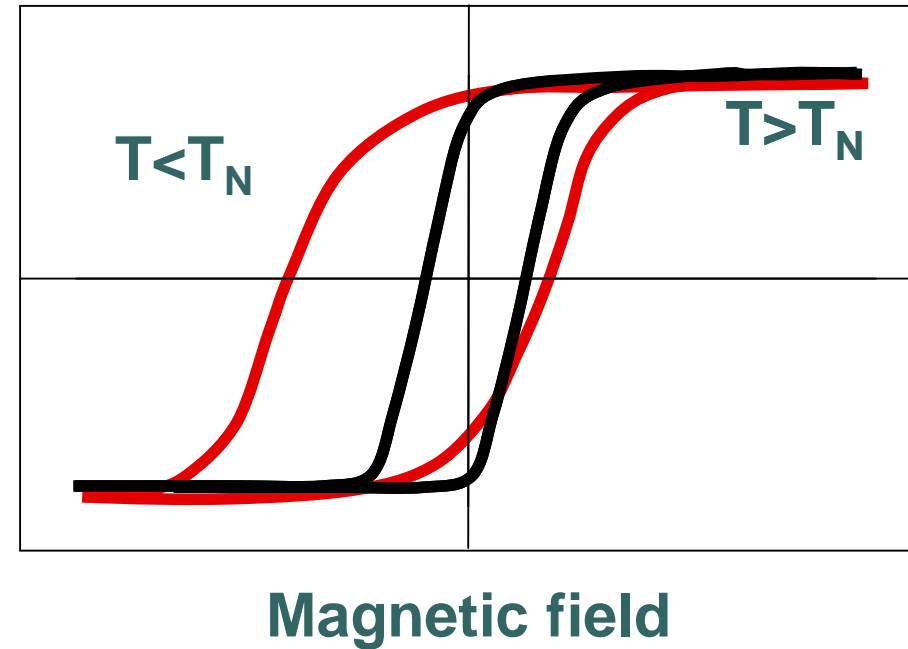
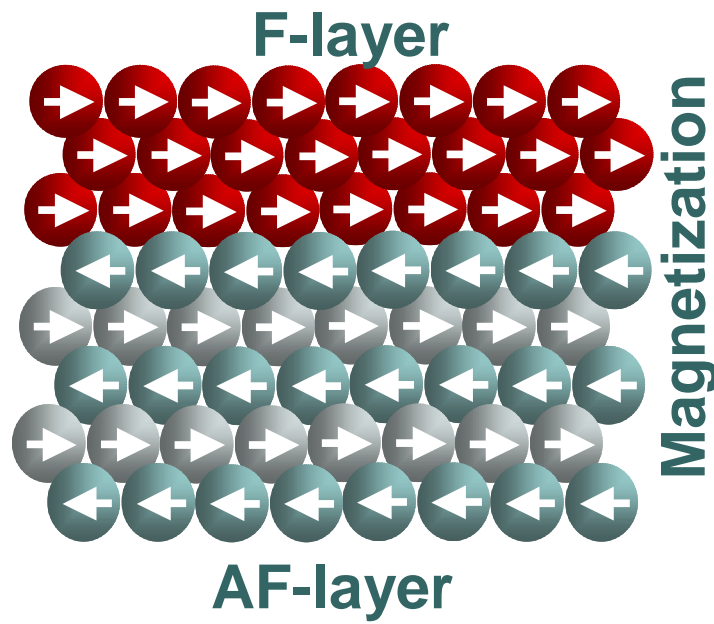
2. Field cooling of AF below T_N

Exchange bias



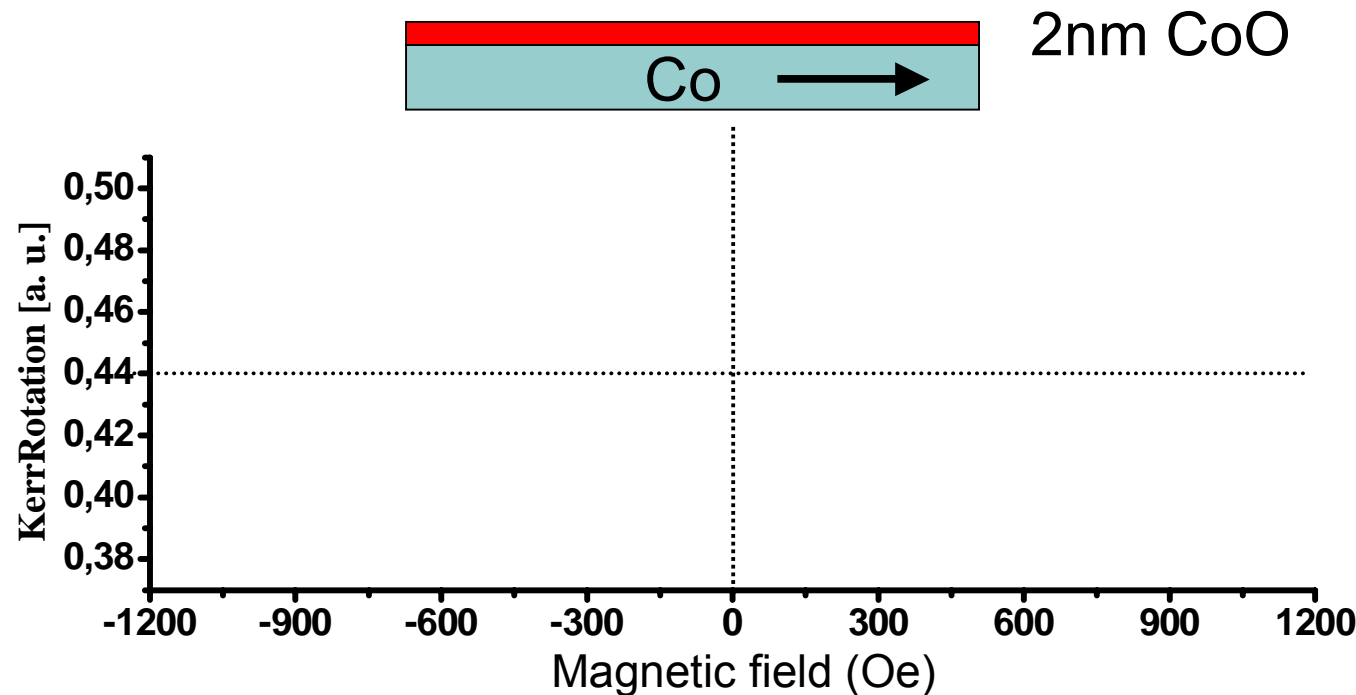
2. Field cooling of AF below T_N

Exchange bias



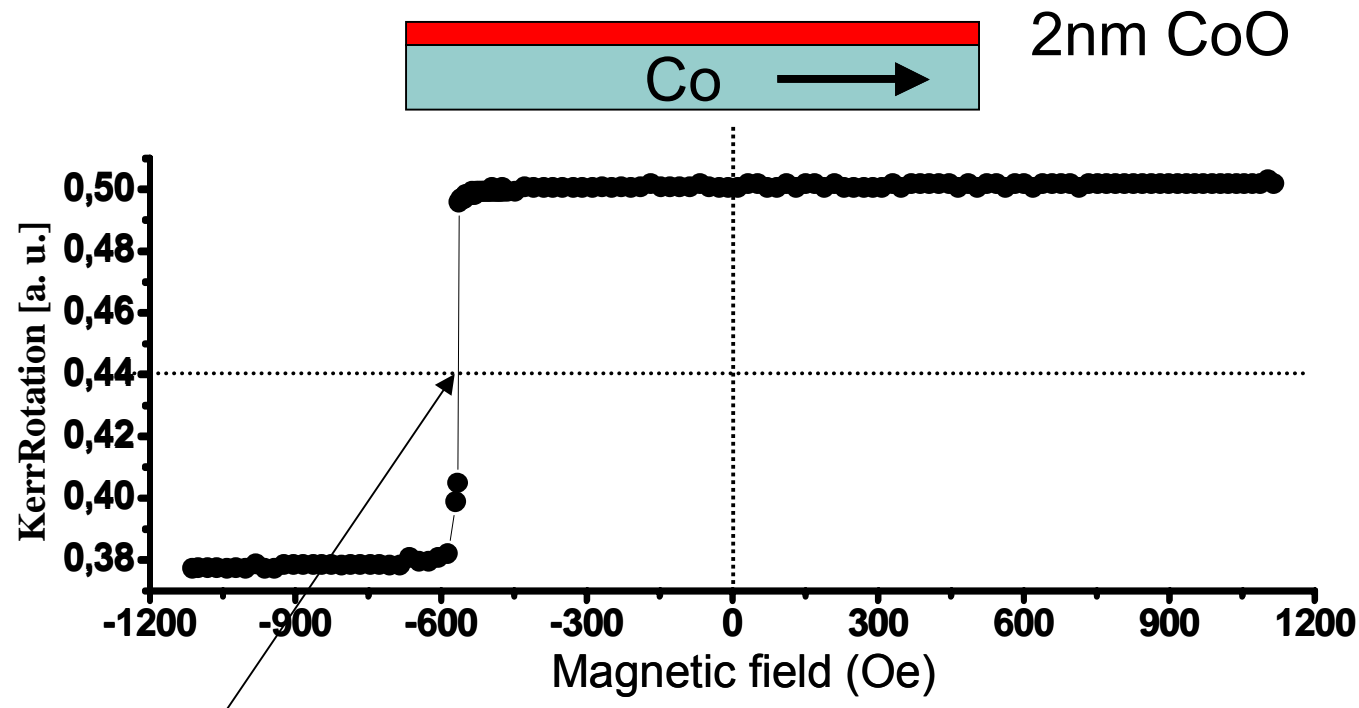
2. Field cooling of AF below T_N

MOKE measurements of a CoO/Co bilayer



F. Radu, M. Etzkorn, R. Siebrecht, T. Schmitte, K. Westerholt, and H. Zabel Phys. Rev. B **67**, 134409 (2003)

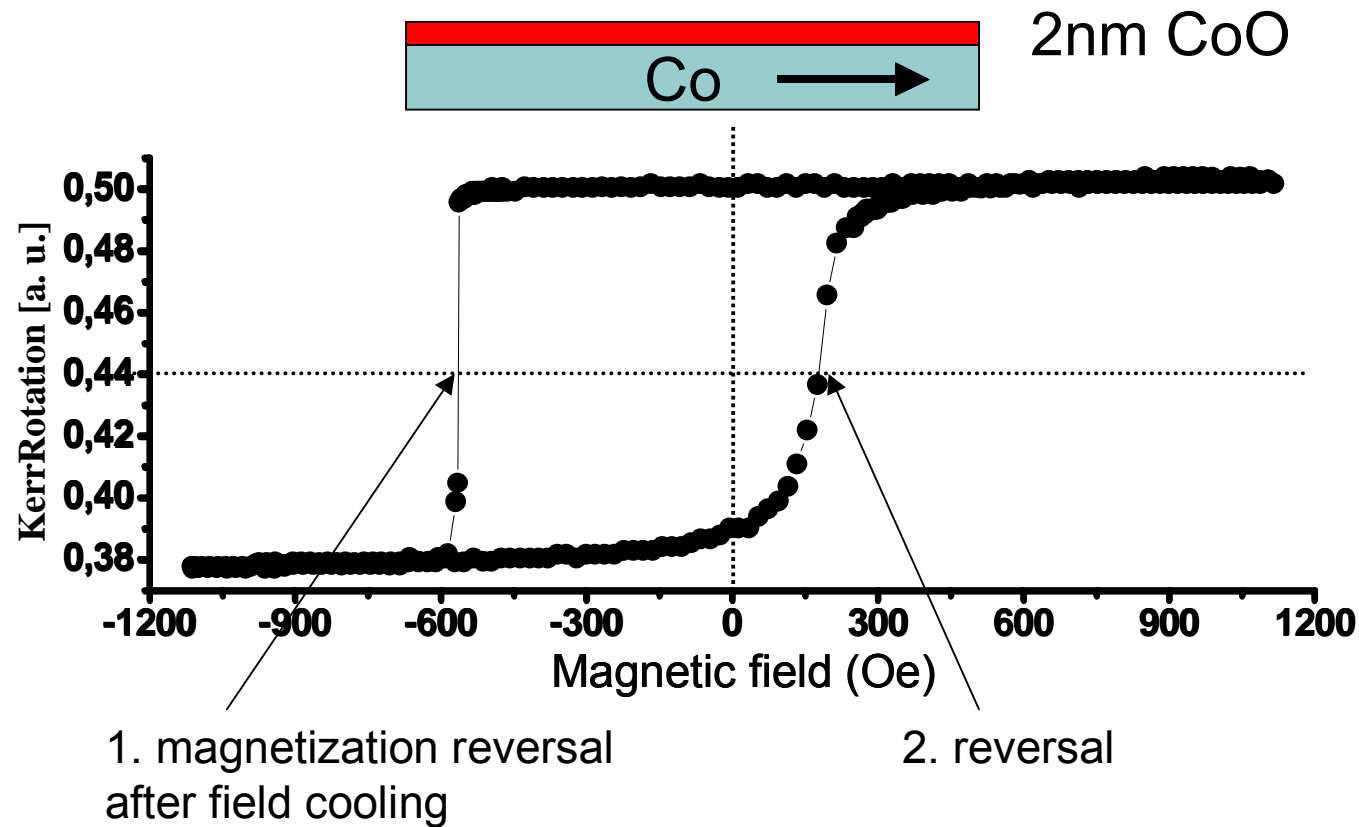
MOKE measurements of a CoO/Co bilayer



1. magnetization reversal
after field cooling

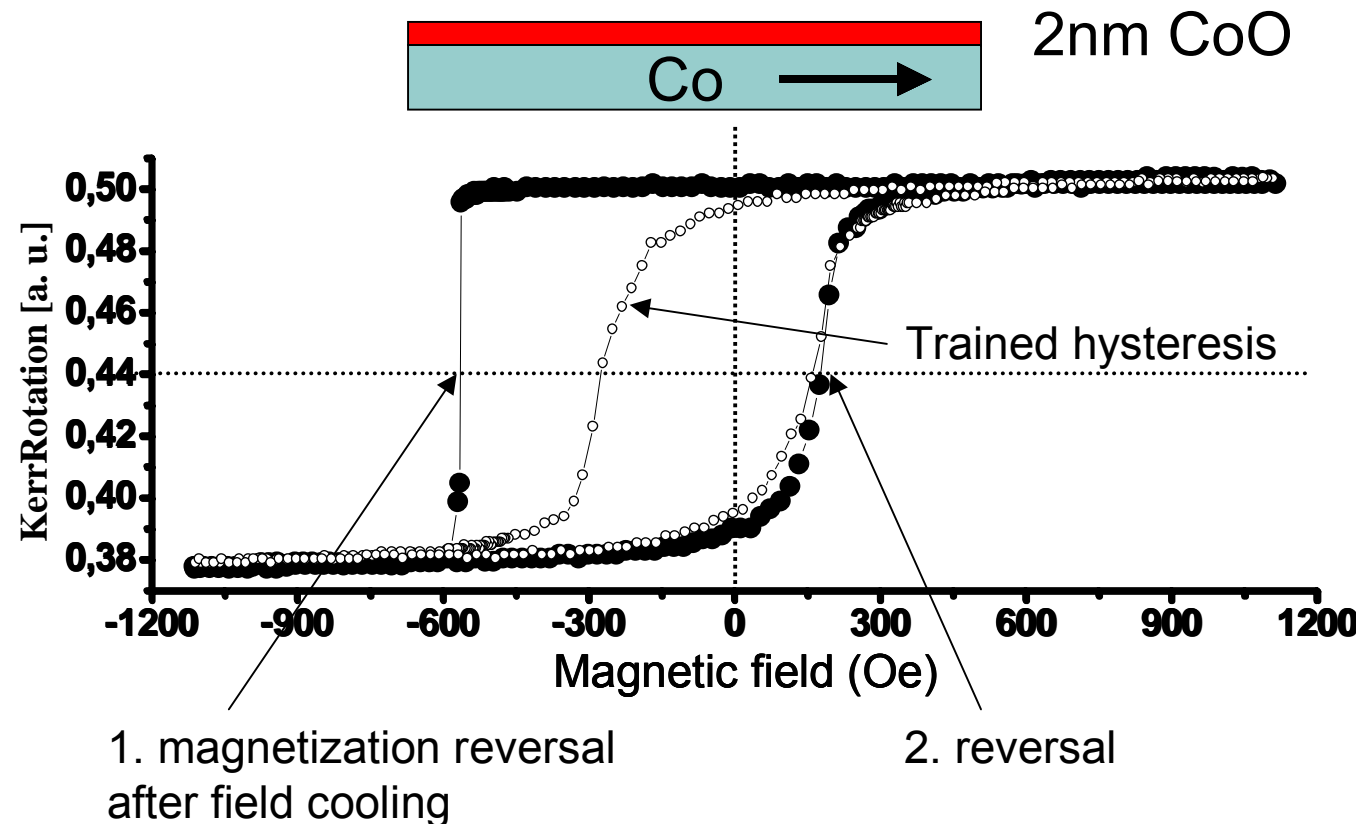
F. Radu, M. Etzkorn, R. Siebrecht, T. Schmitte, K. Westerholt, and H. Zabel Phys. Rev. B **67**, 134409 (2003)

MOKE measurements of a CoO/Co bilayer



F. Radu, M. Etzkorn, R. Siebrecht, T. Schmitte, K. Westerholt, and H. Zabel Phys. Rev. B **67**, 134409 (2003)

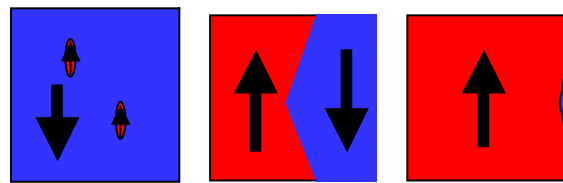
MOKE measurements of a CoO/Co bilayer



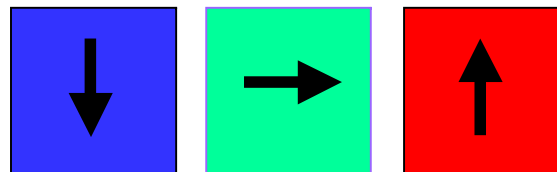
F. Radu, M. Etzkorn, R. Siebrecht, T. Schmitte, K. Westerholt, and H. Zabel Phys. Rev. B **67**, 134409 (2003)

Magnetic hysteresis: neutrons tell the difference

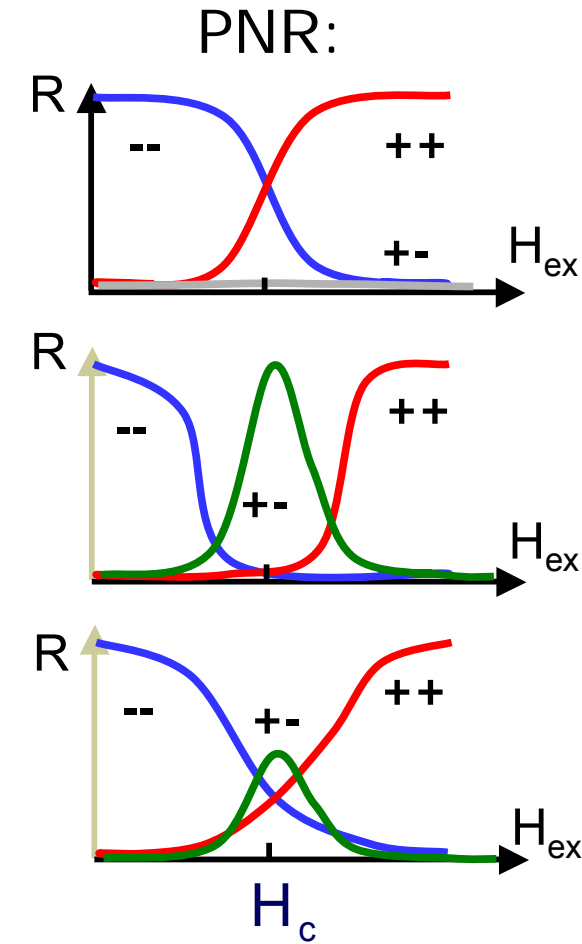
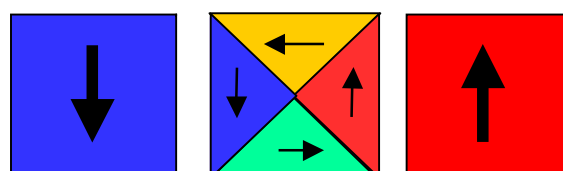
1. Nucleation and domain wall movement:



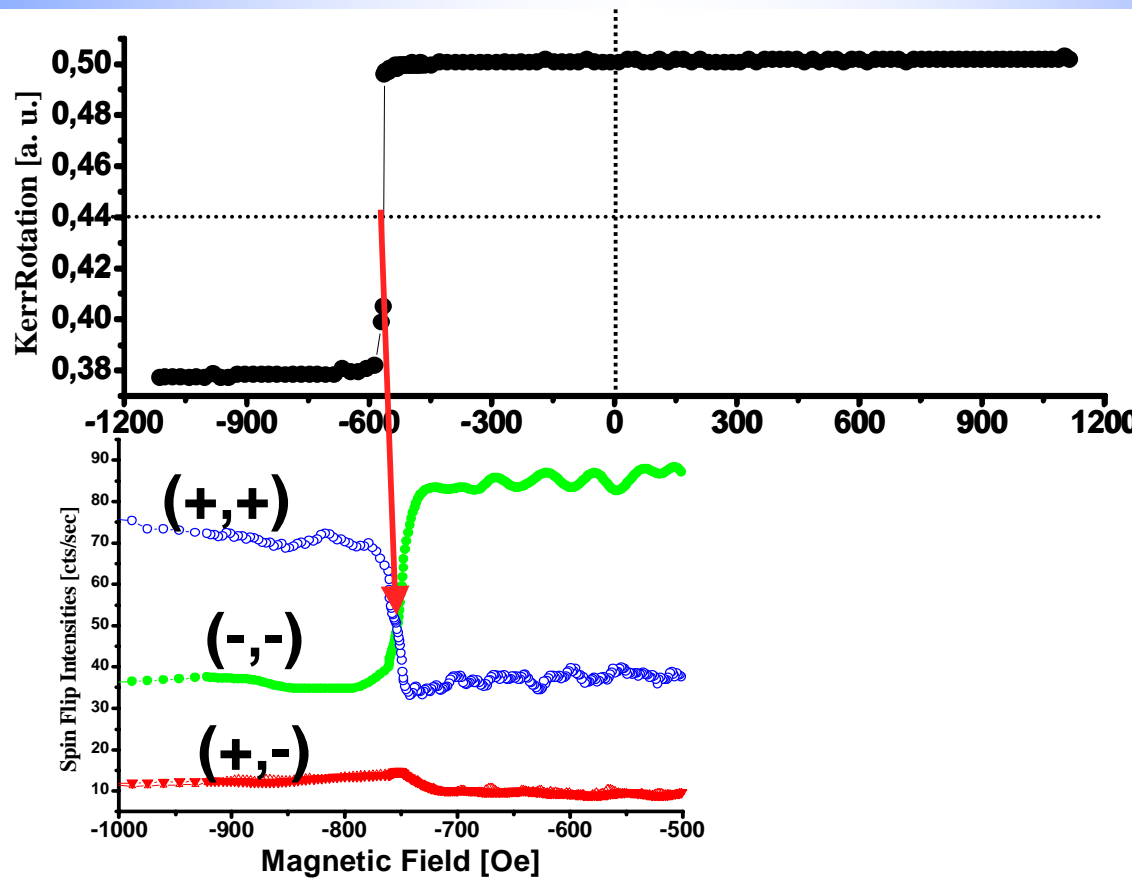
2. Coherent Rotation:



3. Domain formation:

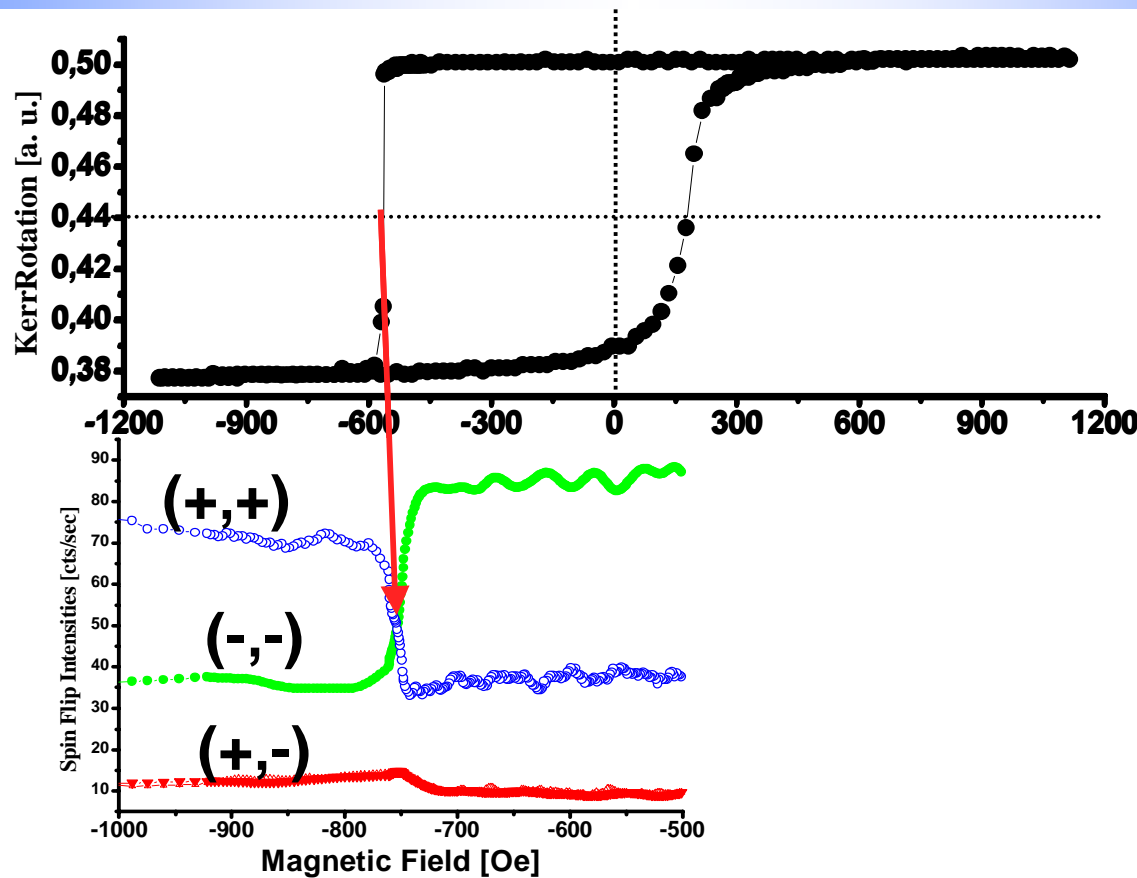


PNR results of CoO/Co bilayer



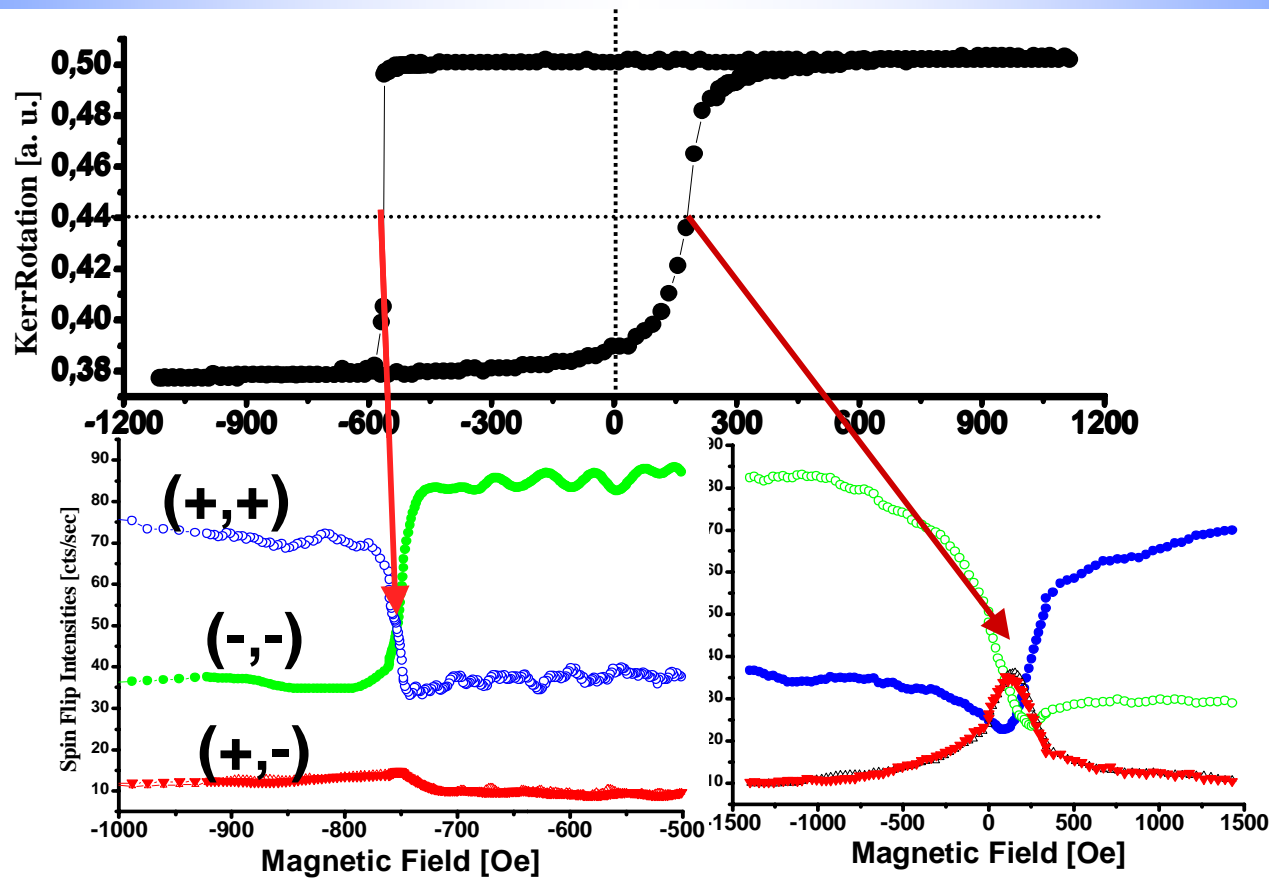
F. Radu, M. Etzkorn, R. Siebrecht, T. Schmitte, K. Westerholt, and H. Zabel
Phys. Rev. B **67**, 134409 (2003)

PNR results of CoO/Co bilayer



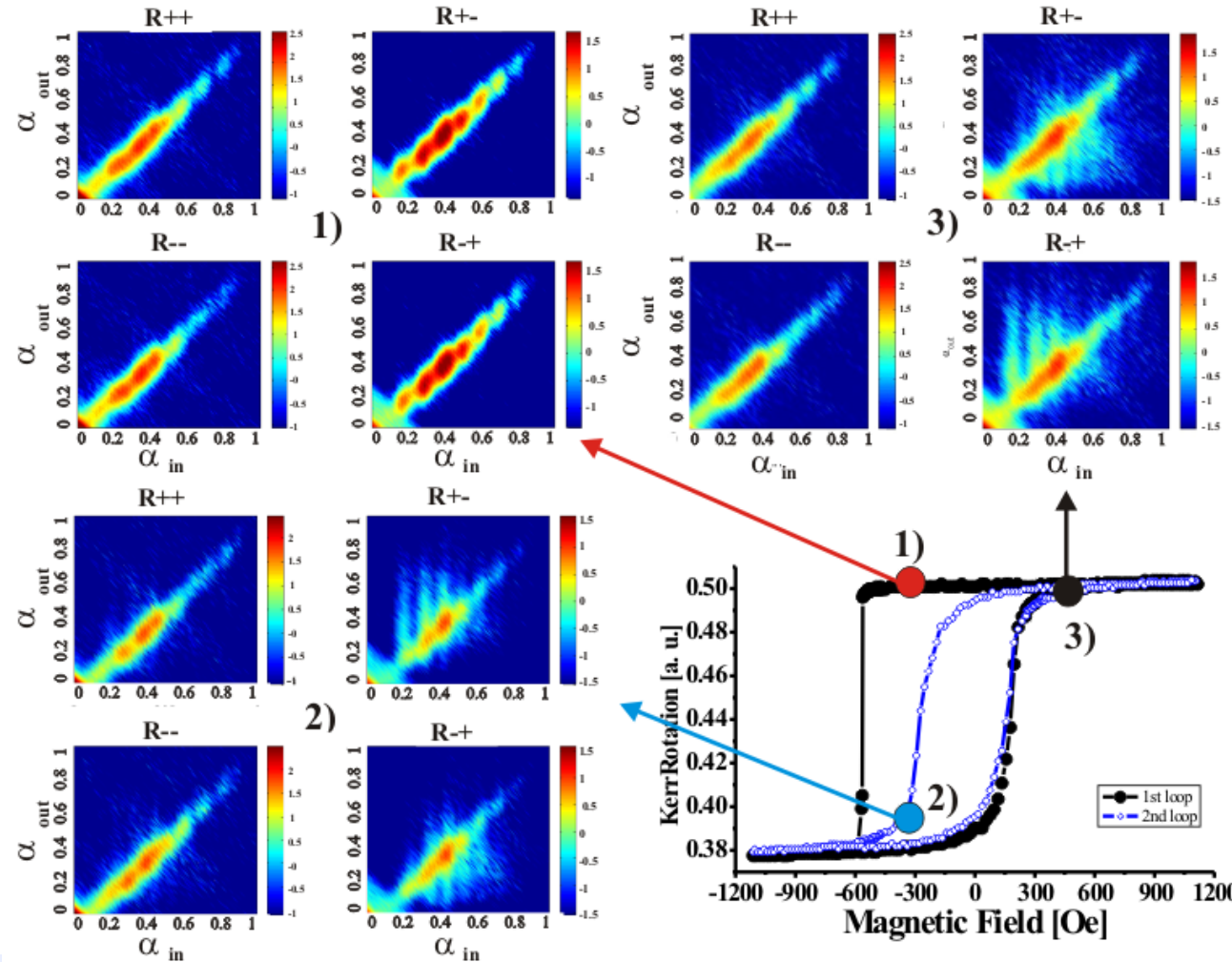
F. Radu, M. Etzkorn, R. Siebrecht, T. Schmitte, K. Westerholt, and H. Zabel
Phys. Rev. B **67**, 134409 (2003)

PNR results of CoO/Co bilayer



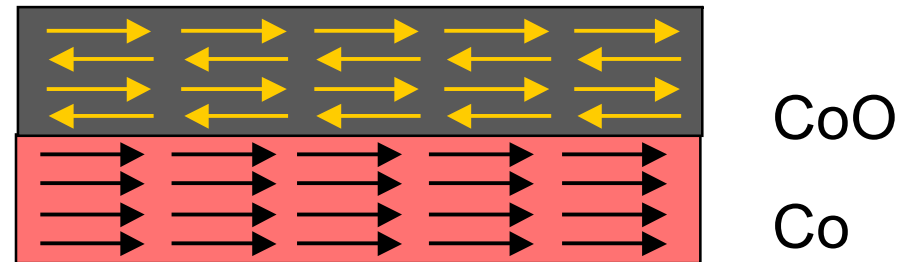
F. Radu, M. Etzkorn, R. Siebrecht, T. Schmitte, K. Westerholt, and H. Zabel
Phys. Rev. B **67**, 134409 (2003)

Diffuse scattering from CoO/Co



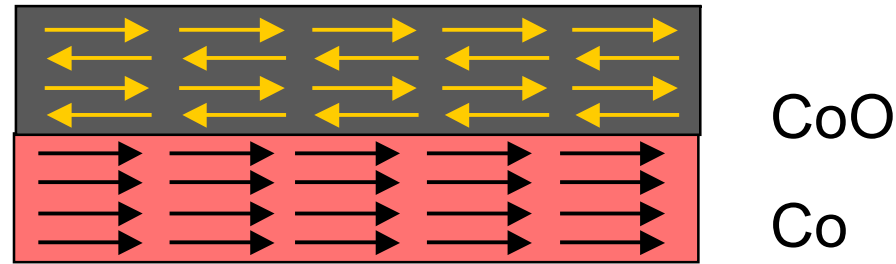
Change of domain structure upon reversal

After first field cooling:
Single domain state,
large H_{c1}



Change of domain structure upon reversal

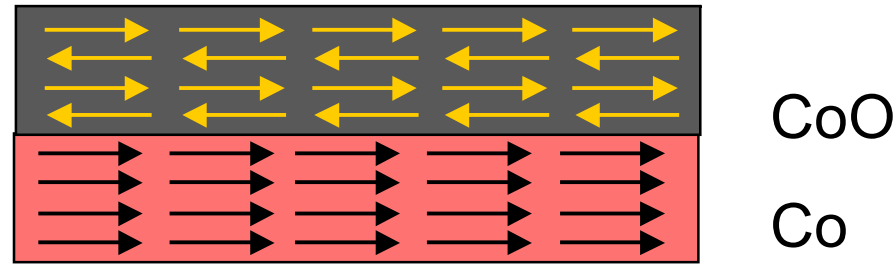
After first field cooling:
Single domain state,
large H_{c1}



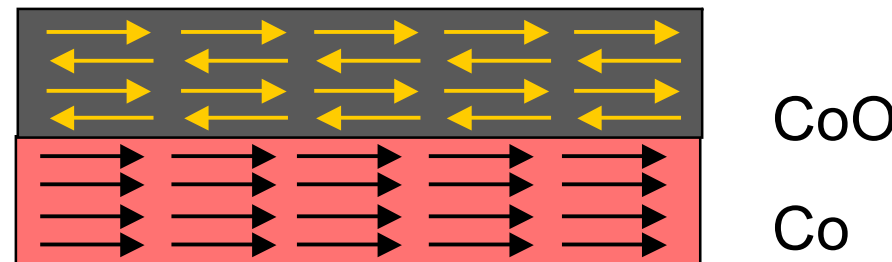
After first reversal:
domain wall motion,
creating AF domains

Change of domain structure upon reversal

After first field cooling:
Single domain state,
large H_{c1}

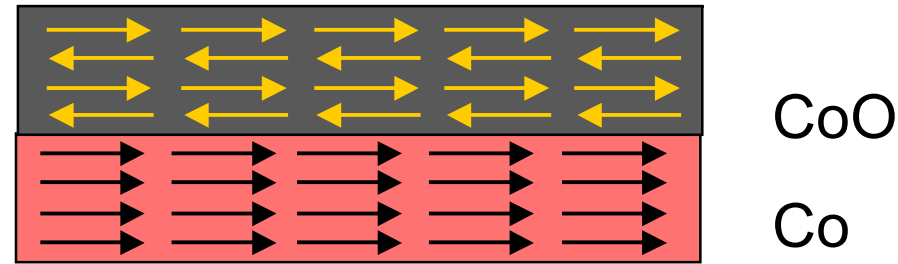


After first reversal:
domain wall motion,
creating AF domains

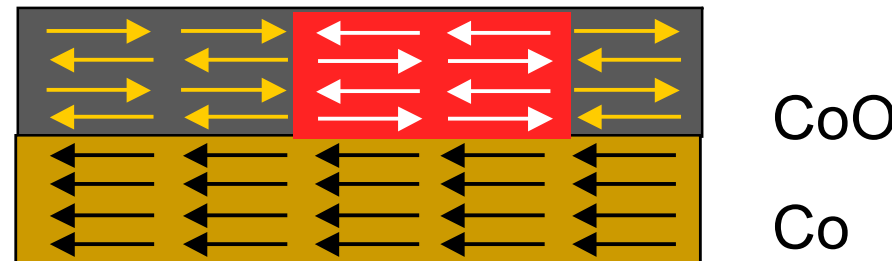


Change of domain structure upon reversal

After first field cooling:
Single domain state,
large H_{c1}

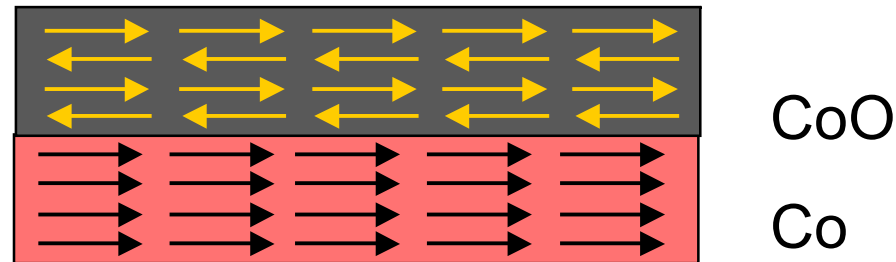


After first reversal:
domain wall motion,
creating AF domains

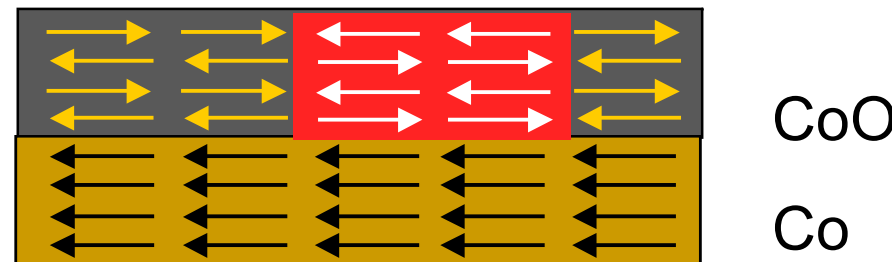


Change of domain structure upon reversal

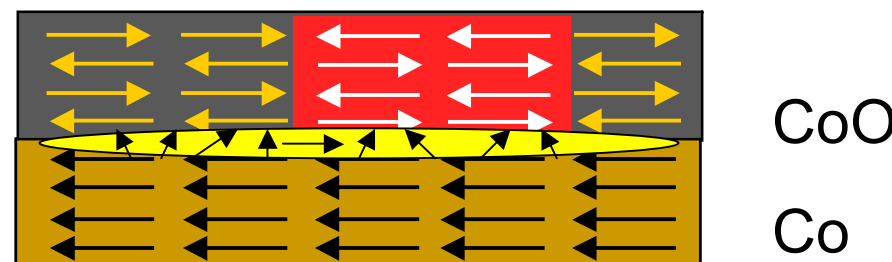
After first field cooling:
Single domain state,
large H_{c1}



After first reversal:
domain wall motion,
creating AF domains



Spin glass type
interfacial layer



Neutron reflectometers with polarization analysis

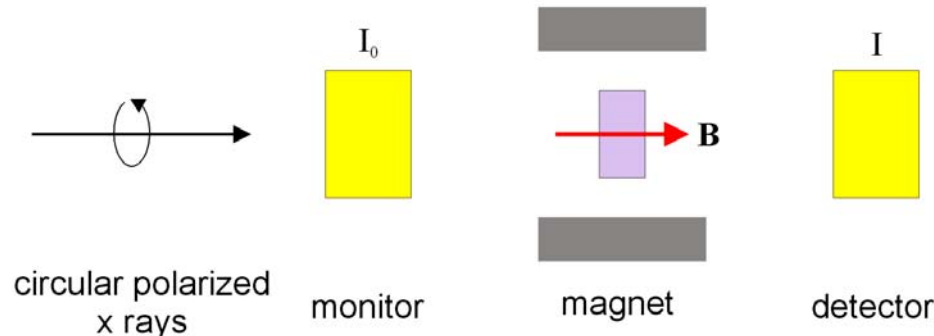
ADAM	ILL	SPN	Dubna
D17	ILL	REFLEX	Dubna
HADAS	FRJ	ROG	Delft
CRISP	ISIS	REFSANS	GKSS/FRM II
AMOR	PSI	N-REX	MPI/FRM II
MORPHEUS	PSI	MIRA	FRM II
V6	HMI	MARIA	Jülich/FRM II
EROS	LLB		
PRISM	LLB		
PNR	GKSS		
NeRo	GKSS		



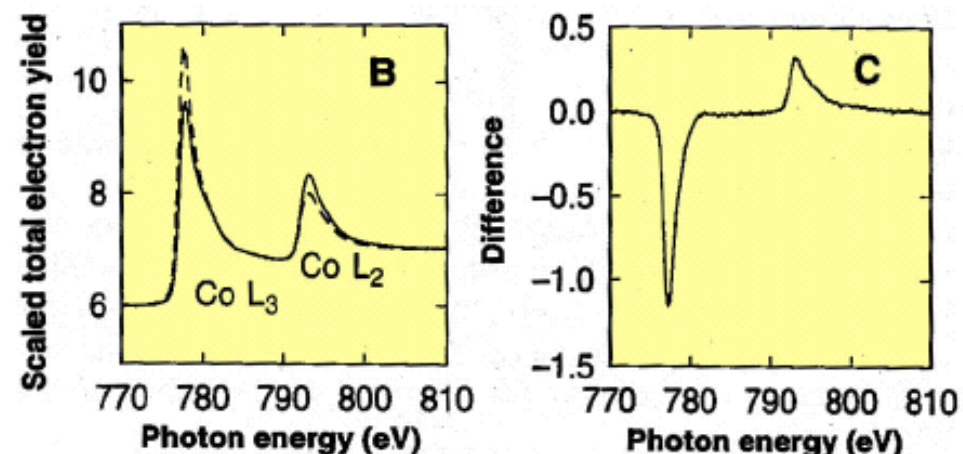
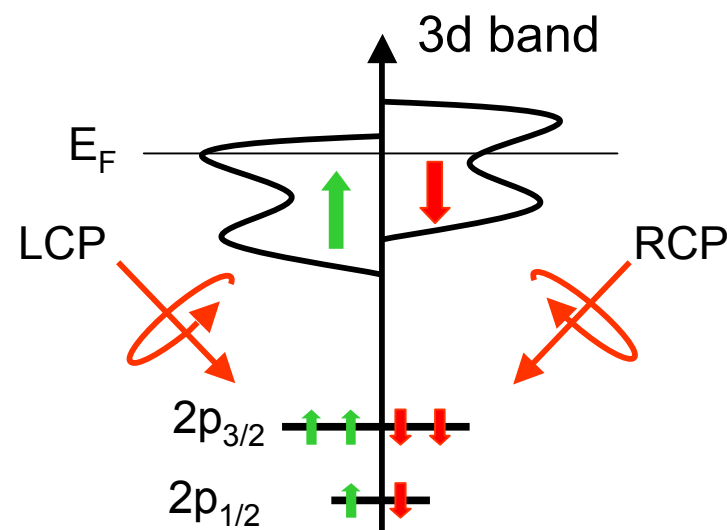
Do we still need PNR?

X-Ray Magnetic Dichroism XMCD

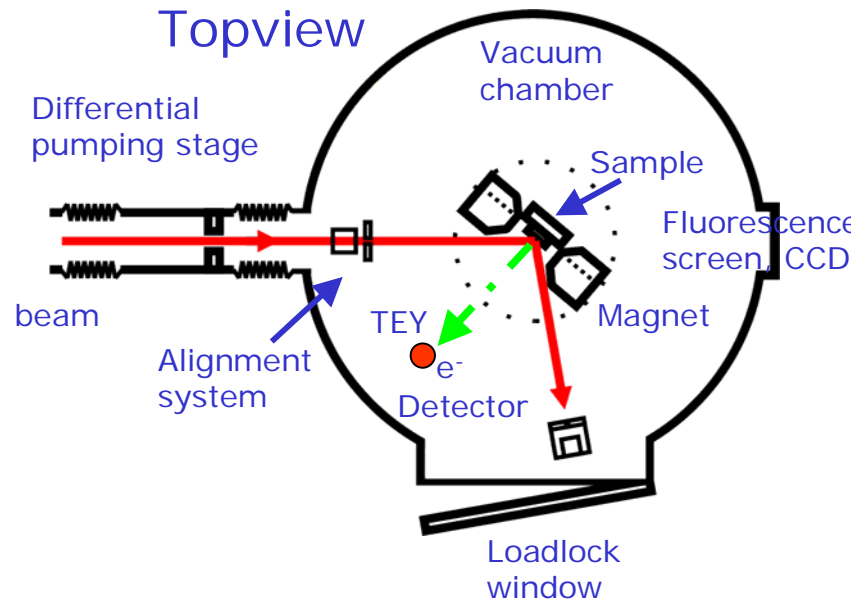
XMCD experimental layout



Absorption and reflection depend on the magnetization



XMCD and XRMS



- Element specific
- Spin and orbital moment analysis
- Magnetic scattering (XRMS)
- Vector magnetometry (similar to MOKE)
- Environment of magnetic ion (metallic versus ionic)
- High time resolution (ns-ps)
- High spatial resolution (x-ray microscopy: 10-20 nm)

YES, PNR is still required!

- The only method to provide depth resolved absolute magnetic moments
- Sensitive to magnetic induction (including stray fields in domain walls and screening fields in superconductors)
- No interference with optical terms, and no independent determination of optical parameters required
- Born approximation is sufficient for analysis at $Q > Q_c$
- Vector magnetometry is measured in the same field configuration
- Deep interfaces and layers are accessible
- Polarization analysis of diffuse scattering possible
- Coherence length of neutrons on the order of magnetic domain sizes (several μm), providing access to fluctuation terms.



Literature

- J.F. Ankner and G.P. Felcher, J. Magn. Magn. Mater. **200**, 751 (1999)
- M.R. Fitzsimmons et al. J. Magn. Magn. Mater. **271**, 103 (2004)
- H. Zabel and K. Theis-Bröhl, J. Phys.: Condens. Matter **15**, S505 (2003)
- H. Zabel, Materials Today, Jan. 2006
- Many further references are in these reviews



Thank you for your attention

